12

Detection of Climate Change and Attribution of Causes

Co-ordinating Lead Authors
J.F.B. Mitchell, D.J. Karoly

Lead Authors
G.C. Hegerl, F.W. Zwiers, M.R. Allen, J. Marengo

Contributing Authors
V. Barros, M. Berliner, G. Boer, T. Crowley, C. Folland, M. Free, N. Gillett, P. Groisman, J. Haigh, K. Hasselmann, P. Jones, M. Kandlikar, V. Kharin, H. Kheshgi, T. Knutson, M. MacCracken, M. Mann, G. North, J. Risbey, A. Robock, B. Santer, R. Schnur, C. Schönwiese, D. Sexton, P. Stott, S. Tett, K. Vinnikov, T. Wigley

Review Editors
F. Semazzi, J. Zillman

Contents

Executive Summary

The IPCC WG1 Second Assessment Report (IPCC, 1996) (hereafter SAR) concluded, "the balance of evidence suggests that there is a discernible human influence on global climate". It noted that the detection and attribution of anthropogenic climate change signals can only be accomplished through a gradual accumulation of evidence. The SAR authors also noted uncertainties in a number of factors, including the magnitude and patterns of internal climate variability, external forcing and climate system response, which prevented them from drawing a stronger conclusion. The results of the research carried out since 1995 on these uncertainties and other aspects of detection and attribution are summarised below.

A longer and more closely scrutinised observational record
Three of the five years (1995, 1996 and 1998) added to the instrumental record since the SAR are the warmest in the instrumental record of global temperatures, consistent with the expectation that increases in greenhouse gases will lead to continued long-term warming. The impact of observational sampling errors has been estimated for the global and hemispheric mean surface temperature record and found to be small relative to the warming observed over the 20th century. Some sources of error and uncertainty in both the Microwave Sounding Unit (MSU) and radiosonde observations have been identified that largely resolve discrepancies between the two data sets. However, current climate models cannot fully account for the observed difference in the trend between the surface and lower-tropospheric temperatures over the last twenty years even when all known external influences are included. New reconstructions of the surface temperature record of the last 1,000 years indicate that the temperature changes over the last 100 years are unlikely to be entirely natural in origin, even taking into account the large uncertainties in palaeo-reconstructions.

New model estimates of internal variability
Since the SAR, more models have been used to estimate the magnitude of internal climate variability. Several of the models used for detection show similar or larger variability than observed on interannual to decadal time-scales, even in the absence of external forcing. The warming over the past 100 years is very unlikely to be due to internal variability alone as estimated by current models. Estimates of variability on the longer time-scales relevant to detection and attribution studies are uncertain. Nonetheless, conclusions on the detection of an anthropogenic signal are insensitive to the model used to estimate internal variability and recent changes cannot be accounted for as pure internal variability even if the amplitude of simulated internal variations is increased by a factor of two or more. In most recent studies, the residual variability that remains in the observations after removal of the estimated anthropogenic signals is consistent with model-simulated variability on the space- and time-scales used for detection and attribution. Note, however, that the power of the consistency test is limited. Detection studies to date have shown that the observed large-scale changes in surface temperature in recent decades are unlikely (bordering on very unlikely) to be entirely the result of internal variability.

New estimates of responses to natural forcing
Fully coupled ocean-atmosphere models have used reconstructions of solar and volcanic forcings over the last one to three centuries to estimate the contribution of natural forcing to climate variability and change. Including their effects produces an increase in variance on all time-scales and brings the low-frequency variability simulated by models closer to that deduced from palaeo-reconstructions. Assessments based on physical principles and model simulations indicate that natural forcing alone is unlikely to explain the increased rate of global warming since the middle of the 20th century or changes in vertical temperature structure. The reasons are that the trend in natural forcing has likely been negative over the last two decades and natural forcing alone is unlikely to account for the observed cooling of the stratosphere. However, there is evidence for a detectable volcanic influence on climate. The available evidence also suggests a solar influence in proxy records of the last few hundred years and also in the instrumental record of the early 20th century. Statistical assessments confirm that natural variability (the combination of internal and naturally forced) is unlikely to explain the warming in the latter half of the 20th century.

Improved representation of anthropogenic forcing
Several studies since the SAR have included an explicit representation of greenhouse gases (as opposed to an equivalent increase in carbon dioxide (CO_2)). Some have also included tropospheric ozone changes, an interactive sulphur cycle, an explicit radiative treatment of the scattering of sulphate aerosols, and improved estimates of the changes in stratospheric ozone. While detection of the climate response to these other anthropogenic factors is often ambiguous, detection of the influence of greenhouse gas increases on the surface temperature changes over the past 50 years is robust.

Sensitivity to estimates of climate change signals
Since the SAR, more simulations with increases in greenhouse gases and some representation of aerosol effects have become available. In some cases, ensembles of simulations have been run to reduce noise in the estimates of the time-dependent response. Some studies have evaluated seasonal variation of the response. Uncertainties in the estimated climate change signals have made it difficult to attribute the observed climate change to one specific combination of anthropogenic and natural influences. Nevertheless, all studies since the SAR have found a significant anthropogenic contribution is required to account for surface and tropospheric trends over at least the last 30 years.

Qualitative consistencies between observed and modelled climate changes
There is a wide range of evidence of qualitative consistencies between observed climate changes and model responses to anthropogenic forcing, including global warming, increasing land-ocean temperature contrast, diminishing Arctic sea-ice extent, glacial retreat and increases in precipitation in Northern Hemisphere high latitudes. Some qualita-

tive inconsistencies remain, including the fact that models predict a faster rate of warming in the mid- to upper troposphere which is not observed in either satellite or radiosonde tropospheric temperature records.

A wider range of detection techniques

A major advance since the SAR is the increase in the range of techniques used, and the evaluation of the degree to which the results are independent of the assumptions made in applying those techniques. There have been studies using pattern correlations, optimal detection studies using one or more fixed patterns and time-varying patterns, and a number of other techniques. Evidence of a human influence on climate is obtained using all these techniques.

Results are sensitive to the range of temporal and spatial scales that are considered. Several decades of data are necessary to separate the forced response from internal variability. Idealised studies have demonstrated that surface temperature changes are detectable only on scales greater than 5,000 km. Studies also show that the level of agreement found between simulations and observations in pattern correlation studies is close to what one would expect in theory.

Attribution studies have applied multi-signal techniques to address whether or not the magnitude of the observed response to a particular forcing agent is consistent with the modelled response and separable from the influence of other forcing agents. The inclusion of time-dependent signals has helped to distinguish between natural and anthropogenic forcing agents. As more response patterns are included, the problem of degeneracy (different combinations of patterns yielding near identical fits to the observations) inevitably arises. Nevertheless, even with the responses to all the major forcing factors included in the analysis, a distinct greenhouse gas signal remains detectable. Overall, the magnitude of the model-simulated temperature response to greenhouse gases is found to be consistent with the observed greenhouse response on the scales considered. However, there remain discrepancies between the modelled and observed responses to other natural and anthropogenic factors, and estimates of signal amplitudes are model-dependent. Most studies find that, over the last 50 years, the estimated rate and magnitude of warming due to increasing concentrations of greenhouse gases alone are comparable with, or larger than, the observed warming. Furthermore, most model estimates that take into account both greenhouse gases and sulphate aerosols are consistent with observations over this period.

The increase in the number of studies, the breadth of techniques, increased rigour in the assessment of the role of anthropogenic forcing in climate, the robustness of results to the assumptions made using those techniques, and consistency of results lead to increased confidence in these results. Moreover, to be consistent with the signal observed to date, the rate of anthropogenic warming is likely to lie in the range 0.1 to 0.2°C/decade over the first half of the 21st century under the IS92a (IPCC, 1992) emission scenario.

Remaining uncertainties

A number of important uncertainties remain. These include:

- Discrepancies between the vertical profile of temperature change in the troposphere seen in observations and models. These have been reduced as more realistic forcing histories have been used in models, although not fully resolved. Also, the difference between observed surface and lower-tropospheric trends over the last two decades cannot be fully reproduced by model simulations.

- Large uncertainties in estimates of internal climate variability from models and observations, though as noted above, these are unlikely (bordering on very unlikely) to be large enough to nullify the claim that a detectable climate change has taken place.

- Considerable uncertainty in the reconstructions of solar and volcanic forcing which are based on proxy or limited observational data for all but the last two decades. Detection of the influence of greenhouse gases on climate appears to be robust to possible amplification of the solar forcing by ozone/solar or solar/cloud interactions, provided these do not alter the pattern or time dependence of the response to solar forcing. Amplification of the solar signal by these processes, which are not yet included in models, remains speculative.

- Large uncertainties in anthropogenic forcing are associated with the effects of aerosols. The effects of some anthropogenic factors, including organic carbon, black carbon, biomass aerosols, and changes in land use, have not been included in detection and attribution studies. Estimates of the size and geographic pattern of the effects of these forcings vary considerably, although individually their global effects are estimated to be relatively small.

- Large differences in the response of different models to the same forcing. These differences, which are often greater than the difference in response in the same model with and without aerosol effects, highlight the large uncertainties in climate change prediction and the need to quantify uncertainty and reduce it through better observational data sets and model improvement.

Synopsis

The SAR concluded: "The balance of evidence suggests a discernible human influence on global climate". That report also noted that the anthropogenic signal was still emerging from the background of natural climate variability. Since the SAR, progress has been made in reducing uncertainty, particularly with respect to distinguishing and quantifying the magnitude of responses to different external influences. Although many of the sources of uncertainty identified in the SAR still remain to some degree, new evidence and improved understanding support an updated conclusion.

- There is a longer and more closely scrutinised temperature record and new model estimates of variability. The warming over the past 100 years is very unlikely to be due to internal

variability alone, as estimated by current models. Reconstructions of climate data for the past 1,000 years also indicate that this warming was unusual and is unlikely to be entirely natural in origin.

- There are new estimates of the climate response to natural and anthropogenic forcing, and new detection techniques have been applied. Detection and attribution studies consistently find evidence for an anthropogenic signal in the climate record of the last 35 to 50 years.

- Simulations of the response to natural forcings alone (i.e., the response to variability in solar irradiance and volcanic eruptions) do not explain the warming in the second half of the 20th century. However, they indicate that natural forcings may have contributed to the observed warming in the first half of the 20th century.

- The warming over the last 50 years due to anthropogenic greenhouse gases can be identified despite uncertainties in forcing due to anthropogenic sulphate aerosol and natural factors (volcanoes and solar irradiance). The anthropogenic sulphate aerosol forcing, while uncertain, is negative over this period and therefore cannot explain the warming. Changes in natural forcing during most of this period are also estimated to be negative and are unlikely to explain the warming.

- Detection and attribution studies comparing model simulated changes with the observed record can now take into account uncertainty in the magnitude of modelled response to external forcing, in particular that due to uncertainty in climate sensitivity.

- Most of these studies find that, over the last 50 years, the estimated rate and magnitude of warming due to increasing concentrations of greenhouse gases alone are comparable with, or larger than, the observed warming. Furthermore, most model estimates that take into account both greenhouse gases and sulphate aerosols are consistent with observations over this period.

- The best agreement between model simulations and observations over the last 140 years has been found when all the above anthropogenic and natural forcing factors are combined. These results show that the forcings included are sufficient to explain the observed changes, but do not exclude the possibility that other forcings may also have contributed.

In the light of new evidence and taking into account the remaining uncertainties, most of the observed warming over the last 50 years is likely to have been due to the increase in greenhouse gas concentrations.

Furthermore, it is very likely that the 20th century warming has contributed significantly to the observed sea level rise, through thermal expansion of sea water and widespread loss of land ice. Within present uncertainties, observations and models are both consistent with a lack of significant acceleration of sea level rise during the 20th century.

12.1 Introduction

12.1.1 The Meaning of Detection and Attribution

The response to anthropogenic changes in climate forcing occurs against a backdrop of natural internal and externally forced climate variability that can occur on similar temporal and spatial scales. Internal climate variability, by which we mean climate variability not forced by external agents, occurs on all time-scales from weeks to centuries and millennia. Slow climate components, such as the ocean, have particularly important roles on decadal and century time-scales because they integrate high-frequency weather variability (Hasselmann, 1976) and interact with faster components. Thus the climate is capable of producing long time-scale internal variations of considerable magnitude without any external influences. Externally forced climate variations may be due to changes in natural forcing factors, such as solar radiation or volcanic aerosols, or to changes in anthropogenic forcing factors, such as increasing concentrations of greenhouse gases or sulphate aerosols.

Definitions

The presence of this natural climate variability means that the detection and attribution of anthropogenic climate change is a statistical "signal-in-noise" problem. *Detection* is the process of demonstrating that an observed change is significantly different (in a statistical sense) than can be explained by natural internal variability. However, the detection of a change in climate does not necessarily imply that its causes are understood. As noted in the SAR, the unequivocal *attribution* of climate change to anthropogenic causes (i.e., the isolation of cause and effect) would require controlled experimentation with the climate system in which the hypothesised agents of change are systematically varied in order to determine the climate's sensitivity to these agents. Such an approach to attribution is clearly not possible. Thus, from a practical perspective, attribution of observed climate change to a given combination of human activity and natural influences requires another approach. This involves statistical analysis and the careful assessment of multiple lines of evidence to demonstrate, within a pre-specified margin of error, that the observed changes are:

- unlikely to be due entirely to internal variability;
- consistent with the estimated responses to the given combination of anthropogenic and natural forcing; and
- not consistent with alternative, physically plausible explanations of recent climate change that exclude important elements of the given combination of forcings.

Limitations

It is impossible, even in principle, to distinguish formally between all conceivable explanations with a finite amount of data. Nevertheless, studies have now been performed that include all the main natural and anthropogenic forcing agents that are generally accepted (on physical grounds) to have had a substantial impact on near-surface temperature changes over the 20th century. Any statement that a model simulation is consistent with observed changes can only apply to a subset of model-simulated variables, such as large-scale near-surface temperature trends: no numerical model will ever be perfect in every respect. To attribute all or part of recent climate change to human activity, therefore, we need to demonstrate that alternative explanations, such as pure internal variability or purely naturally forced climate change, are unlikely to account for a set of observed changes that can be accounted for by human influence. Detection (ruling out that observed changes are only an instance of internal variability) is thus one component of the more complex and demanding process of attribution. In addition to this general usage of the term detection (that some climate change has taken place), we shall also discuss the detection of the influence of individual forcings (see Section 12.4).

Detection and estimation

The basic elements of this approach to detection and attribution were recognised in the SAR. However, detection and attribution studies have advanced beyond addressing the simple question "have we detected a human influence on climate?" to such questions as "how large is the anthropogenic change?" and "is the magnitude of the response to greenhouse gas forcing as estimated in the observed record consistent with the response simulated by climate models?" The task of detection and attribution can thus be rephrased as an estimation problem, with the quantities to be estimated being the factor(s) by which we have to scale the model-simulated response(s) to external forcing to be consistent with the observed change. The estimation approach uses essentially the same tools as earlier studies that considered the problem as one of hypothesis testing, but is potentially more informative in that it allows us to quantify, with associated estimates of uncertainty, how much different factors have contributed to recent observed climate changes. This interpretation only makes sense, however, if it can be assumed that important sources of model error, such as missing or incorrectly represented atmospheric feedbacks, affect primarily the amplitude and not the structure of the response to external forcing. The majority of relevant studies suggest that this is the case for the relatively small-amplitude changes observed to date, but the possibility of model errors changing both the amplitude and structure of the response remains an important caveat. Sampling error in model-derived signals that originates from the model's own internal variability also becomes an issue if detection and attribution is considered as an estimation problem – some investigations have begun to allow for this, and one study has estimated the contribution to uncertainty from observational sampling and instrumental error. The robustness of detection and attribution findings obtained with different climate models has been assessed.

Extensions

It is important to stress that the attribution process is inherently open-ended, since we have no way of predicting what alternative explanations for observed climate change may be proposed, and be accepted as plausible, in the future. This problem is not unique to the climate change issue, but applies to any problem of

establishing cause and effect given a limited sample of observations. The possibility of a confounding explanation can never be ruled out completely, but as successive alternatives are tested and found to be inadequate, it can be seen to become progressively more unlikely. There is growing interest in the use of Bayesian methods (Dempster, 1998; Hasselmann, 1998; Leroy, 1998; Tol and de Vos, 1998; Barnett *et al.*, 1999; Levine and Berliner, 1999; Berliner *et al*., 2000). These provide a means of formalising the process of incorporating additional information and evaluating a range of alternative explanations in detection and attribution studies. Existing studies can be rephrased in a Bayesian formalism without any change in their conclusions, as demonstrated by Leroy (1998). However, a number of statisticians (e.g., Berliner *et al.*, 2000) argue that a more explicitly Bayesian approach would allow greater flexibility and rigour in the treatment of different sources of uncertainty.

12.1.2 Summary of the First and Second Assessment Reports

The first IPCC Scientific Assessment in 1990 (IPCC, 1990) concluded that the global mean surface temperature had increased by 0.3 to 0.6°C over the previous 100 years and that the magnitude of this warming was broadly consistent with the predictions of climate models forced by increasing concentrations of greenhouse gases. However, it remained to be established that the observed warming (or part of it) could be attributed to the enhanced greenhouse effect. Some of the reasons for this were that there was only limited agreement between model predictions and observations, because climate models were still in the early stages of development; there was inadequate knowledge of natural variability and other possible anthropogenic effects on climate and there was a scarcity of suitable observational data, particularly long, reliable time-series.

By the time of the SAR in 1995, considerable progress had been made in attempts to identify an anthropogenic effect on climate. The first area of significant advance was that climate models were beginning to incorporate the possible climatic effects of human-induced changes in sulphate aerosols and stratospheric ozone. The second area of progress was in better defining the background variability of the climate system through multi-century model experiments that assumed no changes in forcing. These provided important information about the possible characteristics of the internal component of natural climate variability. The third area of progress was in the application of pattern-based methods that attempted to attribute some part of the observed changes in climate to human activities, although these studies were still in their infancy at that time.

The SAR judged that the observed trend in global climate over the previous 100 years was unlikely to be entirely natural in origin. This led to the following, now well-known, conclusion: "Our ability to quantify the human influence on global climate is currently limited because the expected signal is still emerging from the noise of natural variability, and because there are uncertainties in key factors. Nevertheless, the balance of evidence suggests that there is a discernible human influence on global climate". It also noted that the magnitude of the influence was uncertain.

12.1.3 Developments since the Second Assessment Report

In the following sections, we assess research developments since the SAR in areas crucial to the detection of climate change and the attribution of its causes. First, in Section 12.2, we review advances in the different elements that are needed in any detection and attribution study, including observational data, estimates of internal climate variability, natural and anthropogenic climate forcings and their simulated responses, and statistical methods for comparing observed and modelled climate change. We draw heavily on the assessments in earlier chapters of this report, particularly Chapter 2 – Observed Climate Variability and Change, Chapter 6 – Radiative Forcing of Climate Change, Chapter 8 – Model Evaluation, and Chapter 9 – Projections of Future Climate Change.

In Section 12.3, a qualitative assessment is made of observed and modelled climate change, identifying general areas of agreement and difference. This is based on the observed climate changes identified with most confidence in Chapter 2 and the model projections of climate change from Chapter 9.

Next, in Section 12.4, advances obtained with quantitative methods for climate change detection and attribution are assessed. These include results obtained with time-series methods, pattern correlation methods, and optimal fingerprint methods. The interpretation of optimal fingerprinting as an estimation problem, finding the scaling factors required to bring the amplitude of model-simulated changes into agreement with observed changes, is discussed. Some remaining uncertainties are discussed in Section 12.5 and the key findings are drawn together in Section 12.6.

12.2 The Elements of Detection and Attribution

12.2.1 Observed Data

Ideally, a detection and attribution study requires long records of observed data for climate elements that have the potential to show large climate change signals relative to natural variability. It is also necessary that the observing system has sufficient coverage so that the main features of natural variability and climate change can be identified and monitored. A thorough assessment of observed climate change, climate variability and data quality was presented in Chapter 2. Most detection and attribution studies have used near-surface air temperature, sea surface temperature or upper air temperature data, as these best fit the requirement above.

The quality of observed data is a vital factor. Homogeneous data series are required with careful adjustments to account for changes in observing system technologies and observing practices. Estimates of observed data uncertainties due to instrument errors or variations in data coverage (assessed in Chapter 2) are included in some recent detection and attribution studies.

There have been five more years of observations since the SAR. Improvements in historical data coverage and processing are described in Chapter 2. Confidence limits for observational sampling error have been estimated for the global and hemispheric mean temperature record. Applications of improved pre-instrumental proxy data reconstructions are described in the next two sections.

12.2.2 Internal Climate Variability

Detection and attribution of climate change is a statistical "signal-in-noise" problem, it requires an accurate knowledge of the properties of the "noise". Ideally, internal climate variability would be estimated from instrumental observations, but a number of problems make this difficult. The instrumental record is short relative to the 30 to 50 year time-scales that are of interest for detection and attribution of climate change, particularly for variables in the free atmosphere. The longest records that are available are those for surface air temperature and sea surface temperature. Relatively long records are also available for precipitation and surface pressure, but coverage is incomplete and varies in time (see Chapter 2). The instrumental record also contains the influences of external anthropogenic and natural forcing. A record of natural internal variability can be reconstructed by removing estimates of the response to external forcing (for example, Jones and Hegerl, 1998; Wigley *et al.*, 1998a). However, the accuracy of this record is limited by incomplete knowledge of the forcings and by the accuracy of the climate model used to estimate the response.

Estimates using palaeoclimatic data

Palaeo-reconstructions provide an additional source of information on climate variability that strengthens our qualitative assessment of recent climate change. There has been considerable progress in the reconstruction of past temperatures. New reconstructions with annual or seasonal resolution, back to 1000 AD, and some spatial resolution have become available (Briffa *et al.*, 1998; Jones *et al.*, 1998; Mann *et al.*, 1998, 2000; Briffa *et al.*, 2000; Crowley and Lowery, 2000; see also Chapter 2, Figure 2.21). However, a number of difficulties, including limited coverage, temporal inhomogeneity, possible biases due to the palaeo-reconstruction process, uncertainty regarding the strength of the relationships between climatic and proxy indices, and the likely but unknown influence of external forcings inhibit the estimation of internal climate variability directly from palaeoclimate data. We expect, however, that the reconstructions will continue to improve and that palaeo-data will become increasingly important for assessing natural variability of the climate system. One of the most important applications of this palaeoclimate data is as a check on the estimates of internal variability from coupled climate models, to ensure that the latter are not underestimating the level of internal variability on 50 to 100 year time-scales (see below). The limitations of the instrumental and palaeo-records leave few alternatives to using long "control" simulations with coupled models (see Figure 12.1) to estimate the detailed structure of internal climate variability.

Estimates of the variability of global mean surface temperature

Stouffer *et al.* (2000) assess variability simulated in three 1,000-year control simulations (see Figure 12.1). The models are found to simulate reasonably well the spatial distribution of variability and the spatial correlation between regional and global mean variability, although there is more disagreement between models at long time-scales (>50 years) than at short time-scales. None of the long model simulations produces a secular trend which is comparable to that observed. Chapter 8, Section 8.6.2. assesses model-simulated variability in detail. Here we assess the aspects that are particularly relevant to climate change detection. The power spectrum of global mean temperatures simulated by the most recent coupled climate models (shown in Figure 12.2) compares reasonably well with that of detrended observations (solid black line) on interannual to decadal time-scales. However, uncertainty of the spectral estimates is large and some models are clearly underestimating variability (indicated by the asterisks). Detailed comparison on inter-decadal time-scales is difficult because observations are likely to contain a response to external forcings that will not be entirely removed by a simple linear trend. At the same time, the detrending procedure itself introduces a negative bias in the observed low-frequency spectrum.

Both of these problems can be avoided by removing an independent estimate of the externally forced response from the observations before computing the power spectrum. This independent estimate is provided by the ensemble mean of a coupled model simulation of the response to the combination of natural and anthropogenic forcing (see Figure 12.7c). The resulting spectrum of observed variability (dotted line in Figure 12.2) will not be subject to a negative bias because the observed data have not been used in estimating the forced response. It will, however, be inflated by uncertainty in the model-simulated forced response and by noise due to observation error and due to incomplete coverage (particularly the bias towards relatively noisy Northern Hemisphere land temperatures in the early part of the observed series). This estimate of the observed spectrum is therefore likely to overestimate power at all frequencies. Even so, the more variable models display similar variance on the decadal to inter-decadal time-scales important for detection and attribution.

Estimates of spatial patterns of variability

Several studies have used common empirical orthogonal function (EOF) analysis to compare the spatial modes of climate variability between different models. Stouffer *et al.* (2000) analysed the variability of 5-year means of surface temperature in 500-year or longer simulations of the three models most commonly used to estimate internal variability in formal detection studies. The distribution of the variance between the EOFs was similar between the models and the observations. HadCM2 tended to overestimate the variability in the main modes, whereas GFDL and ECHAM3 underestimated the variability of the first mode. The standard deviations of the dominant modes of variability in the three models differ from observations by less than a factor of two, and one model (HadCM2) has similar or more variability than the observations in all leading modes. In general, one would expect to obtain conservative detection and attribution results when natural variability is estimated with such a model. One should also expect control simulations to be less variable than observations because they do not contain externally forced variability. Hegerl *et al.* (2000) used common EOFS to compare 50-year June-July-August (JJA) trends of surface temperature in ECHAM3 and HadCM2. Standard deviation differences between models

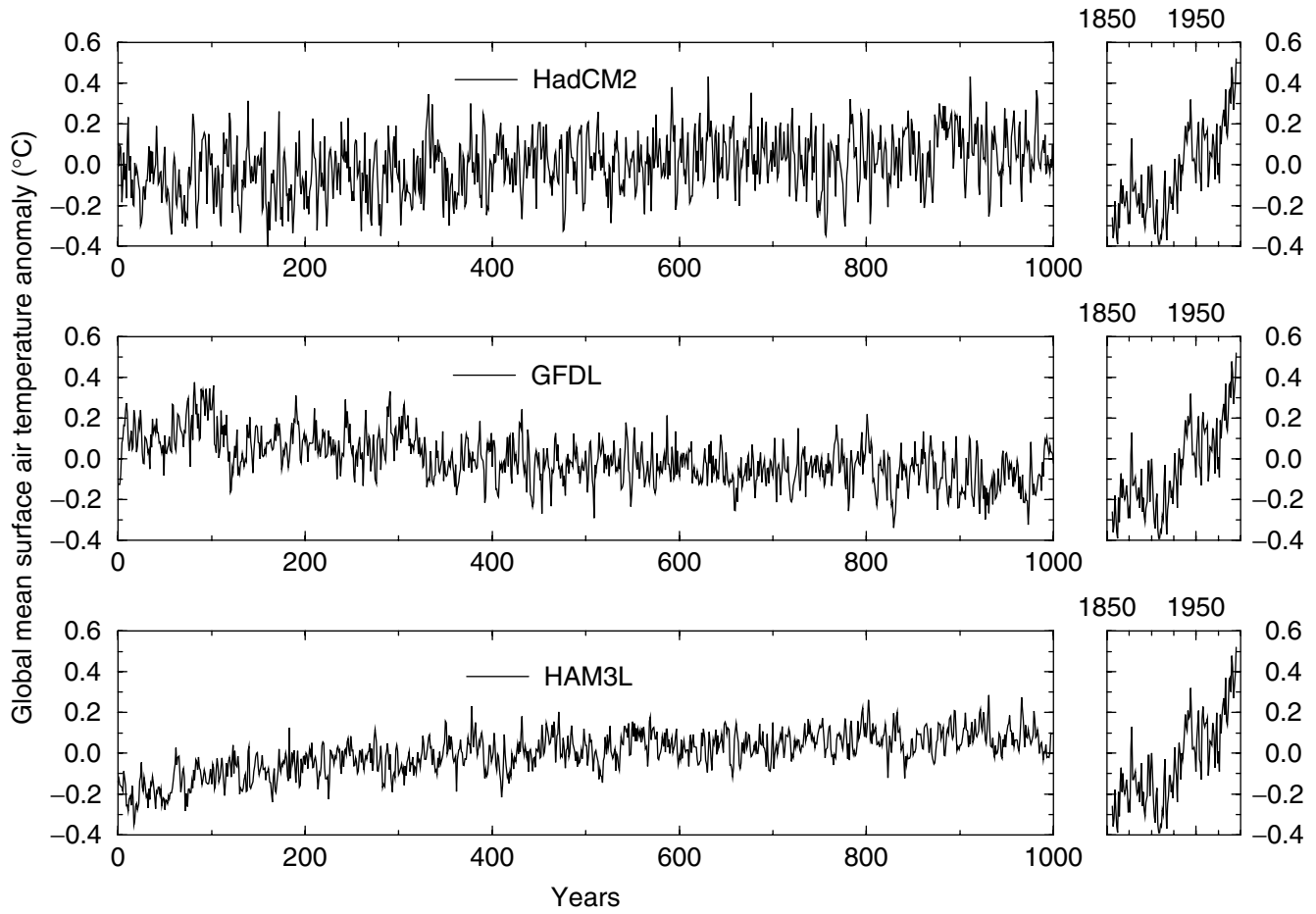

Figure 12.1: Global mean surface air temperature anomalies from 1,000-year control simulations with three different climate models, HadCM2, GFDL R15 and ECHAM3/LSG (labelled HAM3L), compared to the recent instrumental record (Stouffer *et al.*, 2000). No model control simulation shows a trend in surface air temperature as large as the observed trend. If internal variability is correct in these models, the recent warming is likely not due to variability produced within the climate system alone.

were marginally larger on the 50-year time-scale (less than a factor of 2.5). Comparison with direct observations cannot be made on this time-scale because the instrumental record is too short.

Variability of the free atmosphere

Gillett *et al.* (2000a) compared model-simulated variability in the free atmosphere with that of detrended radiosonde data. They found general agreement except in the stratosphere, where present climate models tend to underestimate variability on all time-scales and, in particular, do not reproduce modes of variability such as the quasi-biennial oscillation (QBO). On decadal time-scales, the model simulated less variability than observed in some aspects of the vertical patterns important for the detection of anthropogenic climate change. The discrepancy is partially resolved by the inclusion of anthropogenic (greenhouse gas, sulphate and stratospheric ozone) forcing in the model. However, the authors also find evidence that solar forcing plays a significant role on decadal time-scales, indicating that this should be taken into account in future detection studies based on changes in the free atmosphere (see also discussion in Chapter 6 and Section 12.2.3.1 below).

Comparison of model and palaeoclimatic estimates of variability

Comparisons between the variability in palaeo-reconstructions and climate model data have shown mixed results to date. Barnett *et al.* (1996) compared the spatial structure of climate variability of coupled climate models and proxy time-series for (mostly summer) decadal temperature (Jones *et al.*, 1998). They found that the model-simulated amplitude of the dominant proxy mode of variation is substantially less than that estimated from the proxy data. However, choosing the EOFs of the palaeo-data as the basis for comparison will maximise the variance in the palaeo-data and not the models, and so bias the model amplitudes downwards. The neglect of naturally forced climate variability in the models might also be responsible for part of the discrepancy noted in Barnett *et al.* (1996) (see also Jones *et al.*, 1998). The limitations of the temperature reconstructions (see Chapter 2, Figure 2.21), including for example the issue of how to relate site-specific palaeo-data to large-scale variations, may also contribute to this discrepancy. Collins *et al.* (2000) compared the standard deviation of large-scale Northern Hemisphere averages in a model control simulation and in tree-ring-based proxy data for the last 600 years on decadal time-scales. They found a

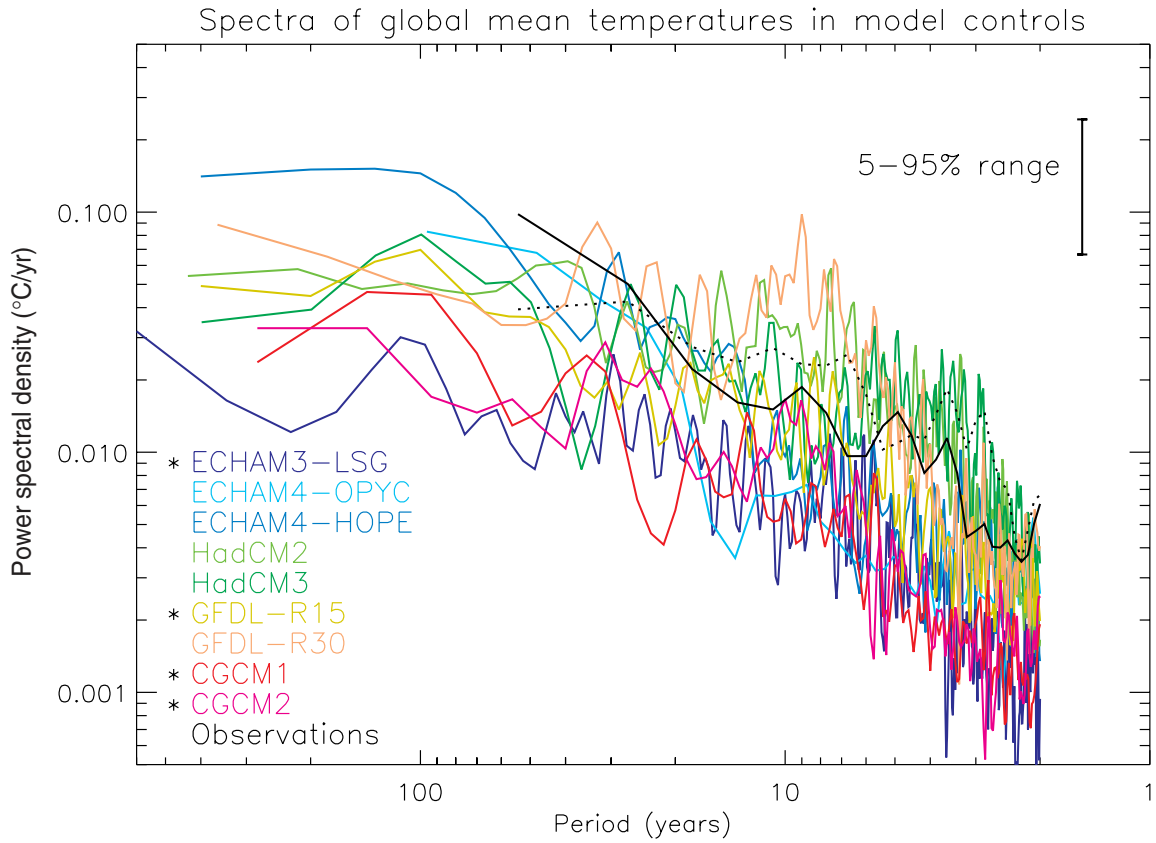

Figure 12.2: Coloured lines: power spectra of global mean temperatures in the unforced control integrations that are used to provide estimates of internal climate variability in Figure 12.12. All series were linearly detrended prior to analysis, and spectra computed using a standard Tukey window with the window width (maximum lag used in the estimate) set to one-fifth of the series length, giving each spectral estimate the same uncertainty range, as shown (see, e.g., Priestley, 1981). The first 300 years were omitted from ECHAM3-LSG, CGCM1 and CGCM2 models as potentially trend-contaminated. Solid black line: spectrum of observed global mean temperatures (Jones *et al.*, 2001) over the period 1861 to 1998 after removing a best-fit linear trend. This estimate is unreliable on inter-decadal time-scales because of the likely impact of external forcing on the observed series and the negative bias introduced by the detrending. Dotted black line: spectrum of observed global mean temperatures after removing an independent estimate of the externally forced response provided by the ensemble mean of a coupled model simulation (Stott *et al.*, 2000b, and Figure 12.7c). This estimate will be contaminated by uncertainty in the model-simulated forced response, together with observation noise and sampling error. However, unlike the detrending procedure, all of these introduce a positive (upward) bias in the resulting estimate of the observed spectrum. The dotted line therefore provides a conservative (high) estimate of observed internal variability at all frequencies. Asterisks indicate models whose variability is significantly less than observed variability on 10 to 60 year time-scales after removing either a best-fit linear trend or an independent estimate of the forced response from the observed series. Significance is based on an F-test on the ratio observed/model mean power over this frequency interval and quoted at the 5% level. Power spectral density (PSD) is defined such that unit-variance uncorrelated noise would have an expected PSD of unity (see Allen *et al.*, 2000a, for details). Note that different normalisation conventions can lead to different values, which appear as a constant offset up or down on the logarithmic vertical scale used here. Differences between the spectra shown here and the corresponding figure in Stouffer *et al.* (2000) shown in Chapter 8, Figure 8.18 are due to the use here of a longer (1861 to 2000) observational record, as opposed to 1881 to 1991 in Figure 8.18. That figure also shows 2.5 to 97.5% uncertainty ranges, while for consistency with other figures in this chapter, the 5 to 95% range is displayed here.

factor of less than two difference between model and data if the tree-ring data are calibrated such that low-frequency variability is better retained than in standard methods (Briffa *et al.*, 2000). It is likely that at least part of this discrepancy can be resolved if natural forcings are included in the model simulation. Crowley (2000) found that 41 to 69% of the variance in decadally smoothed Northern Hemisphere mean surface temperature reconstructions could be externally forced (using data from Mann *et al.* (1998) and Crowley and Lowery (2000)). The residual variability in the reconstructions, after subtracting estimates of volcanic and solar-forced signals, showed no significant difference in variability on decadal and multi-decadal time-scales from three long coupled model control simulations. In summary, while there is substantial uncertainty in comparisons between long-term palaeo-records of surface temperature and model estimates of multi-decadal variability, there is no clear evidence of a serious discrepancy.

Summary

These findings emphasise that there is still considerable uncertainty in the magnitude of internal climate variability. Various approaches are used in detection and attribution studies to account for this uncertainty. Some studies use data from a number of coupled climate model control simulations (Santer *et al.*, 1995; Hegerl *et al.*, 1996, 1997, North and Stevens, 1998) and choose the most conservative result. In other studies, the estimate of internal variance is inflated to assess the sensitivity of detection and attribution results to the level of internal variance (Santer *et al.*, 1996a, Tett *et al.*, 1999; Stott *et al.*, 2001). Some authors also augment model-derived estimates of natural variability with estimates from observations (Hegerl *et al.*, 1996). A method for checking the consistency between the residual variability in the observations after removal of externally forced signals (see equation A12.1.1, Appendix 12.1) and the natural internal variability estimated from control simulations is also available (e.g., Allen and Tett, 1999). Results indicate that, on the scales considered, there is no evidence for a serious inconsistency between the variability in models used for optimal fingerprint studies and observations (Allen and Tett, 1999; Tett *et al.*, 1999; Hegerl *et al.*, 2000, 2001; Stott *et al.*, 2001). The use of this test and the use of internal variability from the models with the greatest variability increases confidence in conclusions derived from optimal detection studies.

12.2.3 Climate Forcings and Responses

The global mean change in radiative forcing (see Chapter 6) since the pre-industrial period may give an indication of the relative importance of the different external factors influencing climate over the last century. The temporal and spatial variation of the forcing from different sources may help to identify the effects of individual factors that have contributed to recent climate change.

The need for climate models

To detect the response to anthropogenic or natural climate forcing in observations, we require estimates of the expected space-time pattern of the response. The influences of natural and anthropogenic forcing on the observed climate can be separated only if the spatial and temporal variation of each component is known. These patterns cannot be determined from the observed instrumental record because variations due to different external forcings are superimposed on each other and on internal climate variations. Hence climate models are usually used to estimate the contribution from each factor. The models range from simpler energy balance models to the most complex coupled atmosphere-ocean general circulation models that simulate the spatial and temporal variations of many climatic parameters (Chapter 8).

The models used

Energy balance models (EBMs) simulate the effect of radiative climate forcing on surface temperature. Climate sensitivity is included as an adjustable parameter. These models are computationally inexpensive and produce noise-free estimates of the climate signal. However, EBMs cannot represent dynamical components of the climate signal, generally cannot simulate variables other than surface temperature, and may omit some of the important feedback processes that are accounted for in more complex models. Most detection and attribution approaches therefore apply signals estimated from coupled Atmosphere Ocean General Circulation Models (AOGCMs) or atmospheric General Circulation Models (GCMs) coupled to mixed-layer ocean models. Forced simulations with such models contain both the climate response to external forcing and superimposed internal climate variability. Estimates of the climate response

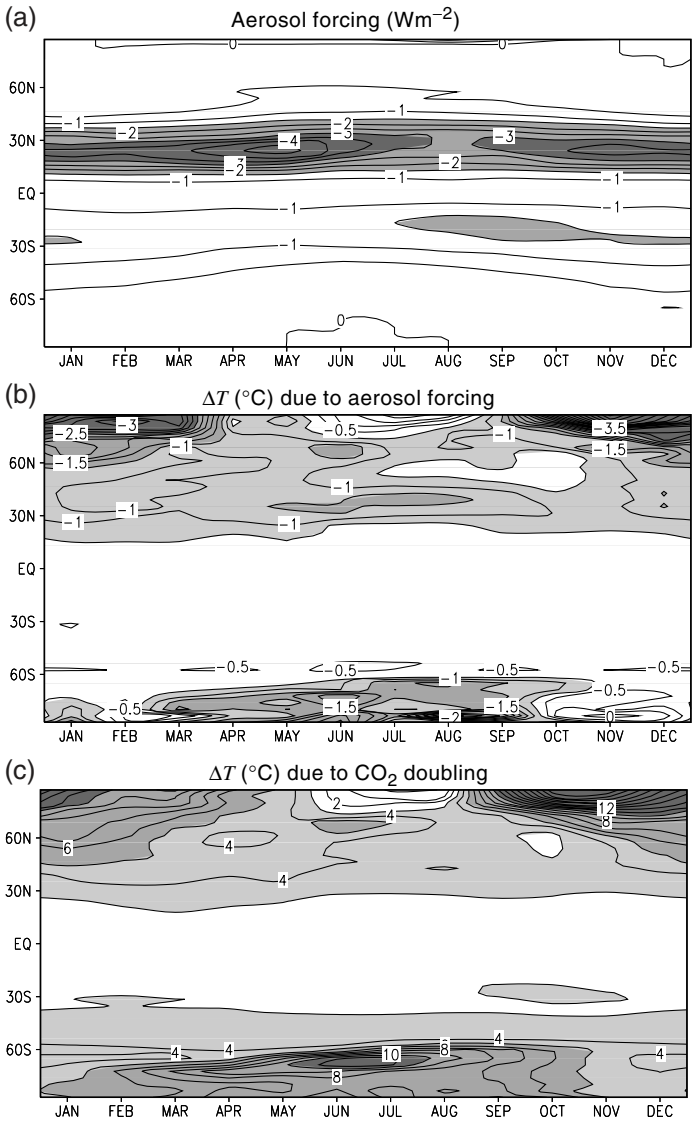

Figure 12.3: Latitude-month plot of radiative forcing and model equilibrium response for surface temperature. (a) Radiative forcing (Wm^{-2}) due to increased sulphate aerosol loading at the time of CO_2 doubling. (b) Change in temperature due to the increase in aerosol loading. (c) Change in temperature due to CO_2 doubling. Note that the patterns of radiative forcing and temperature response are quite different in (a) and (b), but that the patterns of large-scale temperature responses to different forcings are similar in (b) and (c). The experiments used to compute these fields are described by Reader and Boer (1998).

computed from model output will necessarily contain at least some noise from this source, although this can be reduced by the use of ensemble simulations. Note that different models can produce quite different patterns of response to a given forcing due to differences in the representation of feedbacks arising from changes in cloud (in particular), sea ice and land surface processes.

The relationship between patterns of forcing and response

There are several reasons why one should not expect a simple relationship between the patterns of radiative forcing and temperature response. First, strong feedbacks such as those due to water vapour and sea ice tend to reduce the difference in the temperature response due to different forcings. This is illustrated graphically by the response to the simplified aerosol forcing used in early studies. The magnitude of the model response is largest over the Arctic in winter even though the forcing is small, largely due to ice-albedo feedback. The large-scale patterns of change and their temporal variations are similar, but of opposite sign, to that obtained in greenhouse gas experiments (Figure 12.3, see also Mitchell *et al.*, 1995a). Second, atmospheric circulation tends to smooth out temperature gradients and reduce the differences in response patterns. Similarly, the thermal inertia of the climate system tends to reduce the amplitude of short-term fluctuations in forcing. Third, changes in radiative forcing are more effective if they act near the surface, where cooling to space is restricted, than at upper levels, and in high latitudes, where there are stronger positive feedbacks than at low latitudes (Hansen *et al.*, 1997a).

In practice, the response of a given model to different forcing patterns can be quite similar (Hegerl *et al.*, 1997; North and Stevens, 1998; Tett *et al.*, 1999). Similar signal patterns (a condition often referred to as "degeneracy") can be difficult to distinguish from one another. Tett *et al.* (1999) find substantial degeneracy between greenhouse gas, sulphate, volcanic and solar patterns they used in their detection study using HadCM2. On the other hand, the greenhouse gas and aerosol patterns generated by ECHAM3 LSG (Hegerl *et al.*, 2000) are more clearly separable, in part because the patterns are more distinct, and in part because the aerosol response pattern correlates less well with ECHAM3 LSG's patterns of internal variability. The vertical patterns of temperature change due to greenhouse gas and stratospheric ozone forcing are less degenerate than the horizontal patterns.

Summary

Different models may give quite different patterns of response for the same forcing, but an individual model may give a surprisingly similar response for different forcings. The first point means that attribution studies may give different results when using signals generated from different models. The second point means that it may be more difficult to distinguish between the response to different factors than one might expect, given the differences in radiative forcing.

12.2.3.1 Natural climate forcing

Since the SAR, there has been much progress in attempting to understand the climate response to fluctuations in solar luminosity and to volcanism. These appear to be the most important among a broad range of natural external climate forcings at decadal and centennial time-scales. The mechanisms of these forcings, their reconstruction and associated uncertainties are described in Chapter 6, and further details of the simulated responses are given in Chapter 8, Section 8.6.3.

Volcanic forcing

The radiative forcing due to volcanic aerosols from the recent El Chichon and Mt. Pinatubo eruptions has been estimated from satellite and other data to be -3 Wm^{-2} (peak forcing; after Hansen *et al.*, 1998). The forcing associated with historic eruptions before the satellite era is more uncertain. Sato *et al.* (1993) estimated aerosol optical depth from ground-based observations over the last century (see also Stothers, 1996; Grieser and Schoenwiese, 1999). Prior to that, reconstructions have been based on various sources of data (ice cores, historic documents etc.; see Lamb, 1970; Simkin *et al.*, 1981; Robock and Free, 1995; Crowley and Kim, 1999; Free and Robock, 1999). There is uncertainty of about a factor of two in the peak forcing in reconstructions of historic volcanic forcing in the pre-satellite era (see Chapter 6).

Solar forcing

The variation of solar irradiance with the 11-year sunspot cycle has been assessed with some accuracy over more than 20 years, although measurements of the magnitude of modulations of solar irradiance between solar cycles are less certain (see Chapter 6). The estimation of earlier solar irradiance fluctuations, although based on physical mechanisms, is indirect. Hence our confidence in the range of solar radiation on century time-scales is low, and confidence in the details of the time-history is even lower (Harrison and Shine, 1999; Chapter 6). Several recent reconstructions estimate that variations in solar irradiance give rise to a forcing at the Earth's surface of about 0.6 to 0.7 Wm^{-2} since the Maunder Minimum and about half this over the 20th century (see Chapter 6, Figure 6.5; Hoyt and Schatten, 1993; Lean *et al.*, 1995; Lean, 1997; Froehlich and Lean, 1998; Lockwood and Stamper, 1999). This is larger than the 0.2 Wm^{-2} modulation of the 11-year solar cycle measured from satellites. (Note that we discuss here the forcing at the Earth's surface, which is smaller than that at the top of the atmosphere, due to the Earth's geometry and albedo.) The reconstructions of Lean *et al.* (1995) and Hoyt and Schatten (1993), which have been used in GCM detection studies, vary in amplitude and phase. Chapter 6, Figure 6.8 shows time-series of reconstructed solar and volcanic forcing since the late 18th century. All reconstructions indicate that the direct effect of variations in solar forcing over the 20th century was about 20 to 25% of the change in forcing due to increases in the well-mixed greenhouse gases (see Chapter 6).

Reconstructions of climate forcing in the 20th century indicate that the net natural climate forcing probably increased during the first half of the 20th century, due to a period of low volcanism coinciding with a small increase in solar forcing. Recent decades show negative natural forcing due to increasing volcanism, which overwhelms the direct effect, if real, of a small increase in solar radiation (see Chapter 6, Table 6.13).

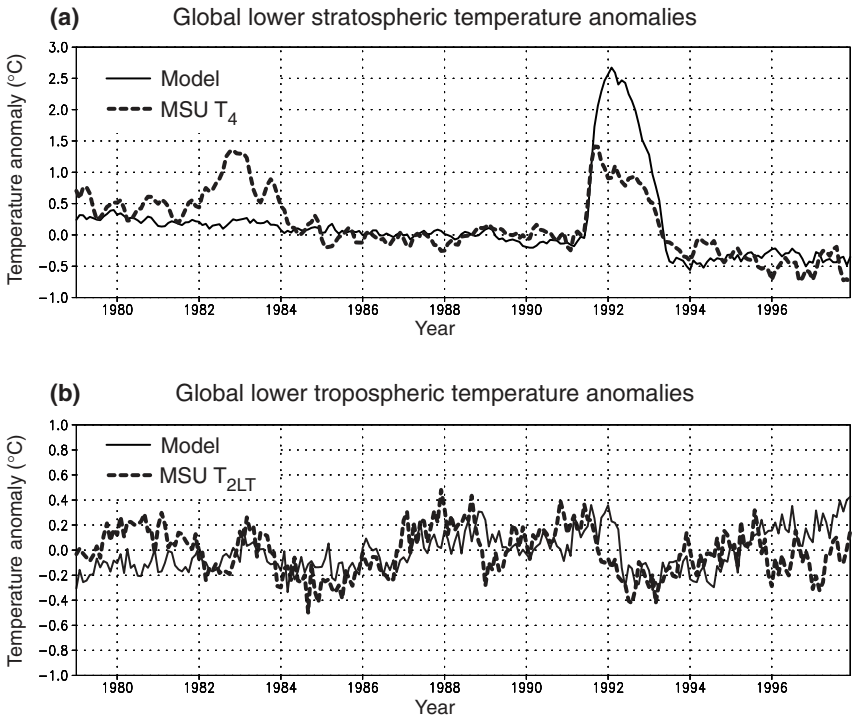

Figure 12.4: (a) Observed microwave sounding unit (MSU) global mean temperature in the lower stratosphere, shown as dashed line, for channel 4 for the period 1979 to 97 compared with the average of several atmosphere-ocean GCM simulations starting with different atmospheric conditions in 1979 (solid line). The simulations have been forced with increasing greenhouse gases, direct and indirect forcing by sulphate aerosols and tropospheric ozone forcing, and Mt. Pinatubo volcanic aerosol and stratospheric ozone variations. The model simulation does not include volcanic forcing due to El Chichon in 1982, so it does not show stratospheric warming then. (b) As for (a), except for 2LT temperature retrievals in the lower troposphere. Note the steady response in the stratosphere, apart from the volcanic warm periods, and the large variability in the lower troposphere (from Bengtsson *et al.*, 1999).

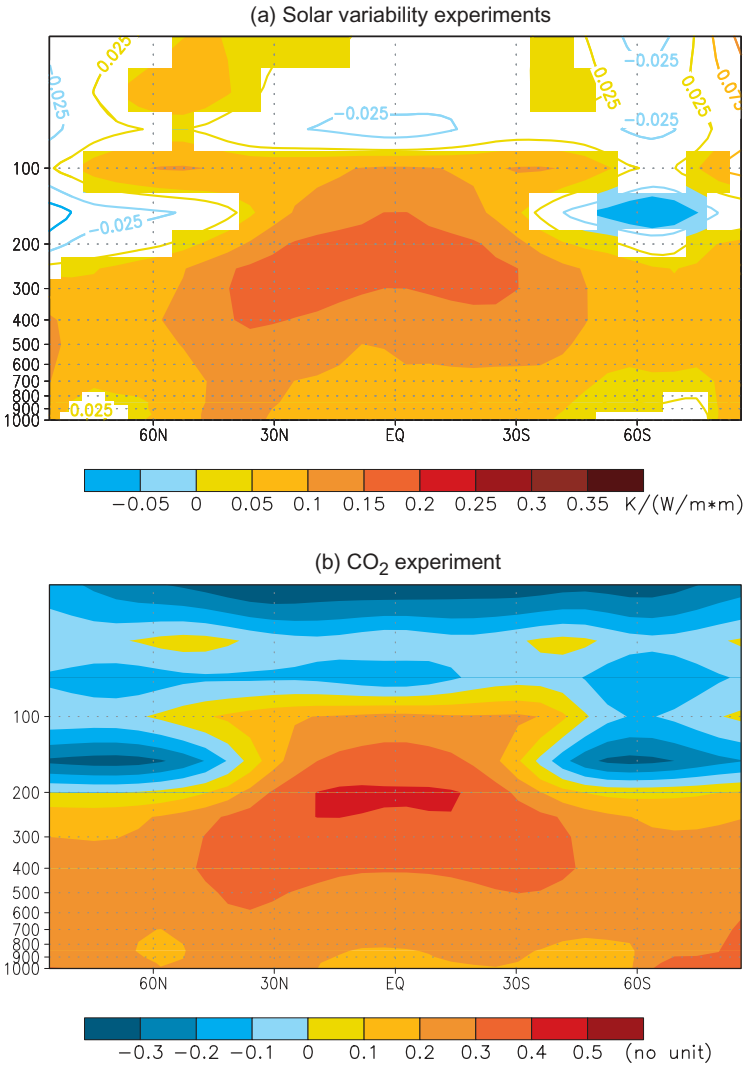

Figure 12.5: (a) Response (covariance, normalised by the variance of radiance fluctuations) of zonally averaged annual mean atmospheric temperature to solar forcing for two simulations with ECHAM3/LSG. Coloured regions indicate locally significant response to solar forcing. (b) Zonal mean of the first EOF of greenhouse gas-induced temperature change simulated with the same model (from Cubasch *et al.*, 1997). This indicates that for ECHAM3/LSG, the zonal mean temperature response to greenhouse gas and solar forcing are quite different in the stratosphere but similar in the troposphere.

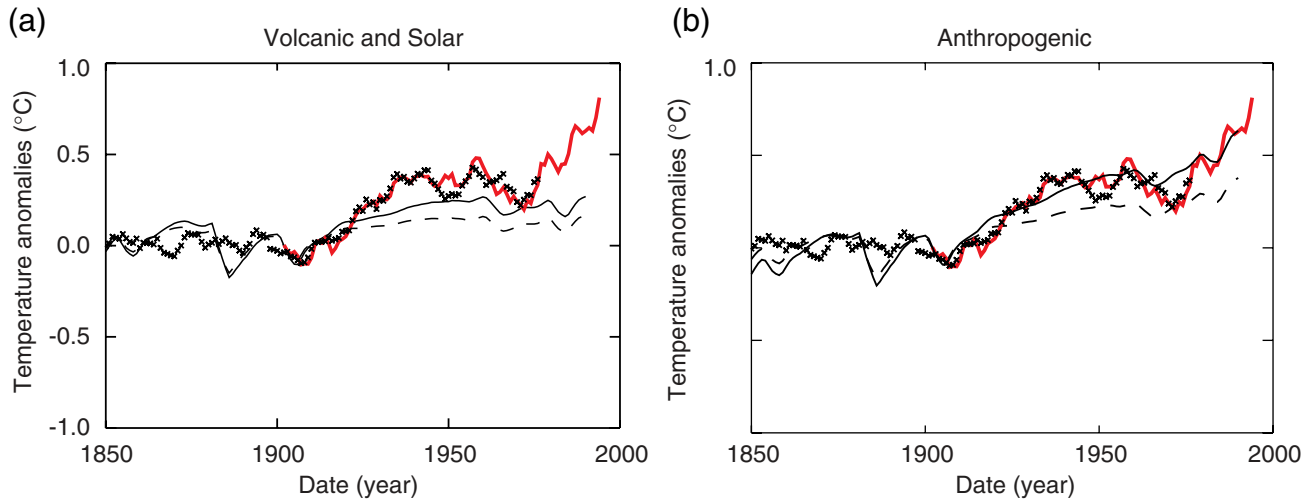

Figure 12.6: (a) Five-year running mean Northern Hemisphere temperature anomalies since 1850 (relative to the 1880 to 1920 mean) from an energy-balance model forced by Dust Veil volcanic index and Lean *et al.* (1995) solar index (see Free and Robock, 1999). Two values of climate sensitivity to doubling CO_2 were used; 3.0°C (thin solid line), and 1.5°C (dashed line). Also shown are the instrumental record (thick red line) and a reconstruction of temperatures from proxy records (crosses, from Mann *et al.*, 1998). The size of both the forcings and the proxy temperature variations are subject to large uncertainties. Note that the Mann temperatures do not include data after 1980 and do not show the large observed warming then. (b) As for (a) but for simulations with volcanic, solar and anthropogenic forcing (greenhouse gases and direct and indirect effects of tropospheric aerosols). The net anthropogenic forcing at 1990 relative to 1760 was 1.3 Wm^{-2}, including a net cooling of 1.3 Wm^{-2} due to aerosol effects.

12.2.3.2 Climatic response to natural forcing

Response to volcanic forcing

The climate response to several recent volcanic eruptions has been studied in observations and simulations with atmospheric GCMs (e.g., Robock and Mao, 1992, 1995; Graf *et al.*, 1996; Hansen *et al.*, 1996; Kelly *et al.*, 1996; Mao and Robock, 1998; Kirchner *et al.*, 1999). The stratosphere warms and the annual mean surface and tropospheric temperature decreases during the two to three years following a major volcanic eruption. A simulation incorporating the effects of the Mt. Pinatubo eruption and observed changes in stratospheric ozone in addition to anthropogenic forcing approximately reproduces the observed stratospheric variations (Figure 12.4; Bengtsson *et al.*, 1999). It shows stratospheric warming after the volcanic eruption, superimposed on a long-term cooling trend. Although the surface temperature response in the Northern Hemisphere warm season following a volcanic eruption is dominated by global scale radiative cooling, some models simulate local warming over Eurasia and North America in the cold season due to changes in circulation (e.g., Graf *et al.*, 1996; Kirchner *et al.*, 1999). Variability from other sources makes assessment of the observed climate response difficult, particularly as the two most recent volcanic eruptions (Mt. Pinatubo and El Chichon) occurred in El Niño-Southern Oscillation (ENSO) warm years. Simulations with simple models (Bertrand *et al.*, 1999; Crowley and Kim, 1999; Grieser and Schoenwiese, 2001) and AOGCMs (Tett *et al.*, 1999; Stott *et al.*, 2001) produce a small decadal mean cooling in the 1980s and 1990s due to several volcanic eruptions in those decades. Some simulations also produce global warming in the early 20th century as a recovery from a series of strong eruptions around the turn of the 20th century. It is unclear whether such a long-term response is realistic.

Response to solar forcing

Since the SAR, there have been new modelling and observational studies on the climate effects of variations in solar irradiance. The surface temperature response to the 11-year cycle is found to be small (e.g., Cubasch *et al.*, 1997; White *et al.*, 1997; North and Stevens, 1998; Crowley and Kim, 1999; Free and Robock, 1999). Low-frequency solar variability over the last few hundred years gives a stronger surface temperature response (Cubasch *et al.*, 1997; Drijfhout *et al.*, 1999; Rind *et al.*, 1999; Tett *et al.*, 1999; Stott *et al.*, 2001). Model results show cooling circa 1800 due to the hypothesised solar forcing minimum and some warming in the 20th century, particularly in the early 20th century. Time-dependent experiments produce a global mean warming of 0.2 to 0.5°C in response to the estimated 0.7 Wm^{-2} change of solar radiative forcing from the Maunder Minimum to the present (e.g., Lean and Rind, 1998, Crowley and Kim, 1999).

Ozone changes in the Earth's atmosphere caused by the 11-year solar cycle could affect the temperature response in the free atmosphere. A relation between 30 hPa geopotential and a solar index has been shown over nearly four solar cycles by Labitzke and van Loon (1997). Van Loon and Shea (1999, 2000) found a related connection between upper to middle tropospheric temperature and a solar index over the last 40 years, which is particularly strong in July and August. Variations in ozone forcing related to the solar cycle may also affect surface temperature via radiative and dynamical processes (see discussion in Chapter 6; Haigh, 1999; Shindell *et al.*, 1999, 2001), but observational evidence remains ambiguous (e.g., van Loon and Shea, 2000). The assessment of ozone-related Sun-climate interactions is uncertain as a result of the lack of long-term, reliable observations. This makes it difficult to separate effects of volcanic eruptions and solar forcing on ozone. There has also been

speculation that the solar cycle might influence cloudiness and hence surface temperature through cosmic rays (e.g., Svensmark and Friis-Christensen, 1997; Svensmark, 1998). The latter effect is difficult to assess due to limitations in observed data and the shortness of the correlated time-series.

As discussed earlier in Section 12.2.3, differences between the response to solar and greenhouse gas forcings would make it easier to distinguish the climate response to either forcing. However, the spatial response pattern of surface air temperature to an increase in solar forcing was found to be quite similar to that in response to increases in greenhouse gas forcing (e.g., Cubasch *et al.*, 1997). The vertical response to solar forcing (Figure 12.5) includes warming throughout most of the troposphere. The response in the stratosphere is small and possibly locally negative, but less so than with greenhouse gas forcing, which gives tropospheric warming and strong stratospheric cooling. The dependence of solar forcing on wavelength and the effect of solar fluctuations on ozone were generally omitted in these simulations. Hence, the conclusion that changes in solar forcing have little effect on large-scale stratospheric temperatures remains tentative.

The different time-histories of the solar and anthropogenic forcing should help to distinguish between the responses. All reconstructions suggest a rise in solar forcing during the early decades of the 20th century with little change on inter-decadal time-scales in the second half. Such a forcing history is unlikely to explain the recent acceleration in surface warming, even if amplified by some unknown feedback mechanism.

Studies linking forcing and response through correlation techniques

A number of authors have correlated solar forcing and volcanic forcing with hemispheric and global mean temperature time-series from instrumental and palaeo-data (Lean *et al.*, 1995; Briffa *et al.*, 1998; Lean and Rind, 1998; Mann *et al.*, 1998) and found statistically significant correlations. Others have compared the simulated response, rather than the forcing, with observations and found qualitative evidence for the influence of natural forcing on climate (e.g., Crowley and Kim, 1996; Overpeck *et al.*, 1997; Wigley *et al.*, 1997; Bertrand *et al.*, 1999) or significant correlations (e.g., Schönwiese *et al.*, 1997; Free and Robock, 1999; Grieser and Schönwiese, 2001). Such a comparison is preferable as the climate response may differ substantially from the forcing. The results suggest that global scale low-frequency temperature variations are influenced by variations in known natural forcings. However, these results show that the late 20th century surface warming cannot be well represented by natural forcing (solar and volcanic individually or in combination) alone (for example Figures 12.6, 12.7; Lean and Rind, 1998; Free and Robock, 1999; Crowley, 2000; Tett *et al.*, 2000; Thejll and Lassen, 2000).

Mann *et al.* (1998, 2000) used a multi-correlation technique and found significant correlations with solar and, less so, with the volcanic forcing over parts of the palaeo-record. The authors concluded that natural forcings have been important on decadal-to-century time-scales, but that the dramatic warming of the 20th century correlates best and very significantly with greenhouse gas forcing. The use of multiple correlations avoids the possibility of spuriously high correlations due to the common trend in the solar and temperature time-series (Laut and Gunderman, 1998). Attempts to estimate the contributions of natural and anthropogenic forcing to 20th century temperature evolution simultaneously are discussed in Section 12.4.

Summary

We conclude that climate forcing by changes in solar irradiance and volcanism have likely caused fluctuations in global and hemispheric mean temperatures. Qualitative comparisons suggest that natural forcings produce too little warming to fully explain the 20th century warming (see Figure 12.7). The indication that the trend in net solar plus volcanic forcing has been negative in recent decades (see Chapter 6) makes it unlikely that natural forcing can explain the increased rate of global warming since the middle of the 20th century. This question will be revisited in a more quantitative manner in Section 12.4.

12.2.3.3 Anthropogenic forcing

In the SAR (Santer *et al.*, 1996c), pattern-based detection studies took into account changes in well-mixed greenhouse gases (often represented by an equivalent increase in CO_2), the direct effect of sulphate aerosols (usually represented by a seasonally constant change in surface albedo) and the influence of changes in stratospheric ozone. Recent studies have also included the effect of increases in tropospheric ozone and a representation of the indirect effect of sulphate aerosols on cloud albedo. Many models now include the individual greenhouse gases (as opposed to a CO_2 equivalent) and include an interactive sulphur cycle and an explicit treatment of scattering by aerosols (as opposed to using prescribed changes in surface albedo). Note that representation of the sulphur cycle in climate models is not as detailed as in the offline sulphur cycle models reported in Chapter 5. Detection and attribution studies to date have not taken into account other forcing agents discussed in Chapter 6, including biogenic aerosols, black carbon, mineral dust and changes in land use. Estimates of the spatial and temporal variation of these factors have not been available long enough to have been included in model simulations suitable for detection studies. In general, the neglected forcings are estimated to be small globally and there may be a large degree of cancellation in their global mean effect (see Chapter 6, Figure 6.8). It is less clear that the individual forcings will cancel regionally. As discussed in Section 12.4, this will add further uncertainty in the attribution of the response to individual forcing agents, although we believe it is unlikely to affect our conclusions about the effects of increases in well-mixed greenhouse gases on very large spatial scales.

Global mean anthropogenic forcing

The largest and most certain change in radiative forcing since the pre-industrial period is an increase of about 2.3 Wm^{-2} due to an increase in well-mixed greenhouse gases (Chapter 6, Figure 6.8 and Table 6.1). Radiative forcing here is taken to be the net downward radiative flux at the tropopause (see Chapter 6). Smaller, less certain contributions have come from increases in tropospheric ozone (about 0.3 Wm^{-2}), the direct effect of increases in sulphate aerosols (about –0.4 Wm^{-2}) and decreases in

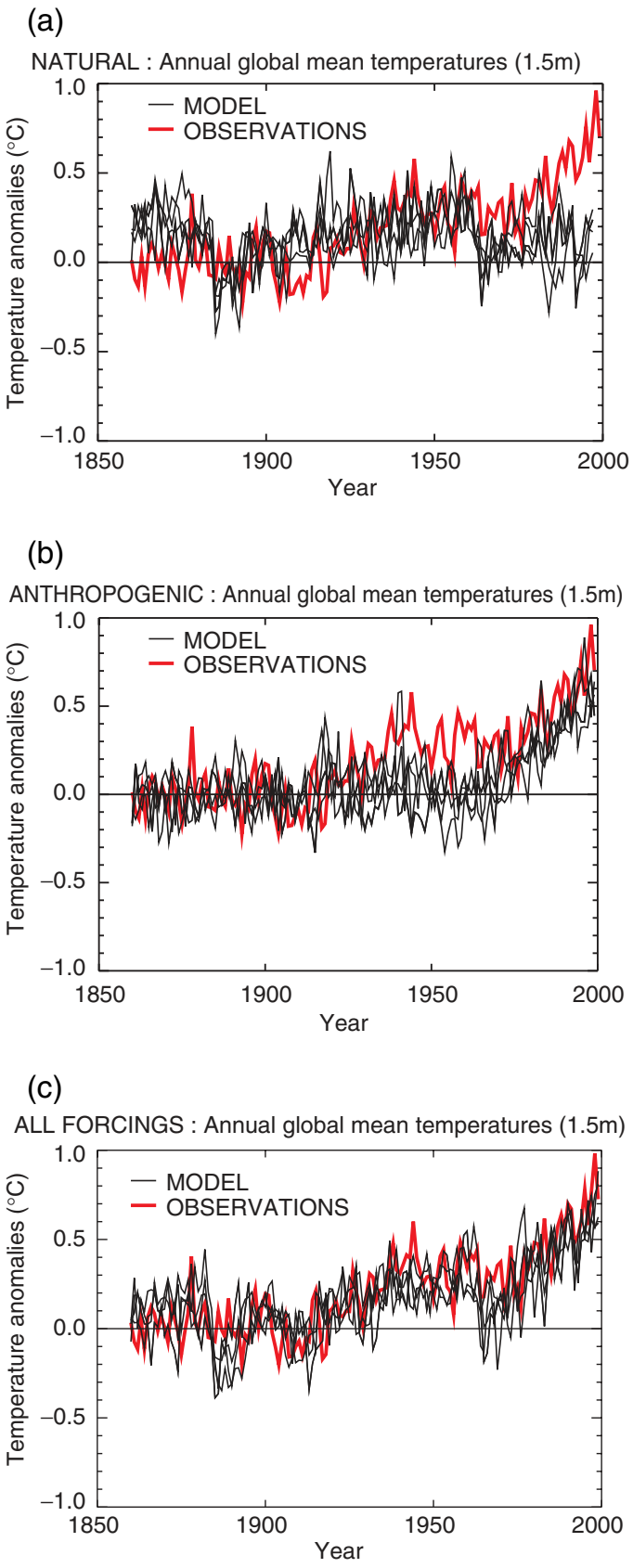

Figure 12.7: Global mean surface temperature anomalies relative to the 1880 to 1920 mean from the instrumental record compared with ensembles of four simulations with a coupled ocean-atmosphere climate model (from Stott *et al.*, 2000b; Tett *et al.*, 2000) forced (a) with solar and volcanic forcing only, (b) with anthropogenic forcing including well mixed greenhouse gases, changes in stratospheric and tropospheric ozone and the direct and indirect effects of sulphate aerosols, and (c) with all forcings, both natural and anthropogenic. The thick line shows the instrumental data while the thin lines show the individual model simulations in the ensemble of four members. Note that the data are annual mean values. The model data are only sampled at the locations where there are observations. The changes in sulphate aerosol are calculated interactively, and changes in tropospheric ozone were calculated offline using a chemical transport model. Changes in cloud brightness (the first indirect effect of sulphate aerosols) were calculated by an offline simulation (Jones *et al.*, 1999) and included in the model. The changes in stratospheric ozone were based on observations. The volcanic forcing was based on the data of Sato *et al.* (1993) and the solar forcing on Lean *et al.* (1995), updated to 1997. The net anthropogenic forcing at 1990 was 1.0 Wm^{-2} including a net cooling of 1.0 Wm^{-2} due to sulphate aerosols. The net natural forcing for 1990 relative to 1860 was 0.5 Wm^{-2}, and for 1992 was a net cooling of 2.0 Wm^{-2} due to Mt. Pinatubo. Other models forced with anthropogenic forcing give similar results to those shown in b (see Chapter 8, Section 8.6.1, Figure 8.15; Hasselmann *et al.*, 1995; Mitchell *et al.*, 1995b; Haywood *et al.*, 1997; Boer *et al.*, 2000a; Knutson *et al.*, 2000).

stratospheric ozone (about –0.2 Wm^{-2}). There is a very uncertain and possibly large negative contribution from the indirect effects of aerosols. Other factors such as that due to increases in fossil fuel organic carbon, aviation, changes in land use and mineral dust are very poorly known and not yet incorporated into simulations used in formal detection studies. Their contribution is generally believed to be small relative to well-mixed greenhouse gases, though they could be of importance on regional scales.

In order to assess temperature changes over the last two decades, Hansen *et al.* (1997b) estimated the net radiative forcing due to changes in greenhouse gases (including ozone), solar variations and stratospheric aerosols from 1979 to 1995 from the best available measurements of the forcing agents. The negative forcing due to volcanoes and decreases in stratospheric ozone compensated for a substantial fraction of the increase in greenhouse gas forcing in this period (see Chapter 6, Table 6.13).

Patterns of anthropogenic forcing

Many of the new detection studies take into account the spatial variation of climate response, which will depend to some extent on the pattern of forcing (see also Section 12.2.3). The patterns of forcing vary considerably (see Chapter 6, Figure 6.7). The magnitude of the overall forcing due to increases in well-mixed greenhouse gases varies from almost 3 Wm^{-2} in the sub-tropics to about 1 Wm^{-2} around the poles. The warming due to increases in tropospheric ozone is mainly in the tropics and northern sub-tropics. Decreases in stratospheric ozone observed over the last couple of decades have produced negative forcing of up to about 0.5 Wm^{-2} around Antarctica. The direct effect of sulphate aerosols predominates in the Northern Hemisphere industrial regions where the negative forcing may exceed 2 Wm^{-2} locally.

Temporal variations in forcing

Some of the new detection studies take into account the temporal as well as spatial variations in climate response (see Section 12.4.3.3). Hence the temporal variation of forcing is also important. The forcing due to well-mixed greenhouse gases (and tropospheric ozone) has increased slowly in the first half of the century, and much more rapidly in recent decades (Chapter 6, Figure 6.8). Contributions from other factors are smaller and more uncertain. Sulphur emissions increased steadily until World War I, then levelled off, and increased more rapidly in the 1950s, though not as fast as greenhouse gas emissions. This is reflected in estimates of the direct radiative effect of increases in sulphate aerosols. Given the almost monotonic increase in greenhouse gas forcing in recent decades, this means the ratio of sulphate to greenhouse gas forcing has probably been decreasing since about 1960 (see Chapter 6, Figure 6.8). This should be borne in mind when considering studies that attempt to detect a response to sulphate aerosols. The decreases in stratospheric ozone have been confined to the last two to three decades.

Uncertainties in aerosol forcing

Some recent studies have incorporated the indirect effect of increases in tropospheric aerosols. This is very poorly understood (see Chapter 6), but contributes a negative forcing which could be negligible or exceed 2 Wm^{-2}. The upper limit would imply very little change in net global mean anthropogenic forcing over the last century although there would still be a quite strong spatial pattern of heating and cooling which may be incompatible with recent observed changes (see, for example, Mitchell *et al.*, 1995a). A negligible indirect sulphate effect would imply a large increase in anthropogenic forcing in the last few decades. There is also a large range in the inter-hemispheric asymmetry in the different estimates of forcing (see Chapter 6, Table 6.4). Given this high level of uncertainty, studies using simulations including estimates of indirect sulphate forcing should be regarded as preliminary.

Summary

Well-mixed greenhouse gases make the largest and best-known contribution to changes in radiative forcing over the last century or so. There remains a large uncertainty in the magnitude and patterns of other factors, particularly those associated with the indirect effects of sulphate aerosol.

12.2.3.4 Climatic response to anthropogenic forcing

We now consider the simulated response to anthropogenic forcing. Models run with increases in greenhouse gases alone give a warming which accelerates in the latter half of the century. When a simple representation of aerosol effects is included (Mitchell *et al.*, 1995b; Cubasch *et al.*, 1996; Haywood *et al.*, 1997; Boer *et al.*, 2000a,b) the rate of warming is reduced (see also Chapter 8, Section 8.6.1). The global mean response is similar when additional forcings due to ozone and the indirect effect of sulphates are included. GCM simulations (Tett *et al.*, 1996; Hansen *et al.*, 1997b) indicate that changes in stratospheric ozone observed over the last two decades yield a global mean surface temperature cooling of about 0.1 to 0.2°C. This may be too small to be distinguishable from the model's internal variability and is also smaller than the warming effects due to the changes in the well-mixed greenhouse gases over the same time period (about 0.2 to 0.3°C). The lack of a statistically significant surface temperature change is in contrast to the large ozone-induced cooling in the lower stratosphere (WMO, 1999; Bengtsson *et al.* 1999).

The response of the vertical distribution of temperature to anthropogenic forcing

Increases in greenhouse gases lead to a warming of the troposphere and a cooling of the stratosphere due to CO_2 (IPCC, 1996). Reductions in stratospheric ozone lead to a further cooling, particularly in the stratosphere at high latitudes. Anthropogenic sulphate aerosols cool the troposphere with little effect on the stratosphere. When these three forcings are included in a climate model (e.g., Tett *et al.*, 1996, 2000) albeit in a simplified way, the simulated changes show tropospheric warming and stratospheric cooling, as observed and as expected on physical principles (Figure 12.8). Note that this structure is distinct from that expected from natural (internal and external) influences.

The response of surface temperature to anthropogenic forcing

The spatial pattern of the simulated surface temperature response to a steady increase in greenhouse gases is well documented (e.g., Kattenberg *et al.*, 1996; Chapter 10). The warming is greater over

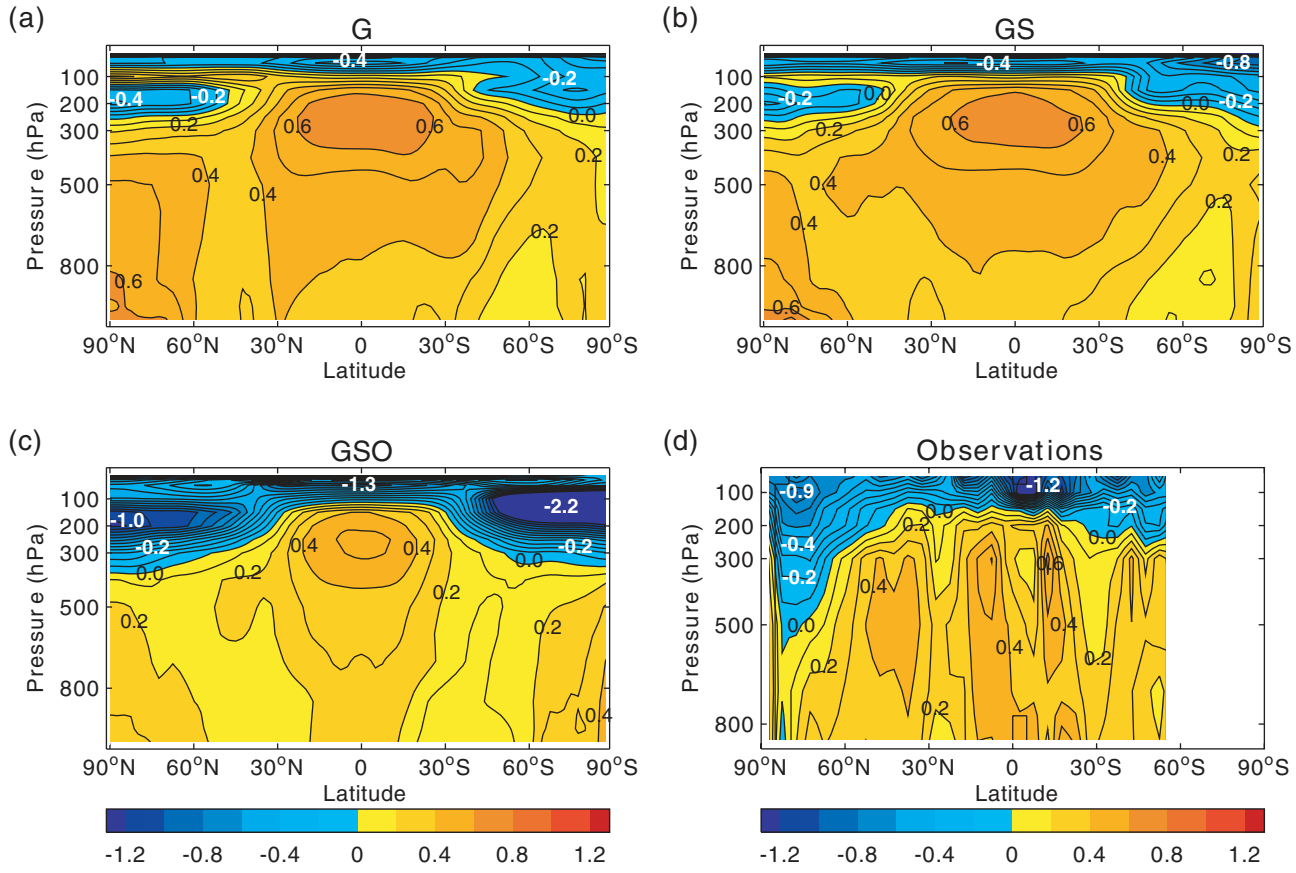

Figure 12.8: Simulated and observed zonal mean temperature change as a function of latitude and height from Tett *et al.* (1996). The contour interval is 0.1°C. All signals are defined to be the difference between the 1986 to 1995 decadal mean and the 20 year 1961 to 1980 mean. (a), increases in CO_2 only (G); (b), as (a), but with a simple representation of sulphate aerosols added (GS); (c), as (b), with observed changes in stratospheric ozone (GSO); (d), observed changes.

land than over ocean and generally small during the 20th century over the Southern Ocean and northern North Atlantic where mixing extends to considerable depth. The warming is amplified in high latitudes in winter by the recession of sea ice and snow, and is close to zero over sea ice in summer.

Despite the qualitative consistency of these general features, there is considerable variation from model to model. In Chapter 9, it was noted that the spatial correlation between the transient response to increasing CO_2 in *different* models in scenarios to the middle of the 21st century was typically 0.65. In contrast, the spatial correlation between the temperature response to greenhouses gases only, and greenhouse gases and aerosols in the *same* model was typically 0.85 (see Chapter 9, Table 9.2). Hence, attempts to detect separate greenhouse gas and aerosol patterns in different models may not give consistent results (see Section 12.4.3.2).

12.2.4 Some Important Statistical Considerations

Most recent studies (Hegerl *et al.*, 1996, 1997, 2000, 2001; North and Stevens, 1998; Allen and Tett, 1999; Tett *et al.*, 1999, 2000; Berliner *et al.*, 2000; North and Wu, 2001; Stott *et al.*, 2001) have used a regression approach in which it is assumed that observations can be represented as a linear combination of candidate signals plus noise (see Appendices 12.1 and 12.2). Other approaches, such as pattern correlation (Santer *et al.*, 1995, 1996a; see also Appendix 12.3), complement the regression approach, being particularly valuable in cases where model-simulated response patterns are particularly uncertain. In all cases, the signal patterns are obtained from climate models. In the regression approach, the unknown signal amplitudes are estimated from observations. The uncertainty of these estimates that is caused by natural variability in the observations is expressed with confidence intervals. Detection of an individual signal is achieved when the confidence interval for its amplitude does not include zero. Overall detection (that some climate change has taken place) is achieved when the joint confidence interval on the signals considered does not encompass the origin.

Attribution and consistency

Detecting that some climate change has taken place does not immediately imply that we know the cause of the detected change. The practical approach to attribution that has been taken by climatologists includes a demand for consistency between the signal amplitudes projected by climate models and estimated from observations (Hasselmann, 1997). Consequently, several

studies, including Hegerl *et al.* (1997, 2000) and Tett *et al.* (1999, 2000) have performed an "attribution" consistency test that is designed to detect inconsistency between observed and model projected signal amplitudes. This test is a useful adjunct to detection because it provides an objective means of identifying model-simulated signal amplitudes that are significantly different from those estimated from observations. However, the test does not give the final word on attribution because it is designed to identify evidence of inconsistency rather than evidence for consistency between modelled and observed estimates of signal strength. A further refinement (e.g., Stott *et al.*, 2001) is to consider the full range of signals believed, on physical grounds, to be likely to have had a significant impact on recent climate change and to identify those subsets of these signals that are consistent with recent observations. If all these subsets contain an anthropogenic component, for example, then at least part of the observed change can be attributed to anthropogenic influence. Levine and Berliner (1999) point out that a test that searches for consistency is available (Brown *et al.*, 1995), but it has not yet been used in attribution studies. Bayesian statisticians approach the problem more directly by estimating the posterior probability that the signal amplitudes projected by climate models are close to those in the observed climate. Berliner *et al.* (2000) provides a demonstration.

The use of climate models to estimate natural internal variability
Climate models play a critical role in these studies because they provide estimates of natural internal variability as well as the signals. In most studies an estimate of natural internal variability is needed to optimise the search for the signal and this is usually obtained from a long control simulation. In addition, a separate estimate of natural variability is required to determine the uncertainty of the amplitude estimates. Unfortunately, the short instrumental record gives only uncertain estimates of variability on the 30 to 50 year time-scales that are important for detection and attribution and palaeo-data presently lacks the necessary spatial coverage (see Section 12.2.2). Thus a second control integration is generally used to estimate the uncertainty of the amplitude estimates that arises from natural climate variability (e.g., Hegerl *et al.*, 1996; Tett *et al.*, 1999).

Temporal and spatial scales used in detection studies
While a growing number of long control simulations are becoming available, there remain limitations on the spatial scales that can be included in global scale detection and attribution studies. Present day control simulations, which range from 300 to about 2,000 years in length, are not long enough to simultaneously estimate internal variability on the 30 to 50 year time-scale over a broad range of spatial scales. Consequently, detection and attribution studies are conducted in a reduced space that includes only large spatial scales. This space is selected so that it represents the signals well and allows reliable estimation of internal variability on the scales retained (see Appendix 12.4). Recently, the scale selection process has been augmented with a statistical procedure that checks for consistency between model simulated and observed variability on the scales that are retained (Allen and Tett, 1999).

Fixed and temporally-varying response patterns
Detection and attribution studies performed up to the SAR used fixed signal patterns that did not evolve with time. These studies were hampered because the mean large-scale response of climate to different types of anomalous forcing tends to be similar (e.g., Mitchell *et al.*, 1995a; Reader and Boer, 1998; see also Figure 12.3). Recent studies have been able to distinguish more clearly between signals from anthropogenic and other sources by including information from climate models about their temporal evolution. Tett *et al.* (1999, 2000) and Stott *et al.* (2001) in related studies have used a *space-time* approach in which the signal pattern evolves on the decadal time-scale over a 50-year period. North and Wu (2001) also use a space-time approach. North and Stevens (1998) used a related *space-frequency* approach (see Appendix 12.2).

Allowance for noise in signal patterns
Most studies have assumed that signal patterns are noise free. This is a reasonable assumption for fixed pattern studies (see Appendix 12.2) but space-time estimates of the 20th century climate change obtained from small ensembles of forced climate simulations are contaminated by the model's internal variability. Allen and Tett (1999) point out that noise in the signal patterns will tend to make the standard detection algorithm (e.g., Hasselmann, 1993, 1997) somewhat conservative. Methods for accommodating this source of noise have been available for more than a century (Adcock, 1878; see also Ripley and Thompson, 1987). Allen and Stott (2000) recently applied such a method and found that, while the question of which signals could be detected was generally unaffected, the estimated amplitude of individual signals was sensitive to this modification of the procedure. Another source of uncertainty concerns differences in signal patterns between different models. Recent studies (Allen *et al.*, 2000a,b; Barnett *et al.*, 2000; Hegerl *et al.*, 2000) consider the sensitivity of detection and attribution results to these differences.

12.3 Qualitative Comparison of Observed and Modelled Climate Change

12.3.1 Introduction

This section presents a qualitative assessment of consistencies and inconsistencies between the observed climate changes identified in Chapter 2 and model projections of anthropogenic climate change described in Chapter 9.

Most formal detection and attribution studies concentrate on variables with high climate change signal-to-noise ratios, good observational data coverage, and consistent signals from different model simulations, mainly using mean surface air temperatures or zonal mean upper-air temperatures. To enhance the signal-to-noise ratio, they generally consider variations on large spatial scales and time-scales of several decades or longer.

There are many studies that have identified areas of qualitative consistency and inconsistency between observed and modelled climate change. While the evidence for an anthropogenic influence on climate from such studies is less compelling than from formal attribution studies, a broad range of evidence of

qualitative consistency between observed and modelled climate change is also required. In addition, areas of qualitative consistency may suggest the possibility for further formal detection and attribution study.

12.3.2 Thermal Indicators

Surface temperature

Global mean surface air temperature has been used in many climate change detection studies. The warming shown in the instrumental observations over the last 140 years is larger than that over a comparable period in any of the multi-century control simulations carried out to date (e.g., Figure 12.1; Stouffer *et al.*, 2000). If the real world internal variability on this time-scale is no greater than that of the models, then the temperature change over the last 140 years has been unusual and therefore likely to be externally forced. This is supported by palaeo-reconstructions of the last six centuries (Mann *et al.*, 1998) and the last 1,000 years (Briffa *et al.*, 1998; 2000; Jones *et al.*, 1998; Crowley, 2000; Crowley and Lowery, 2000; Mann *et al.*, 2000), which show that the 20th century warming is highly unusual. Three of the five years (1995, 1996 and 1998) added to the instrumental record since the SAR are the warmest globally in the instrumental record, consistent with the expectation that increases in greenhouse gases will lead to sustained long-term warming.

When anthropogenic factors are included, models provide a plausible explanation of the changes in global mean temperature over the last hundred years (Figure 12.7). It is conceivable that this agreement between models and observations is spurious. For example, if a model's response to greenhouse gas increases is too large (small) and the sulphate aerosol forcing too large (small), these errors could compensate. Differences in the spatio-temporal patterns of response to greenhouse gases and sulphate forcing nevertheless allow some discrimination between them, so this compensation is not complete. On the other hand, when forced with known natural forcings, models produce a cooling over the second half of the 20th century (see Figure 12.7) rather than the warming trend shown in the observed record. The discrepancy is too large to be explained through model estimates of internal variability and unlikely to be explained through uncertainty in forcing history (Tett *et al.*, 2000). Schneider and Held (2001) applied a technique to isolate those spatial patterns of decadal climate change in observed surface temperature data over the 20th century which are most distinct from interannual variability. They find a spatial pattern which is similar to model-simulated greenhouse gas and sulphate aerosol fingerprints in both July and December. The time evolution of this pattern shows a strong trend with little influence of interannual variability. (Note that this technique is related to optimal fingerprinting, but does not use prior information on the pattern of expected climate change.)

Other thermal indicators

While most attention in formal detection and attribution studies has been paid to mean surface air temperatures, a number of other thermal indicators of climate variations are also discussed in Chapter 2. Many of these, including warming in sub-surface land temperatures measured in bore holes, warming indicators in ice cores and corresponding bore holes, warming in sub-surface ocean temperatures, retreat of glaciers, and reductions in Arctic sea-ice extent and in snow cover, are consistent with the recent observed warming in surface air temperatures and with model projections of the response to increasing greenhouse gases. Other observed changes in thermal indicators include a reduction in the mean annual cycle (winters warming faster than summers) and in the mean diurnal temperature range (nights warming faster than days) over land (see Chapter 2). While the changes in annual cycle are consistent with most model projections, the observed changes in diurnal temperature range are larger than simulated in most models for forcings due to increasing greenhouse gases and sulphate aerosols this century (see Chapters 2 and 8). However, the spatial and temporal coverage of data for changes in observed diurnal temperature range is less than for changes in mean temperatures, leading to greater uncertainty in the observed global changes (Karoly and Braganza, 2001; Schnur, 2001). Also, the observed reductions in diurnal temperature range are associated with increases in cloudiness (see Chapter 2), which are not simulated well by models. Few models include the indirect effects of sulphate aerosols on clouds.

Changes in sea-ice cover and snow cover in the transition seasons in the Northern Hemisphere are consistent with the observed and simulated high latitude warming. The observed trends in Northern Hemisphere sea-ice cover (Parkinson *et al.*, 1999) are consistent with those found in climate model simulations of the last century including anthropogenic forcing (Vinnikov *et al.*, 1999). Sea-ice extent in the Southern Hemisphere does not show any consistent trends.

Compatibility of surface and free atmosphere temperature trends

There is an overall consistency in the patterns of upper air temperature changes with those expected from increasing greenhouse gases and decreasing stratospheric ozone (tropospheric warming and stratospheric cooling). It is hard to explain the observed changes in the vertical in terms of natural forcings alone, as discussed in Section 12.2.3.2 (see Figure 12.8). However, there are some inconsistencies between the observed and modelled vertical patterns of temperature change. Observations indicate that, over the last three to four decades, the tropical atmosphere has warmed in the layer up to about 300 hPa and cooled above (Parker *et al*., 1997; Gaffen *et al*., 2000). Model simulations of the recent past produce a warming of the tropical atmosphere to about 200 hPa, with a maximum at around 300 hPa not seen in the observations. This discrepancy is less evident when co-located model and radiosonde data are used (Santer *et al.*, 2000), or if volcanic forcing is taken into account, but does not go away entirely (Bengtsson *et al.*, 1999; Brown *et al.*, 2000b). The MSU satellite temperature record is too short and too poorly resolved in the vertical to be of use here.

Comparison of upper air and surface temperature data in Chapter 2 shows that the lower to mid-troposphere has warmed less than the surface since 1979. The satellite-measured temperature over a broad layer in the lower troposphere around 750 hPa since 1979 shows no significant trend, in contrast to the warming trend measured over the same time period at the surface. This disparity has been assessed recently by a panel of experts

(National Academy of Sciences, 2000). They concluded that "the troposphere actually may have warmed much less rapidly than the surface from 1979 to the late 1990s, due both to natural causes (e.g., the sequence of volcanic eruptions that occurred within this particular 20-year period) and human activities (e.g., the cooling in the upper troposphere resulting from ozone depletion in the stratosphere)" (see also Santer *et al.*, 2000). They also concluded that "it is not currently possible to determine whether or not there exists a fundamental discrepancy between modelled and observed atmospheric temperature changes since the advent of satellite data in 1979". Over the last 40 years, observed warming trends in the lower troposphere and at the surface are similar, indicating that the lower troposphere warmed faster than the surface for about two decades prior to 1979 (Brown *et al.*, 2000a; Gaffen *et al.*, 2000). However, in the extra-tropical Eurasian winter some additional warming of the surface relative to the lower or mid-troposphere might be expected since 1979. This is due to an overall trend towards an enhanced positive phase of the Arctic Oscillation (Thompson *et al.*, 2000) which has this signature.

Model simulations of large-scale changes in tropospheric and surface temperatures are generally statistically consistent with the observed changes (see Section 12.4). However, models generally predict an enhanced rate of warming in the mid- to upper troposphere over that at the surface (i.e., a negative lapse-rate feedback on the surface temperature change) whereas observations show mid-tropospheric temperatures warming no faster than surface temperatures. It is not clear whether this discrepancy arises because the lapse-rate feedback is consistently over-represented in climate models or because of other factors such as observational error or neglected forcings (Santer *et al.*, 2000). Note that if models do simulate too large a negative lapse-rate feedback, they will tend to underestimate the sensitivity of climate to a global radiative forcing perturbation.

Stratospheric trends

A recent assessment of temperature trends in the stratosphere (Chanin and Ramaswamy, 1999) discussed the cooling trends in the lower stratosphere described in Chapter 2. It also identified large cooling trends in the middle and upper stratosphere, which are consistent with anthropogenic forcing due to stratospheric ozone depletion and increasing greenhouse gas concentrations. An increase in water vapour, possibly due to increasing methane oxidation, is another plausible explanation for the lower stratospheric cooling (Forster and Shine, 1999) but global stratospheric water vapour trends are poorly understood.

12.3.3 Hydrological Indicators

As discussed in Chapter 2, there is less confidence in observed variations in hydrological indicators than for surface temperature, because of the difficulties in taking such measurements and the small-scale variations of precipitation. There is general consistency between the changes in mean precipitation in the tropics over the last few decades and changes in ENSO. There is no general consistency between observed changes in mean tropical precipitation and model simulations. In middle and high latitudes in the Northern Hemisphere, the observed increase in precipitation is consistent with most model simulations. Observed changes in ocean salinity in the Southern Ocean appear to be consistent with increased precipitation there, as expected from model simulations (Wong *et al.*, 1999; Banks *et al.*, 2000).

The observed increases in the intensity of heavy precipitation in the tropics and in convective weather systems described in Chapter 2 are consistent with moist thermodynamics in a warmer atmosphere and model simulations. Observed increases of water vapour in the lower troposphere in regions where there is adequate data coverage are also consistent with model simulations. As discussed in Chapter 7, different theories suggest opposite variations of water vapour in the upper troposphere associated with an increased greenhouse effect and surface warming. The quality, amount and coverage of water vapour data in the upper troposphere do not appear to be sufficient to resolve this issue.

12.3.4 Circulation

In middle and high latitudes of both hemispheres, there has been a trend over the last few decades towards one phase of the North Atlantic Oscillation/Arctic Oscillation and of the Antarctic high latitude mode, sometimes also referred to as "annular modes", (Chapter 2; Thompson *et al.*, 2000). These are approximately zonally symmetric modes of variability of the atmospheric circulation. Both trends have been associated with reduced surface pressure at high latitudes, stronger high latitude jets, a stronger polar vortex in the winter lower stratosphere and, in the Northern Hemisphere, winter warming over the western parts of the continents associated with increased warm advection from ocean regions. The trend is significant and cannot be explained by internal variability in some models (Gillett *et al.*, 2000b). These dynamical changes explain only part of the observed Northern Hemisphere warming (Gillett *et al.*, 2000b; Thompson *et al.*, 2000). Modelling studies suggest a number of possible causes of these circulation changes, including greenhouse gas increases (Fyfe *et al.*, 1999; Paeth *et al.*, 1999; Shindell *et al.*, 1999) and stratospheric ozone decreases (Graf *et al.*, 1998; Volodin and Galin, 1999). Some studies have also shown that volcanic eruptions (Graf *et al.*, 1998; Mao and Robock, 1998; Kirchner *et al.*, 1999) can induce such changes in circulation on interannual time-scales. Shindell *et al.* (2001) show that both solar and volcanic forcing are unlikely to explain the recent trends in the annular modes.

The majority of models simulate the correct sign of the observed trend in the North Atlantic or Arctic Oscillation when forced with anthropogenic increases in greenhouse gases and sulphate aerosols, but almost all underestimate the magnitude of the trend (e.g., Osborn *et al.*, 1999; Gillett *et al.*, 2000b; Shindell *et al.*, 1999). Some studies suggest that a better resolved stratosphere is necessary to simulate the correct magnitude of changes in dynamics involving the annular modes (e.g., Shindell *et al.*, 2001).

12.3.5 Combined Evidence

The combination of independent but consistent evidence should strengthen our confidence in identifying a human influence on climate. The physical and dynamical consistency of most of the

thermal and hydrological changes described above supports this conclusion. However, it is important to bear in mind that much of this evidence is associated with a global and regional pattern of warming and therefore cannot be considered to be completely independent evidence.

An elicitation of individual experts' subjective assessment of evidence for climate change detection and attribution is being carried out (Risbey *et al.*, 2000). This will help to better understand the nature of the consensus amongst experts on the subject of climate change attribution.

12.4 Quantitative Comparison of Observed and Modelled Climate Change

A major advance since the SAR has been the increase in the range of techniques used to assess the quantitative agreement between observed and modelled climate change, and the evaluation of the degree to which the results are independent of the assumptions made in applying those techniques (Table 12.1). Also, some studies have based their conclusions on estimates of the amplitude of anthropogenic signals in the observations and consideration of their consistency with model projections. Estimates of the changes in forcing up to 1990 used in these studies, where available, are given in Table 12.2. In this section we assess new studies using a number of techniques, ranging from descriptive analyses of simple indices to sophisticated optimal detection techniques that incorporate the time and space-dependence of signals over the 20th century.

We begin in Section 12.4.1 with a brief discussion of detection studies that use simple indices and time-series analyses. In Section 12.4.2 we discuss recent pattern correlation studies (see Table 12.1) that assess the similarity between observed and modelled climate changes. Pattern correlation studies were discussed extensively in the SAR, although subsequently they received some criticism. We therefore also consider the criticism and studies that have evaluated the performance of pattern correlation techniques. Optimal detection studies of various kinds are assessed in Section 12.4.3. We consider first studies that use a single fixed spatial signal pattern (Section 12.4.3.1) and then studies that simultaneously incorporate more than one fixed signal pattern (Section 12.4.3.2). Finally, optimal detection studies that take into account temporal as well as spatial variations (so-called space-time techniques) are assessed in Section 12.4.3.3.

We provide various aids to the reader to clarify the distinction between the various detection and attribution techniques that have been used. Box 12.1 in Section 12.4.3 provides a simple intuitive description of optimal detection. Appendix 12.1 provides a more technical description and relates optimal detection to general linear regression. The differences between fixed pattern, space-time and space-frequency optimal detection methods are detailed in Appendix 12.2 and the relationship between pattern correlation and optimal detection methods is discussed in Appendix 12.3. Dimension reduction, a necessary part of optimal detection studies, is discussed in Appendix 12.4.

12.4.1 Simple Indices and Time-series Methods

An index used in many climate change detection studies is global mean surface temperature, either as estimated from the instrumental record of the last 140 years, or from palaeo-reconstructions. Some studies of the characteristics of the global mean and its relationship to forcing indices are assessed in Section 12.2.3. Here we consider briefly some additional studies that examine the spatial structure of observed trends or use more sophisticated time-series analysis techniques to characterise the behaviour of global, hemispheric and zonal mean temperatures.

Spatial patterns of trends in surface temperature

An extension of the analysis of global mean temperature is to compare the spatial structure of observed trends (see Chapter 2, Section 2.2.2.4) with those simulated by models in coupled control simulations. Knutson *et al.* (2000) examined observed 1949 to 1997 surface temperature trends and found that over about half the globe they are significantly larger than expected from natural low-frequency internal variability as simulated in long control simulations with the GFDL model (Figure 12.9). A similar result was obtained by Boer *et al.* (2000a) using 1900 to 1995 trends. The level of agreement between observed and simulated trends increases substantially in both studies when observations are compared with simulations that incorporate transient greenhouse gases and sulphate aerosol forcing (compare Figure 12.9c with Figure 12.9d, see also Chapter 8, Figure 8.18). While there are areas, such as the extra-tropical Pacific and North Atlantic Ocean, where the GFDL model warms significantly more than has been observed, the anthropogenic climate change simulations do provide a plausible explanation of temperature trends over the last century over large areas of the globe. Delworth and Knutson (2000) find that one in five of their anthropogenic climate change simulations showed a similar evolution of global mean surface temperature over the 20th century to that observed, with strong warming, particularly in the high latitude North Atlantic, in the first half of the century. This would suggest that the combination of anthropogenic forcing and internal variability may be sufficient to account for the observed early-century warming (as suggested by, e.g., Hegerl *et al.*, 1996), although other recent studies have suggested that natural forcing may also have contributed to the early century warming (see Section 12.4.3).

Correlation structures in surface temperature

Another extension is to examine the lagged and cross-correlation structure of observed and simulated hemispheric mean temperature as in Wigley *et al.*, (1998a). They find large differences between the observed and model correlation structure that can be explained by accounting for the combined influences of anthropogenic and solar forcing and internal variability in the observations. Solar forcing alone is not found to be a satisfactory explanation for the discrepancy between the correlation structures of the observed and simulated temperatures. Karoly and Braganza (2001) also examined the correlation structure of surface air temperature variations. They used several simple indices, including the land-ocean contrast, the meridional

Table 12.1: *Summary of the main detection and attribution studies considered.*

Study	Signals	Signal source	Noise source	Method	S, V	Sources of uncertainty	Time-scale	No. of patterns	Detect
Santer *et al.*, 1996	G, GS, O etc.	Equilibrium / future LLNL, GFDL R15, HadCM2	GFDL R15, HadCM2, ECHAM1	F, Corr	V	Internal variability	25 year Annual and seasonal	1	GSO
Hegerl, 1996, 1997	G, GS	Future ECHAM3, HadCM2	GFDL R15, ECHAM1, HadCM2; observation	F, Pattern	S	Internal variability	30, 50 years Annual and JJA	1, 2	G, GS, S
Tett *et al.*, 1996	G, GS, GSO	Historical HadCM2	HadCM2	F, Corr	V	Internal variability	35 years	1	GSO
Hegerl *et al.*, 2000	G, GS, Vol, Sol	Future, ECHAM3, HadCM2	ECHAM3, HadCM2	F, Pattern	S	Internal variability; model uncertainty	30, 50 years Annual and JJA	1, 2	GS, G, S (not all cases)
Allen and Tett, 1999	G, GS, GSO	Historical HadCM2	HadCM2	F, pattern	V	Internal variability	35 years Annual	1, 2	GSO and also G
Tett *et al.*, 1999 Stott *et al.*, 2001	G,GS, Sol, Vol	Historical HadCM2	HadCM2	Time-space	S	Internal variability, 2 solar signals	50 years decadal and seasonal	2 or more	G, GS, Sol (Vol)
North and Stevens, 1998 Leroy, 1998 North and Wu, 2001	G, GS, Sol, Vol	Historical EBM	GFDL ECHAM1, EBM Same+Had CM2	Freq-Space Time-space	S	Internal variability	Annual and hemispheric summer Annual	4	G, S, Vol G, Vol
Barnett *et al.*, 1999	G, GS, GSIO Sol+vol	Future ECHAM3, ECHAM4, HadCM2, GFDL R15	ECHAM3, ECHAM4, HadCM2, GFDL R15	F, Pattern	S	Observed sampling error, model uncertainty, internal variability	50 years JJA trends	2	GS, G, S (S not all cases)
Hill *et al.*, 2001	G, GSO,Sol	Historical HadCM2	HadCM2	F, pattern	V	Internal variability	35 years annual	3	G
Tett *et al.*, 2000	G,GSTI, GSTIO, Nat	Historical HadCM3	HadCM3	Time-space F, pattern	S V	Internal variability Internal variability	50, 100 years decadal 35 years, annual	2 or more 2	G, SIT, GSTIO and Nat GSTI

The columns contain the following information:

Study : the main reference to the study.

Signals : outlines the principal signals considered: G-greenhouse gases, S-sulphate aerosol direct effect, T-tropospheric ozone, I-sulphate aerosol indirect effect, O-stratospheric ozone, Sol-solar, Vol-volcanoes, Nat-solar and volcanoes.

Signal source : "historical" indicates the signal is taken from a historical hindcast simulation, "future" indicates that the pattern is taken from a prediction.

Noise source : origin of the noise estimates.

Method : "F" means fixed spatial pattern, "corr" indicates a correlation study, "pattern" an optimal detection study.

S, V : "V" indicates a vertical temperature pattern, "S" a horizontal temperature pattern.

Sources of uncertainty : any additional uncertainties allowed for are indicated. Modelled internal variability is allowed for in all studies.

Time-scale : the lengths of time interval considered. (JJA= June-July-August)

No. of patterns : the number of patterns considered simultaneously.

Detect : signals detected.

Table 12.2: *Estimated forcing from pre-industrial period to 1990 in simulations used in detection studies (Wm^{-2}). GS indicates only direct sulphate forcing included, GSI indicates both direct and indirect effects included. Other details of the detection studies are given in Table 12.1. Details of the models are given in Chapter 8, Table 8.1.*

Model	Aerosol	Baseline forcing	1990 aerosol forcing	1990 greenhouse gas forcing	Source of estimate
HadCM2	GS	1760	–0.6	1.9	Mitchell and Johns, 1997
HadCM3	GSI	1860	–1.0	2.0	Tett *et al.*, 2000
ECHAM3/LSG	GS	1880	–0.7	1.7	Roeckner
ECHAM4/OPYC	GSI	1760	–0.9	2.2	Roeckner *et al.*, 1999
GFDL_R30	GS	1760	–0.6	2.1	Stouffer
CGCM1,2	GS	1760	~ –1.0	~2.2	Boer *et al.*, 2000a,b

gradient, and the magnitude of the seasonal cycle, to describe global climate variations and showed that for natural variations, they contain information independent of the global mean temperature. They found that the observed trends in these indices over the last 40 years are unlikely to have occurred due to natural climate variations and that they are consistent with model simulations of anthropogenic climate change.

Statistical models of time-series

Further extensions involve the use of statistical "models" of global, hemispheric and regional temperature time-series. Note however, that the stochastic models used in these time-series studies are generally not built from physical principles and are thus not as strongly constrained by our knowledge of the physical climate system as climate models. All these studies depend on inferring the statistical properties of the time-series from an assumed noise model with parameters estimated from the residuals. As such, the conclusions depend on the appropriateness or otherwise of the noise model.

Tol and de Vos (1998), using a Bayesian approach, fit a hierarchy of time-series models to global mean near-surface temperature. They find that there is a robust statistical relationship between atmospheric CO_2 and global mean temperature and that natural variability is unlikely to be an explanation for the observed temperature change of the past century. Tol and Vellinga (1998) further conclude that solar variation is also an unlikely explanation. Zheng and Basher (1999) use similar time-series models and show that deterministic trends are detectable over a large part of the globe. Walter *et al.* (1998), using neural network models, estimate that the warming during the past century due to greenhouse gas increases is 0.9 to 1.3°C and that the counterbalancing cooling due to sulphate aerosols is 0.2 to 0.4°C. Similar results are obtained with a multiple regression model (Schönwiese *et al.*, 1997). Kaufmann and Stern (1997) examine the lagged-covariance structure of hemispheric mean temperature and find it consistent with unequal anthropogenic aerosol forcing in the two hemispheres. Smith *et al.* (2001), using similar bivariate time-series models, find that the evidence for causality becomes weak when the effects of ENSO are taken into account. Bivariate time-series models of hemispheric mean temperature that account for box–diffusion estimates of the response to anthropogenic and solar forcing are found to fit the observations significantly better than competing statistical models. All of these studies draw conclusions that are consistent with those of earlier trend detection studies (as described in the SAR).

In summary, despite various caveats in each individual result, time-series studies suggest that natural signals and internal variability alone are unlikely to explain the instrumental record, and that an anthropogenic component is required to explain changes in the most recent four or five decades.

12.4.2 Pattern Correlation Methods

12.4.2.1 Horizontal patterns

Results from studies using pattern correlations were reported extensively in the SAR (for example, Santer *et al.*, 1995, 1996c; Mitchell *et al.*, 1995b). They found that the patterns of simulated surface temperature change due to the main anthropogenic factors in recent decades are significantly closer to those observed than expected by chance. Pattern correlations have been used because they are simple and are insensitive to errors in the amplitude of the spatial pattern of response and, if centred, to the global mean response. They are also less sensitive than regression-based optimal detection techniques to sampling error in the model-simulated response. The aim of pattern-correlation studies is to use the differences in the large-scale patterns of response, or "fingerprints", to distinguish between different causes of climate change.

Strengths and weaknesses of correlation methods

Pattern correlation statistics come in two types – centred and uncentred (see Appendix 12.3). The centred (uncentred) statistic measures the similarity of two patterns after (without) removal of the global mean. Legates and Davis (1997) criticised the use of centred correlation in detection studies. They argued that correlations could increase while observed and simulated global means diverge. This was precisely the reason centred correlations were introduced (e.g., Santer *et al.*, 1993): to provide an indicator that was statistically independent of global mean temperature changes. If both global mean changes and centred pattern correlations point towards the same explanation of observed temperature changes, it provides more compelling evidence than either of these indicators in isolation. An explicit analysis of the role of the global mean in correlation-based studies can be provided by the

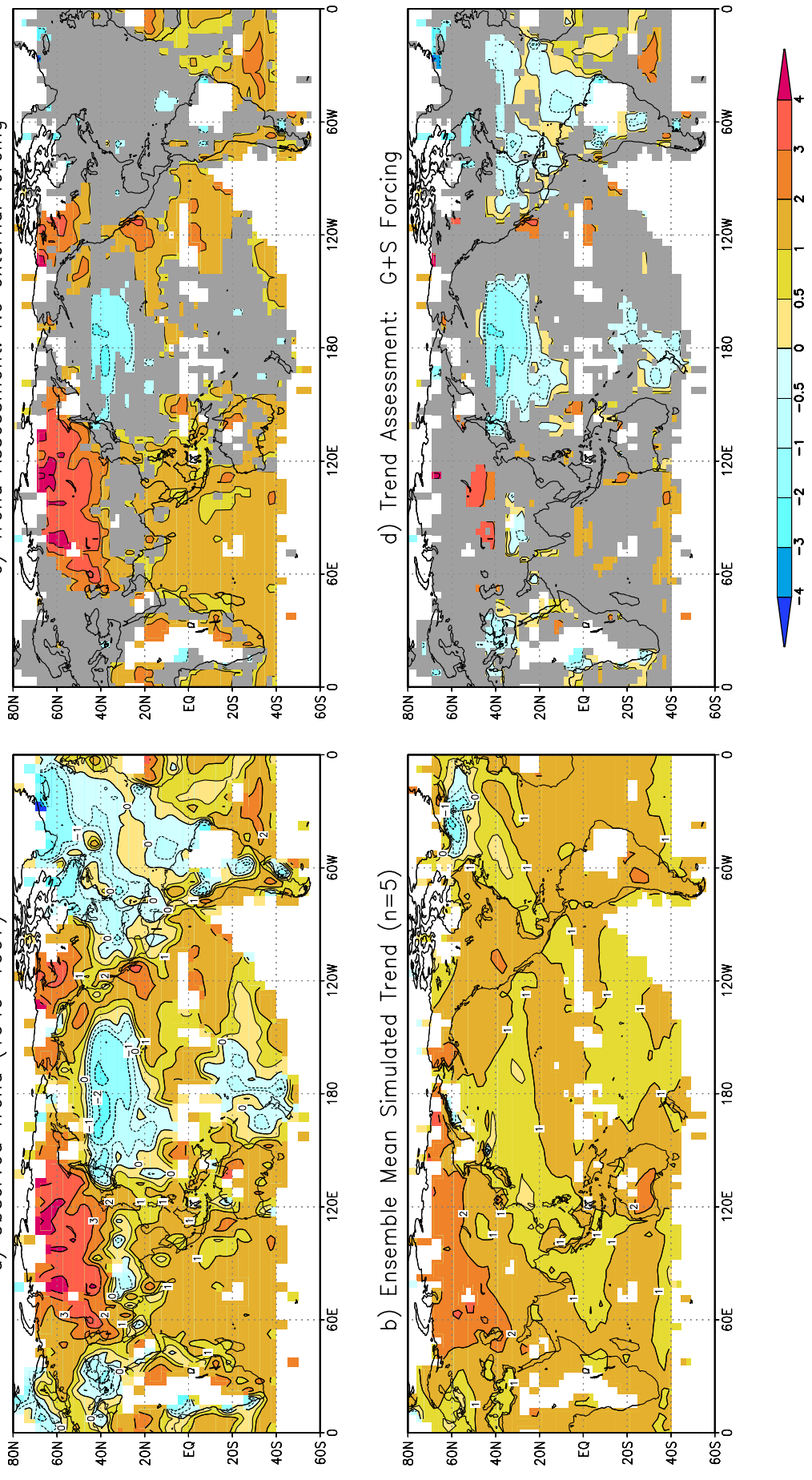

Figure 12.9: (a) Observed surface air temperature trends for 1949 to 1997. (b) Simulated surface air temperature trends for the same period as estimated from a five-member greenhouse gas plus sulphate ensemble run with the GFDL R30 model. (c) Observed trends (in colour) that lie outside the 90% natural variability confidence bounds as estimated from the GFDL R30 control run. Grey areas show regions where the observed trends are consistent with the local 49-year temperature trends in the control run. (d) As for (c) but showing observed 1949 to 1997 trends (in colour) that are significantly different (as determined with a t-test at the 10% level) from those simulated by the greenhouse gas plus aerosol simulations performed with the GFDL R30 model (from Knutson *et al.*, 2000). The larger grey areas in (d) than (c) indicate that the observed trends are consistent with the anthropogenic forced simulations over larger regions than the control simulations.

use of both centred and uncentred statistics. Pattern correlation-based detection studies account for spatial auto-correlation implicitly by comparing the observed pattern correlation with values that are realised in long control simulations (see Wigley *et al.*, 2000). These studies do not consider the amplitude of anthropogenic signals, and thus centred correlations alone are not sufficient for the attribution of climate change.

Wigley *et al.* (1998b) studied the performance of correlation statistics in an idealised study in which known spatial signal patterns were combined with realistic levels of internal variability. The statistics were found to perform well even when the signal is contaminated with noise. They found, in agreement with Johns *et al.* (2001), that using an earlier base period can enhance detectability, but that much of this advantage is lost when the reduced data coverage of earlier base periods is taken into account. They also found that reasonable combinations of greenhouse gas and aerosol patterns are more easily detected than the greenhouse gas pattern on its own. This last result indicates the importance of reducing the uncertainty in the estimate of aerosol forcing, particularly the indirect effects. In summary, we have a better understanding of the behaviour of pattern correlation statistics and reasons for the discrepancies between different studies.

12.4.2.2 Vertical patterns

As noted in Section 12.3.2, increases in greenhouse gases produce a distinctive change in the vertical profile of temperature. Santer *et al.* (1996c) assessed the significance of the observed changes in recent decades using equilibrium GCM simulations with changes in greenhouse gases, sulphate aerosols and stratospheric ozone. This study has been extended to include results from the transient AOGCM simulations, additional sensitivity studies and estimates of internal variability from three different models (Santer *et al.*, 1996a). Results from this study are consistent with the earlier results – the 25-year trend from 1963 to 1988 in the centred correlation statistic between the observed and simulated patterns for the full atmosphere was significantly different from the population of 25-year trends in the control simulations. The results were robust even if the estimates of noise levels were almost doubled, or the aerosol response (assumed linear and additive) was halved. The aerosol forcing leads to a smaller warming in the Northern Hemisphere than in the Southern Hemisphere.

Tett *et al.* (1996) refined Santer *et al.*'s (1996a) study by using ensembles of transient simulations which included increases in CO_2, and sulphate aerosols, and reductions in stratospheric ozone, as well as using an extended record of observations (see Figure 12.8). They found that the best and most significant agreement with observations was found when all three factors were included[1]. Allen and Tett (1999) find that the effect of greenhouse gases can be detected with these signal patterns using optimal detection (see Appendix 12.1).

Folland *et al.* (1998) and Sexton *et al.* (2001) take a complementary approach using an atmospheric model forced with sea surface temperatures (SST) and ice extents prescribed from observations. The correlation between the observed and simulated temperature changes in the vertical relative to the base period from 1961 to 1975 was computed. The experiments with anthropogenic forcing (including some with tropospheric ozone changes), give significantly higher correlations than when only SST changes are included.

Interpretation of results

Weber (1996) and Michaels and Knappenburger (1996) both criticised the Santer *et al.* (1996a) results, quoting upper air measurements analysed by Angell (1994). Weber argued that the increasing pattern similarity over the full atmosphere (850 to 50 hPa) resulted mainly from a Southern Hemisphere cooling associated with stratospheric ozone depletion. Santer *et al.* (1996b) pointed out that when known biases in the radiosonde data are removed (e.g., Parker *et al.*, 1997), or satellite or operationally analysed data are used, the greater stratospheric cooling in the Southern Hemisphere all but disappears. Weber (1996) is correct that stratospheric cooling due to ozone will contribute to the pattern similarity over the full atmosphere, but decreases in stratospheric ozone alone would be expected to produce a tropospheric cooling, not a warming as observed. This point should be born in mind when considering a later criticism of the pattern correlation approach. Both Weber (1996) and Michaels and Knappenburger (1996) note that the greater warming of the Southern Hemisphere relative to the Northern Hemisphere from 1963 to 1988 has since reversed. They attribute the Southern Hemisphere warming from 1963 to the recovery from the cooling following the eruption of Mount Agung. Santer *et al.* (1996b) claim that this change in asymmetry is to be expected, because the heating due to increases in greenhouse gases over the most recent years has probably been growing faster than the estimated cooling due to increases in aerosols (see Section 12.2.3.3). Calculations of the difference in the rate of warming between the Northern and Southern Hemispheres vary between different climate models and as a function of time, depending on the relative forcing due to greenhouse gases and sulphate aerosols, and on the simulated rate of oceanic heat uptake in the Southern Hemisphere (Santer *et al.*, 1996b; Karoly and Braganza, 2001).

Assessing statistical significance of changes in the vertical patterns of temperature

There are some difficulties in assessing the statistical significance in detection studies based on changes in the vertical temperature profile. First, the observational record is short, and subject to error, particularly at upper levels (Chapter 2). Second, the model estimates of variability may not be realistic (Section 12.2.2), particularly in the stratosphere. Third, because of data and model limitations, the number of levels used to represent the stratosphere in detection studies to date is small, and hence may not be adequate to allow an accurate representation of the stratospheric response. Fourth, all models produce a maximum warming in the upper tropical troposphere that is not apparent in the observations and whose impact on detection results is difficult to quantify. Nevertheless, all the studies indicate that

[1] Correction of an error in a data mask (Allen and Tett, 1999) did not affect these conclusions, though the additional improvement due to adding sulphate and ozone forcing was no longer significant.

Box 12.1: Optimal detection

Optimal detection is a technique that may help to provide a clearer separation of a climate change fingerprint from natural internal climate variations. The principle is sketched in Figure 12.B1, below (after Hasselmann, 1976).

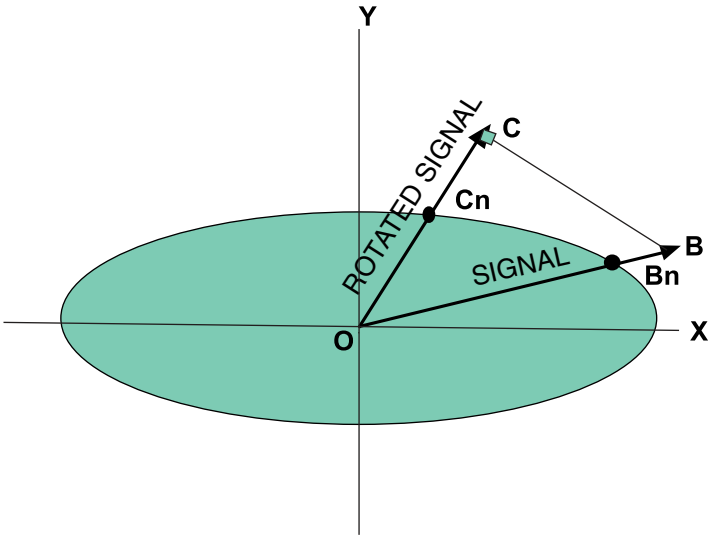

Suppose for simplicity that most of the natural variability can be described in terms of two modes (well-defined spatial patterns) of variability. In the absence of climate change, the amplitudes of these two modes, plotted on a 2D diagram along OX and OY will vary with time, and for a given fraction of occasions (usually chosen as 95 %), the amplitude of each mode will lie within the shaded ellipse. Suppose we are attempting to detect a fingerprint that can be made up of a linear combination of the two patterns such that it lies along OB. The signal to noise ratio is given by OB/OBn. Because our signal lies close to the direction of the main component of variability, the signal to noise ratio is small. On the other hand, we can choose a direction OC that overlaps less with the main component of natural variability such that the signal to noise ratio OC/OCn for the component of the signal that lies in direction OC is larger even though the projected signal OC is smaller then the full signal OB. Optimal detection techniques merely choose the direction OC that maximises the signal to noise ratio. This is equivalent to general linear regression (see Appendix 12.1). A good estimate of natural internal variability is required to optimise effectively.

anthropogenic factors account for a significant part of recent observed changes, whereas internal and naturally forced variations alone, at least as simulated by current models, cannot explain the observed changes. In addition, there are physical arguments for attributing the changes in the vertical profile of temperature to anthropogenic influence (Section 12.3.2).

12.4.3 Optimal Fingerprint Methods

The use of "optimal" techniques can increase the detectability of forced climate changes. These techniques increase the signal-to-noise ratio by looking at the component of the response away from the direction of highest internal variability (see, e.g., Hasselmann, 1979, 1997, 1993; North *et al.*, 1995; see also Box 12.1 on optimal detection and Appendix 12.1). Several new approaches to the optimal detection of anthropogenic climate change have been undertaken since the SAR. We focus on optimal detection studies that use a single pattern of climate change in the following section. Attribution (see Section 12.1.1), which requires us to consider several signals simultaneously, will be considered in Sections 12.4.3.2 and 12.4.3.3.

12.4.3.1 Single pattern studies

Since the SAR, optimal detection studies of surface temperature have been extended (Hegerl *et al.*, 1997, 2000; Barnett *et al.*, 1999) and new studies of data other than surface air temperature have been conducted (Allen and Tett, 1999; Paeth and Hense, 2001; Tett *et al.*, 2000).

Surface temperature patterns

The Hegerl *et al.* (1996) optimal detection study was extended to include more recent estimates of internal variability and simulations with a representation of sulphate aerosols (Hegerl *et al.*, 1997). As in the previous study, different control simulations were used to determine the optimal fingerprint and the significance level of recent temperature change. The authors find significant evidence for a "greenhouse gas plus sulphate aerosol" (GS) fingerprint in the most recent observed 30-year temperature trends regardless of whether internal variability is estimated from models or observations. The 30-year trend ending in the 1940s was found to be significantly larger than expected from internal variability, but less so than the more recent trends. This work has been extended to include other models (Figure 12.10a; see also Barnett *et al.*, 1999: Hegerl *et*

al., 2000), examining whether the amplitude of the 50-year summer surface temperature trends in the GS simulations is consistent with that estimated in the observations. In eleven out of fourteen cases (seven models each evaluated using the fingerprints from the two original models), the model trends are consistent with observations. The greenhouse gas only simulations are generally not consistent with observations, as their warming trends are too large. Berliner *et al.* (2000) detect a combined greenhouse gas and sulphate signal in a fixed pattern detection study of temperature changes using Bayesian techniques.

Vertical patterns of temperature

Allen and Tett (1999) use optimal detection methods to study the change in the vertical profile of zonal mean temperature between 1961 to 1980 and 1986 to 1995. Estimated signals from ensemble AOGCM simulations with greenhouse gas alone (G), greenhouse gas plus direct sulphate (GS), and also including stratospheric ozone forcing (GSO; Tett *et al.*, 1996) are considered. The G and GSO signals are detected separately. The amplitude of the GSO fingerprint estimated from observations is found to be consistent with that simulated by the model, while the model-simulated response to greenhouse gases alone was found to be unrealistically strong. The variance of the residuals that remain after the estimated signal is removed from the observations is consistent with internal variability estimated from a control run.

Other climatic variables

Schnur (2001) applied the optimal detection technique to trends in a variety of climate diagnostics. Changes in the annual mean surface temperature were found to be highly significant (in agreement with previous results from Hegerl *et al.*, 1996, 1997). The predicted change in the annual cycle of temperature as well as winter means of diurnal temperature range can also be detected in most recent observations. The changes are most consistent with those expected from increasing greenhouse gases and aerosols. However, changes in the annual mean and annual cycle of precipitation were small and not significant.

Paeth and Hense (2001) applied a correlation method related to the optimal fingerprint method to 20-year trends of lower tropospheric mean temperature (between 500 and 1,000 hPa) in the summer half of the year in the Northern Hemisphere north of 55°N. Greenhouse gas fingerprints from two models were detected. The combined greenhouse gas plus (direct) sulphate (GS) fingerprints from the two models were not detected.

Summary

All new single-pattern studies published since the SAR detect anthropogenic fingerprints in the global temperature observations, both at the surface and aloft. The signal amplitudes estimated from observations and modelled amplitudes are consistent at the surface if greenhouse gas and sulphate aerosol forcing are taken into account, and in the free atmosphere if ozone forcing is also included. Fingerprints based on smaller areas or on other variables yield more ambiguous results at present.

12.4.3.2 Optimal detection studies that use multiple fixed signal patterns

Surface temperature patterns

Hegerl *et al.* (1997) applied a two-fingerprint approach, using a greenhouse gas fingerprint and an additional sulphate aerosol fingerprint that is made spatially independent (orthogonalised) of the greenhouse fingerprint. They analysed 50-year trends in observed northern summer temperatures. The influence of greenhouse gas and sulphate aerosol signals were both detected simultaneously in the observed pattern of 50-year temperature trends, and the amplitudes of both signals were found to be consistent between model and observations. Simulations forced with greenhouse gases alone and solar irradiance changes alone were not consistent with observations.

Hegerl *et al.* (2000) repeated this analysis using parallel simulations from a different climate model. The combined effect of greenhouse gases and aerosols was still detectable and consistent with observations, but the separate influence of sulphate aerosol forcing, as simulated by this second model, was not detectable. This was because the sulphate response was weaker in the second model, and closely resembled one of the main modes of natural variability. Hence, the detection of the net anthropogenic signal is robust, but the detection of the sulphate aerosol component is very sensitive to differences in model-simulated responses.

As in the single-pattern case, this study has been extended to include seven model GS simulations and to take into account observational sampling error (Figure 12.10b,c, see also Barnett *et al.*, 1999; Hegerl *et al.* 2001). A simple linear transformation allows results to be displayed in terms of individual greenhouse and sulphate signal amplitudes, which assists comparison with other results (see Figure 12.10; Hegerl and Allen, 2000). The amplitudes of the greenhouse gas and sulphate components are simultaneously consistent with the observed amplitudes in 10 of the fourteen GS cases (seven models for two sets of fingerprints) displayed. This contrasts with eleven out of fourteen in the combined amplitude test described in Section 12.4.3.1. If the trends to 1995 are used (Figure 12.10c), the results are similar, though in this case, the ellipse just includes the origin and six out of the fourteen GS cases are consistent with observations. The inconsistency can be seen to be mainly due to large variations in the amplitudes of the model-simulated responses to sulphate aerosols (indicated by the vertical spread of results). Model-simulated responses to greenhouse gases are generally more consistent both with each other and with observations. Two of the cases of disagreement are based on a single simulation rather than an ensemble mean and should therefore be viewed with caution (see Barnett *et al.*, 2000). Barnett *et al.* (1999) found that the degree of agreement between the five models and observations they considered was similar, whether or not the global mean response was removed from the patterns. Signal amplitudes from simulations with greenhouse gas forcing only are generally inconsistent with those estimated from observations (Figure 12.10b,c).

In most of the cases presented here, the response to natural forcings was neglected. In a similar analysis to that just described, Hegerl *et al.* (2000); see also Barnett *et al.*, 1999) also assessed simulations of the response to volcanic and solar

forcing. They find, in agreement with Tett *et al.* (1999), that there is better agreement between observations and simulations when these natural forcings are included, particularly in the early 20th century, but that natural forcings alone cannot account for the late-century warming.

In summary, the estimation of the contribution of individual factors to recent climate change is highly model dependent, primarily due to uncertainties in the forcing and response due to sulphate aerosols. However, although the estimated amplitude varies from study to study, all studies indicate a substantial contribution from anthropogenic greenhouse gases to the changes observed over the latter half of the 20th century.

Vertical patterns of temperature

Allen and Tett (1999) also used spatial fingerprints in the vertical derived from simulations with greenhouse gas forcing alone and simulations with greenhouse gas, sulphate aerosol and stratospheric ozone forcing. These authors show that, even if both greenhouse and other anthropogenic signals are estimated simultaneously in the observed record, a significant response to greenhouse gases remains detectable. Hill *et al.* (2001) extended this analysis to include model-simulated responses to both solar and volcanic forcing, and again found that the response to greenhouse gases remains detectable. Results with non-optimised fingerprints are consistent with the optimised case, but the uncertainty range is larger.

In summary, the fixed pattern studies indicate that the recent warming is unlikely (bordering on very unlikely) to be due to internal climate variability. A substantial response to anthropogenic greenhouse gases appears to be necessary to account for recent temperature trends but the majority of studies indicate that greenhouse gases alone do not appear to be able to provide a full explanation. Inclusion of the response to the direct effect of sulphate aerosols usually leads to a more satisfactory explanation of the observed changes, although the amplitude of the sulphate signal depends on the model used. These studies also provide some evidence that solar variations may have contributed to the early century warming.

12.4.3.3 Space-time studies

Here we consider studies that incorporate the time evolution of forced signals into the optimal detection formalism. These studies use evolving patterns of historical climate change in the 20th century that are obtained from climate models forced with historical anthropogenic and natural forcing. Explicit representation of the time dimension of the signals yields a more powerful approach for both detecting and attributing climate change (see Hasselmann, 1993; North *et al.*, 1995) since it helps to distinguish between responses to external forcings with similar spatial patterns (e.g., solar and greenhouse gas forcing). The time variations of the signals can be represented either directly in the time domain or transformed to the frequency domain.

Surface temperature

Tett *et al.* (1999) and Stott *et al.* (2001) describe a detection and attribution study that uses the space-time approach (see Appendix 12.2). They estimate the magnitude of modelled 20th century greenhouse gas, aerosol, solar and volcanic signals in decadal mean data. Signals are fitted by general linear regression to moving fifty-year intervals beginning with 1906 to 1956 and ending 1946 to 1996. The signals are obtained from four ensembles of transient change simulations, each using a different historical forcing scenario. Greenhouse gas, greenhouse gas plus direct sulphate aerosol, low frequency solar, and volcanic forcing scenarios were used. Each ensemble contains four independent simulations with the same transient forcing. Two estimates of natural variability, one used for optimisation and the other for the estimation of confidence intervals, are obtained from separate segments of a long control simulation.

Signal amplitudes estimated with multiple regression become uncertain when the signals are strongly correlated ("degenerate"). Despite the problem of degeneracy, positive and significant greenhouse gas and sulphate aerosol signals are consistently detected in the most recent fifty-year period (Figure 12.11) regardless of which or how many other signals are included in the analysis (Allen *et al.*, 2000a; Stott *et al.*, 2001). The residual variation that remains after removal of the signals is consistent with the model's internal variability. In contrast, recent decadal temperature changes are not consistent with the model's internal climate variability alone, nor with any combination of internal variability and naturally forced signals, even allowing for the possibility of unknown processes amplifying the response to natural forcing.

Tett *et al.* (2000) have completed a study using a model with no flux adjustments, an interactive sulphur cycle, an explicit representation of individual greenhouse gases and an explicit treatment of scattering by aerosols. Two ensembles of four simulations for the instrumental period were run, one with natural (solar and volcanic) forcing only and the other anthropogenic (well-mixed greenhouse gases, ozone and direct and indirect sulphate aerosol) forcing only (see Figure 12.4). They find a substantial response to anthropogenic forcing is needed to explain observed changes in recent decades, and that natural forcing may have contributed significantly to early 20th century climate change. The best agreement between model simulations and observations over the last 140 years has been found when all the above anthropogenic and natural forcing factors are included (Stott *et al.*, 2000b; Figure 12.7c). These results show that the forcings included are sufficient to explain the observed changes, but do not exclude the possibility that other forcings may also have contributed.

The detection of a response to solar forcing in the early part of the century (1906 to 1956) is less robust and depends on the details of the analysis. If seasonally stratified data are used (Stott *et al.*, 2001), the detection of a significant solar influence on climate in the first half of the century becomes clearer with the solar irradiance reconstruction of Hoyt and Schatten (1993), but weaker with that from Lean *et al.* (1995). Volcanism appears to show only a small signal in recent decadal temperature trends and could only be detected using either annual mean data or specifically chosen decades (Stott *et al.*, 2001). The residual variability that remains after the naturally forced signals are removed from the observations of the most recent five decades are not consistent with model internal variability, suggesting that natural

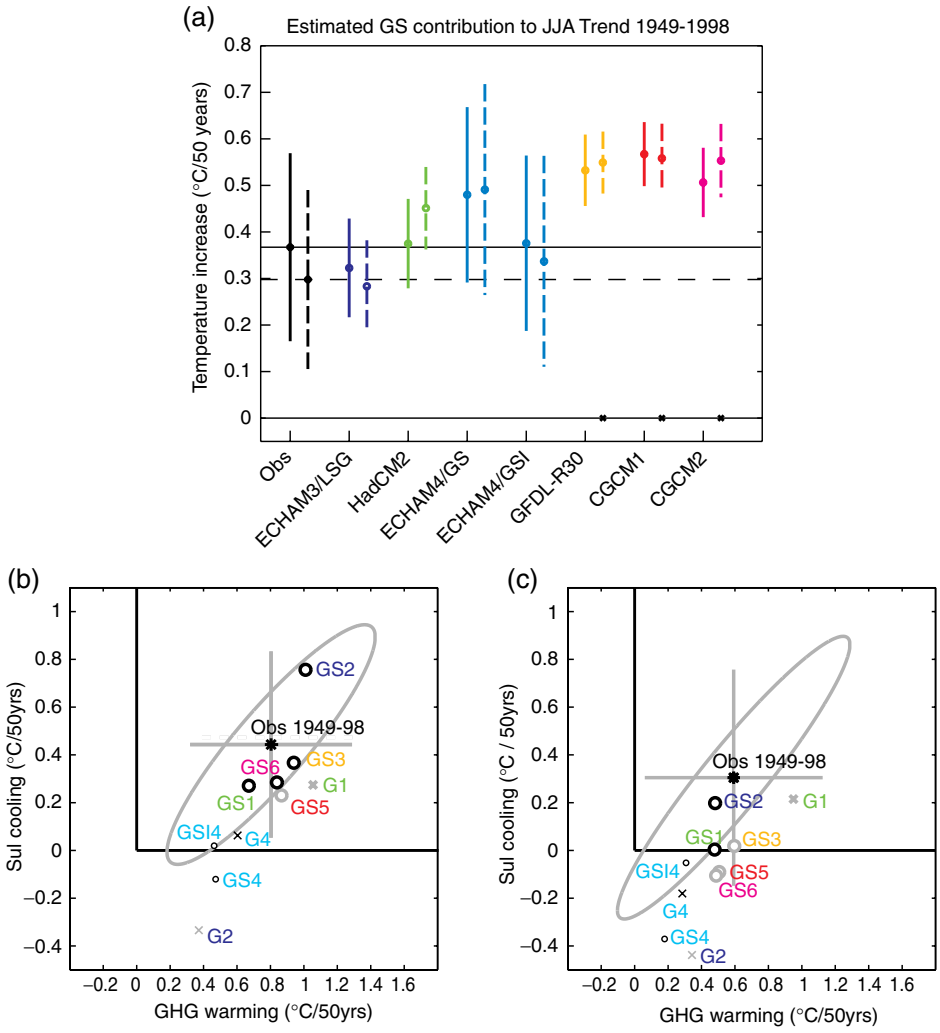

Figure 12.10: Comparison between the amplitude of anthropogenic signals from observed and modelled JJA trend patterns using fingerprints from two different climate models (ECHAM3/LSG and HadCM2) and data from five climate models. (a) Comparison of the amplitude of a single greenhouse gas + sulphate aerosol (GS) signal (expressed as change in global mean temperature [°C] over 50 years). Results show that a significant GS signal can be detected in observed trend patterns 1949 to 1998 at a 5% significance level (one-sided test), independent of which pair of fingerprints was used. The observed signal amplitude is consistent with contemporaneous GS amplitudes for most models' GS simulations. 90% confidence intervals are shown by solid lines for estimates using ECHAM3/LSG fingerprints and by dashed lines for estimates based on HadCM2 fingerprints. Cases where a model's and the observed amplitude disagree are marked by a cross on the axis. (b) and (c) show an estimate of the observed amplitude of a greenhouse gas signal (horizontal axis) and a sulphate aerosol signal (vertical axis) estimated simultaneously. Both signal amplitudes can be estimated as positive from observations based on ECHAM3/LSG fingerprints shown in (b) while only the greenhouse gas signal is detected based on HadCM2 fingerprints shown in panel (c). The amplitudes of both signals from the observations are compared with those from model simulations forced with various forcing histories and using different climate models (1: HadCM2; 2: ECHAM3/LSG; 3: GFDL; 4: ECHAM4/OPYC; 5: CCCma1; 6: CCCma2). Simulations with symbols shown in black are consistent with observations relative to the uncertainty in observations (grey ellipse) and that of the model simulations (not shown). Simulations which are inconsistent are shown in grey. Model simulations where only a single ensemble member is available are illustrated by thin symbols, those based on ensembles of simulations by fat symbols.

Results from consistency tests indicate that most greenhouse gas only simulations (G, shown by "×") are inconsistent with observations. Ten of the GS simulations in both panels are in agreement with observed trend patterns, discrepancies arise mostly from the magnitude of a sulphate signal (vertical axis). The failure to detect a sulphate signal as well as a greenhouse gas signal in panel (c) is due to the two signals being very highly correlated if only spatial patterns are used- this makes separation of the signals difficult. These results show that estimates of a sulphate aerosol signal from observations are model dependent and quite uncertain, while a single anthropogenic signal can be estimated with more confidence.

All units are in °C/50 year, values in the upper right quadrant refer to a physically meaningful greenhouse warming and sulphate aerosol cooling signal. The consistency test establishes whether the difference between a model's and the observed amplitude estimate is significantly larger than the combined uncertainty in the observations (internal variability + observational uncertainty) and the model simulation (internal variability). The figure is derived by updating the data used by Barnett *et al.* (1999) (for details of the analysis see Hegerl *et al.*, 2000) and then applying a simple linear transformation of the multi-regression results (Hegerl and Allen, 2000).

Results for 1946 to 1995 period used by Barnett *et al.* (1999) are similar, except fewer of the models in b and c agree with observations and the case of both signals being zero in c is not rejected. Simulations of natural forcing only ending before 1998 are also rejected in that case.

forcing alone cannot explain the observed 20th century temperature variations. Note that Delworth and Knutson (2000) find one out of five of their simulations with only anthropogenic forcing can reproduce the early century global mean warming, including the enhanced warming in Northern Hemisphere high latitudes. Hence a substantial response to anthropogenic (specifically greenhouse) forcing appears necessary to account for the warming over the past 50 years, but it remains unclear whether natural external forcings are necessary to explain the early 20th century warming.

Sensitivity of results

A variety of sensitivity tests confirm that the detection of anthropogenic signals is insensitive to differences between solar forcing reconstructions, the inclusion of additional forcing through the specification of observed stratospheric ozone concentrations, and to varying details of the analysis (including omitting the signal-to-noise optimisation). Tett *et al.* (1999, 2000) also found that detection of an anthropogenic signal continues to hold even when the standard deviation of the control simulation is inflated by a factor of two. Uncertainty in the signals is unavoidable when ensembles are small, as is the case in Tett *et al.* (1999), and biases the estimates of the signal amplitudes towards zero. Consistent results are obtained when this source of uncertainty is taken into account (Allen and Stott, 2000; Stott *et al.*, 2000a). However amplitude estimates become more uncertain, particularly if the underlying signal is small compared with internal climate variability. Accounting for sampling uncertainty in model-simulated signals indicates a greater degree of greenhouse warming and compensating aerosol cooling in the latter part of the century than shown by Tett *et al.* (1999). Gillett *et al.* (2000b) find that discounting the temperature changes associated with changes in the Arctic Oscillation (Thompson and Wallace, 1998; Thompson *et al.*, 2000), which are not simulated by the model, does not significantly alter the Tett *et al.* (1999) results.

Confidence intervals and scaling factors

Confidence intervals for the signal amplitudes that are obtained from the regression of modelled signals onto observations can be re-expressed as ranges of scaling factors that are required to make modelled signal amplitudes consistent with those estimated from observations (see, e.g., Allen and Tett, 1999). The results show that the range of scaling factors includes unity (i.e., model is consistent with observations) for both the greenhouse gas and the sulphate aerosol signal, and that the scaling factors vary only to a reasonable (and consistent) extent between 50-year intervals.

The scaling factors can also be used to estimate the contribution from anthropogenic factors other than well-mixed greenhouse gases. Using the methodology of Allen and Stott (2000) on the simulations described by Tett *et al.* (2000), the 5 to 95% uncertainty range for scaling the combined response changes in tropospheric ozone and direct and indirect sulphate forcing over the last fifty years is 0.6 to 1.6. The simulated indirect effect of aerosol forcing is by far the biggest contributor to this signal. Ignoring the possible effects of neglected forcings and assuming that the forcing can be scaled in the same way as the response, this translates to a –0.5 to –1.5 Wm^{-2} change in forcing due to the indirect effect since pre-industrial times. This range lies well within that given in Chapter 6 but the limits obtained are sensitive to the model used. Note that large values of the indirect response are consistently associated with a greater sensitivity to greenhouse gases. This would increase this model's estimate of future warming: a large indirect effect coupled with decreases in sulphate emissions would further enhance future warming (Allen *et al.*, 2000b).

Allen *et al.* (2000a) have determined scaling factors from other model simulations (Figure 12.12) and found that the modelled response to the combination of greenhouse gas and sulphate aerosol forcing is consistent with that observed. The scaling factors ranging from 0.8 to 1.2 and the corresponding 95% confidence intervals cover the range 0.5 to 1.6. Scaling factors for 50-year JJA trends are also easily derived from the results published in Hegerl *et al.* (2000). The resulting range of factors is consistent with that of Allen *et al.* (2000a), but wider because the diagnostic used in Allen *et al.* (2000b) enhances the signal-to-noise ratio. If it is assumed that the combination of greenhouse warming and sulphate cooling simulated by these AOGCMs is the only significant external contributor to inter-decadal near-surface temperature changes over the latter half of the 20th century, then Allen *et al.* (2000a) estimate that the anthropogenic warming over the last 50 years is 0.05 to 0.11°C/decade. Making a similar assumption, Hegerl *et al.* (2000) estimate 0.02 to 0.12°C/decade with a best guess of 0.06 to 0.08°C/decade (model dependent, Figure 12.10). The smallness of the range of uncertainty compared with the observed change indicates that natural internal variability alone is unlikely (bordering on very unlikely) to account for the observed warming.

Given the uncertainties in sulphate aerosol and natural forcings and responses, these single-pattern confidence intervals give an incomplete picture. We cannot assume that the response to sulphate forcing (relative to the greenhouse signal) is as simulated in these greenhouse-plus-sulphate simulations; nor can we assume the net response to natural forcing is negligible even though observations of surface temperature changes over the past 30 to 50 years are generally consistent with both these assumptions. Hence we need also to consider uncertainty ranges based on estimating several signals simultaneously (Figure 12.12, right hand panels). These are generally larger than the single-signal estimates because we are attempting to estimate more information from the same amount of data (Tett *et al.*, 1999; Allen and Stott, 2000; Allen *et al.*, 2000a). Nevertheless, the conclusion of a substantial greenhouse contribution to the recent observed warming trend is unchanged.

Estimation of uncertainty in predictions

The scaling factors derived from optimal detection can also be used to constrain predictions of future climate change resulting from anthropogenic emissions (Allen *et al.*, 2000b). The best guess scaling and uncertainty limits for each component can be applied to the model predictions, providing objective uncertainty limits that are based on observations. These estimates are independent of possible errors in the individual model's climate sensitivity and time-scale of oceanic adjustment, provided these

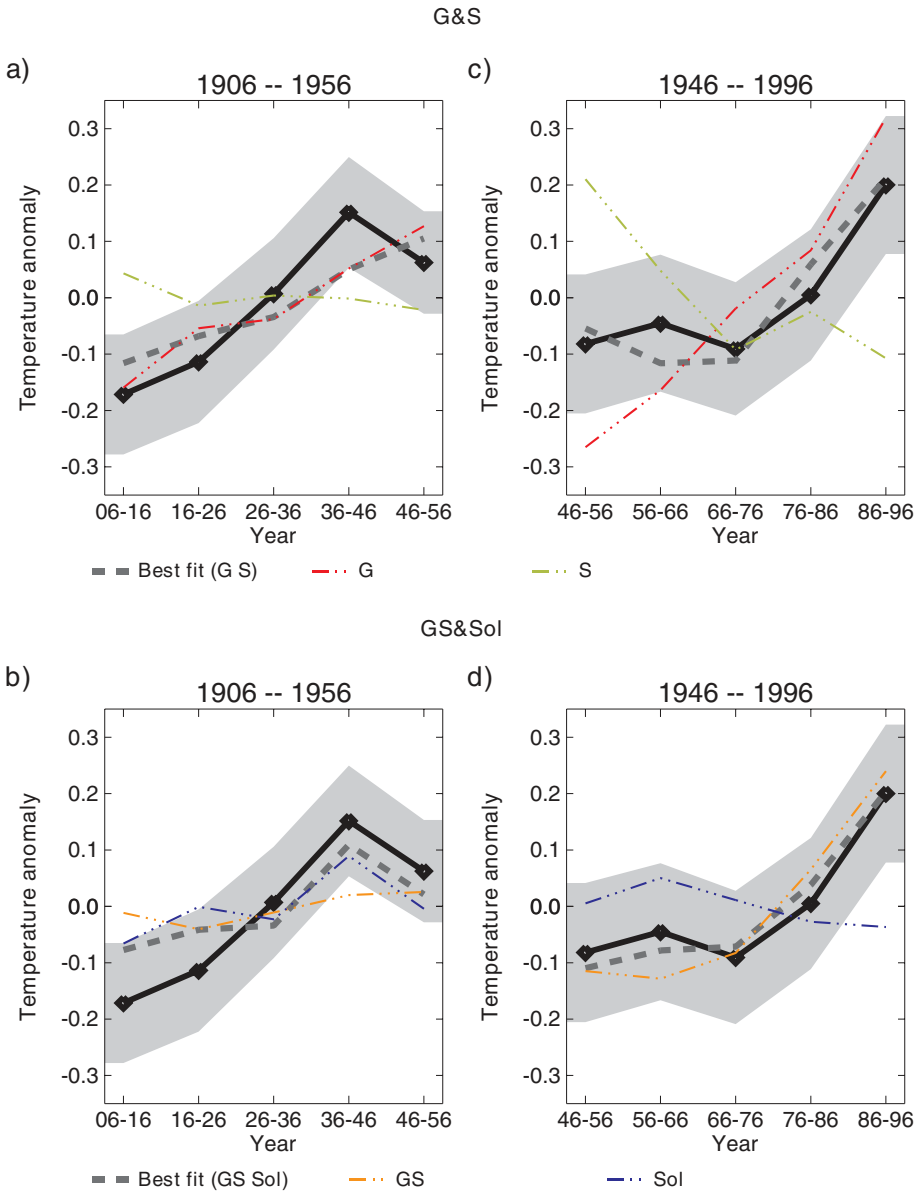

Figure 12.11: Best-estimate contributions to global mean temperature change. Reconstruction of temperature variations for 1906 to 1956 (a and b) and 1946 to 1995 (c and d) for G and S (a and c) and GS and SOL (b and d). (G denotes the estimated greenhouse gas signal, S the estimated sulphate aerosol signal, GS the greenhouse gas / aerosol signal obtained from simulations with combined forcing, SOL the solar signal). Observed (thick black), best fit (dark grey dashed), and the uncertainty range due to internal variability (grey shading) are shown in all plots. (a) and (c) show contributions from GS (orange) and SOL (blue). (b) and (d) show contributions from G (red) and S (green). All time-series were reconstructed with data in which the 50-year mean had first been removed. (Tett *et al.*, 1999).

errors are persistent over time. An example based on the IS92a (IPCC, 1992) GS scenario (whose exact forcing varies between models, see Chapter 9, Table 9.1 for details) is shown in Figure 12.13 based on a limited number of model simulations. Note that in each case, the original warming predicted by the model lies in the range consistent with the observations. A rate of warming of 0.1 to 0.2°C/decade is likely over the first few decades of the 21st century under this scenario. Allen *et al*. (2000b) quote a 5 to 95% ("very likely") uncertainty range of 0.11 to 0.24°C/decade for the decades 1996 to 2046 under the IS92a scenario, but, given the uncertainties and assumptions behind their analysis, the more cautious "likely" qualifier is used here. For comparison, the simple model tuned to the results of seven AOGCMs used for projections in Chapter 9 gives a range of 0.12 to 0.22°C/decade under the IS92a scenario, although it should be noted that this similarity may reflect some cancellation of errors and equally good agreement between the two approaches should not be expected for all scenarios, nor for time-scales longer than the few decades for which the Allen *et al*. (2000b) approach is valid. Figure 12.13 also shows that a similar range of uncertainty is obtained if the greenhouse gas and sulphate components are estimated separately, in which case the estimate of future warming for this particular scenario is independent of possible errors in the amplitude of the sulphate forcing and response. Most of the recent emission scenarios indicate that future sulphate emissions will decrease rather than increase in the near future. This would lead to a larger global warming since the greenhouse gas component would no longer be reduced by sulphate forcing at the same rate as in the past. The level of uncertainty also increases (see Allen *et al.*, 2000b). The final error bar in Figure 12.13 shows that including the model-simulated response to natural forcing over the 20th century into the analysis has little impact on the estimated anthropogenic warming in the 21st century.

It must be stressed that the approach illustrated in Figure 12.13 only addresses the issue of uncertainty in the large-scale climate response to a particular scenario of future greenhouse gas

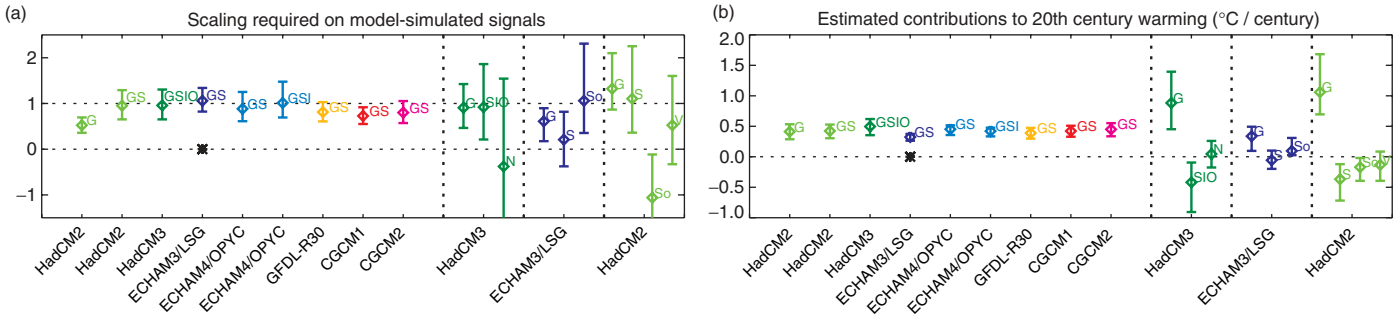

Figure 12.12: (a) Estimates of the "scaling factors" by which we have to multiply the amplitude of several model-simulated signals to reproduce the corresponding changes in the observed record. The vertical bars indicate the 5 to 95% uncertainty range due to internal variability. A range encompassing unity implies that this combination of forcing amplitude and model-simulated response is consistent with the corresponding observed change, while a range encompassing zero implies that this model-simulated signal is not detectable (Allen and Stott, 2000; Stott *et al.*, 2000a). Signals are defined as the ensemble mean response to external forcing expressed in large-scale (>5000 km) near-surface temperatures over the 1946 to 1996 period relative to the 1896 to 1996 mean. The first entry (G) shows the scaling factor and 5 to 95% confidence interval obtained if we assume the observations consist only of a response to greenhouse gases plus internal variability. The range is significantly less than one (consistent with results from other models), meaning that models forced with greenhouse gases alone significantly overpredict the observed warming signal. The next eight entries show scaling factors for model-simulated responses to greenhouse and sulphate forcing (GS), with two cases including indirect sulphate and tropospheric ozone forcing, one of these also including stratospheric ozone depletion (GSI and GSIO respectively). All but one (CGCM1) of these ranges is consistent with unity. Hence there is little evidence that models are systematically over- or under-predicting the amplitude of the observed response under the assumption that model-simulated GS signals and internal variability are an adequate representation (i.e. that natural forcing has had little net impact on this diagnostic). Observed residual variability is consistent with this assumption in all but one case (ECHAM3, indicated by the asterisk). We are obliged to make this assumption to include models for which only a simulation of the anthropogenic response is available, but uncertainty estimates in these single-signal cases are incomplete since they do not account for uncertainty in the naturally forced response. These ranges indicate, however, the high level of confidence with which we can reject internal variability as simulated by these various models as an explanation of recent near-surface temperature change.

A more complete uncertainty analysis is provided by the next three entries, which show corresponding scaling factors on individual greenhouse (G), sulphate (S), solar-plus-volcanic (N), solar-only (So) and volcanic-only (V) signals for those cases in which the relevant simulations have been performed. In these cases, we estimate multiple factors simultaneously to account for uncertainty in the amplitude of the naturally forced response. The uncertainties increase but the greenhouse signal remains consistently detectable. In one case (ECHAM3) the model appears to be overestimating the greenhouse response (scaling range in the G signal inconsistent with unity), but this result is sensitive to which component of the control is used to define the detection space. It is also not known how it would respond to the inclusion of a volcanic signal. In cases where both solar and volcanic forcing is included (HadCM2 and HadCM3), G and S signals remain detectable and consistent with unity independent of whether natural signals are estimated jointly or separately (allowing for different errors in S and V responses). (b) Estimated contributions to global mean warming over the 20th century, based on the results shown in (a), with 5 to 95% confidence intervals. Although the estimates vary depending on which model's signal and what forcing is assumed, and are less certain if more than one signal is estimated, all show a significant contribution from anthropogenic climate change to 20th century warming (from Allen *et al.*, 2000a).

concentrations. This is only one of many interlinked uncertainties in the climate projection problem, as illustrated in Chapter 13, Figure 13.2. Research efforts to attach probabilities to climate projections and scenarios are explored in Chapter 13, Section 13.5.2.3.

Forest *et al.* (2000) used simulations with an intermediate complexity climate model in a related approach. They used optimal detection results following the procedure of Allen and Tett (1999) to rule out combinations of model parameters that yield simulations that are not consistent with observations. They find that low values of the climate sensitivity (<1°C) are consistently ruled out, but the upper bound on climate sensitivity and the rate of ocean heat uptake remain very uncertain.

Other space-time approaches

North and Stevens (1998) use a space-frequency method that is closely related to the space-time approach used in the studies discussed above (see Appendix 12.2). They analyse 100-year surface temperature time-series of grid box mean surface temperatures in a global network of thirty six large (10°×10°) grid boxes for greenhouse gas, sulphate aerosol, volcanic and solar cycle signals in the frequency band with periods between about 8 and 17 years. The signal patterns were derived from simulations with an EBM (see Section 12.2.3). The authors found highly significant responses to greenhouse gas, sulphate aerosol, and volcanic forcing in the observations. Some uncertainty in their conclusions arises from model uncertainty (see discussion in Section 12.2.3) and from the use of control simulations from older AOGCMs, which had relatively low variability, for the estimation of internal climate variability.

A number of papers extend and analyse the North and Stevens (1998) approach. Kim and Wu (2000) extend the methodology to data with higher (monthly) time resolution and demonstrate that this may improve the detectability of climate change signals. Leroy (1998) casts the results from North and Stevens (1998) in a Bayesian framework. North and

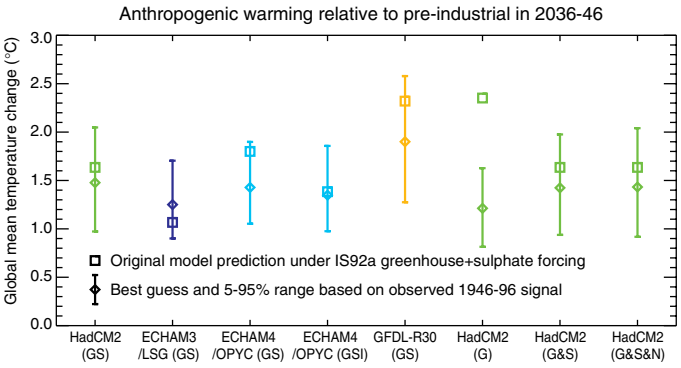

Figure 12.13: Global mean temperature in the decade 2036 to 2046 (relative to pre-industrial, in response to greenhouse gas and sulphate aerosol forcing following the IS92a (IPCC, 1992) scenario), based on original model simulations (squares) and after scaling to fit the observed signal as in Figure 12.12(a) (diamonds), with 5 to 95% confidence intervals. While the original projections vary (depending, for example, on each model's climate sensitivity), the scale should be independent of errors in both sensitivity and rate of oceanic heat uptake, provided these errors are persistent over time. GS indicates combined greenhouse and sulphate forcing. G shows the impact of setting the sulphate forcing to zero but correcting the response to be consistent with observed 20th century climate change. G&S indicates greenhouse and sulphate responses estimated separately (in which case the result is also approximately independent, under this forcing scenario, to persistent errors in the sulphate forcing and response) and G&S&N indicates greenhouse, sulphate and natural responses estimated separately (showing the small impact of natural forcing on the diagnostic used for this analysis). (From Allen *et al.*, 2000b.)

Wu (2001) modified the method to perform space-time (rather than space-frequency) detection in the 100-year record. Their results are broadly similar to those of Tett *et al.*, (1999), Stott *et al.* (2001) and North and Stevens (1998). However, their best guess includes a small sulphate aerosol signal countered by a relatively small, but highly significant, greenhouse gas signal.

All of the space-time and space-frequency optimal detection studies to date indicate a discernible human influence on global climate and yield better-constrained estimates of the magnitude of anthropogenic signals than approaches using spatial information alone. In particular, the inclusion of temporal information can reduce the degeneracy that may occur when more than one climate signal is included. Thus, results from time-space methods generally detect anthropogenic signals even if natural forcings are estimated simultaneously and show that the combination of natural signals and internal variability is inconsistent with the observed surface temperature record.

12.4.3.4 Summary of optimal fingerprinting studies

Results from optimal fingerprint methods indicate a discernible human influence on climate in temperature observations at the surface and aloft and over a range of applications. These methods can also provide a quantitative estimate of the magnitude of this influence. The use of a number of forced climate signals, and the extensive treatment of various (but not all) sources of uncertainty increases our confidence that a considerable part of the recent warming can be attributed to anthropogenic influences. The estimated signals and scaling factors remain subject to the considerable uncertainty in our knowledge of historic climate forcing from sources other than greenhouse gases. While estimates of the amplitude of a single anthropogenic signal are quite consistent between different model signals (see Figures 12.10, 12.12) and different approaches, joint estimates of the amplitude of several signals vary between models and approaches. Thus quantitative separation of the observed warming into anthropogenic and naturally forced components requires considerable caution. Nonetheless, all recent studies reject natural forcing and internal variability alone as a possible explanation of recent climate change. Analyses based on a single anthropogenic signal focusing on continental and global scales indicate that:

- Changes over the past 30 to 50 years are very unlikely to be due to internal variability as simulated by current models.
- The combined response to greenhouse and sulphate forcing is more consistent with the observed record than the response to greenhouse gases alone.
- Inclusion of the simulated response to stratospheric ozone depletion improves the simulation of the vertical structure of the response.

Analyses based on multiple anthropogenic and natural signals indicate that:

- The combination of natural external forcing (solar and volcanic) and internal variability is unlikely to account for the spatio-temporal pattern of change over the past 30 to 50 years, even allowing for possible amplification of the amplitude of natural responses by unknown feedback processes.
- Anthropogenic greenhouse gases are likely to have made a significant and substantial contribution to the warming observed over the second half of the 20th century, possibly larger than the total observed warming.
- The contribution from anthropogenic sulphate aerosols is less clear, but appears to lie in a range broadly consistent with the spread of current model simulations. A high sulphate aerosol forcing is consistently associated with a stronger response to greenhouse forcing.
- Natural external forcing may have contributed to the warming that occurred in the early 20th century.

Results based on variables other than continental and global scale temperature are more ambiguous.

12.5 Remaining Uncertainties

The SAR identified a number of factors that limited the degree to which any human influence on climate could be quantified. It was noted that detection and attribution of anthropogenic climate change signals would be accomplished through a gradual accumulation of evidence, and that there were appreciable uncertainties in the magnitude and patterns of natural variability, and in the radiative forcing and climate response resulting from human activity.

The SAR predicted an increase in the anthropogenic contribution to global mean temperature of slightly over 0.1°C in the five years following the SAR, which is consistent with the observed change since the SAR (Chapter 2). The predicted increase in the anthropogenic signal (and the observed change) are small compared to natural variability, so it is not possible to distinguish an anthropogenic signal from natural variability on five year time-scales.

Differences in surface and free atmosphere temperature trends
There are unresolved differences between the observed and modelled temperature variations in the free atmosphere. These include apparent changes in the temperature difference between the surface and the lower atmosphere, and differences in the tropical upper troposphere. While model simulations of large-scale changes in free atmospheric and surface temperatures are generally consistent with the observed changes, simulated and observed trends in troposphere minus surface temperature differences are not consistent. It is not clear whether this is due to model or observational error, or neglected forcings in the models.

Internal climate variability
The precise magnitude of natural internal climate variability remains uncertain. The amplitude of internal variability in the models most often used in detection studies differs by up to a factor of two from that seen in the instrumental temperature record on annual to decadal time-scales, with some models showing similar or larger variability than observed (Section 12.2; Chapter 8). However, the instrumental record is only marginally useful for validating model estimates of variability on the multi-decadal time-scales that are relevant for detection. Some palaeoclimatic reconstructions of temperature suggest that multi-decadal variability in the pre-industrial era was higher than that generated internally by models (Section 12.2; Chapter 8). However, apart from the difficulties inherent in reconstructing temperature accurately from proxy data, the palaeoclimatic record also includes the climatic response to natural forcings arising, for example, from variations in solar output and volcanic activity. Including the estimated forcing due to natural factors increases the longer-term variability simulated by models, while eliminating the response to external forcing from the palaeo-record brings palaeo-variability estimates closer to model-based estimates (Crowley, 2000).

Natural forcing
Estimates of natural forcing have now been included in simulations over the period of the instrumental temperature record. Natural climate variability (forced and/or internally generated) on its own is generally insufficient to explain the observed changes in temperature over the last few decades. However, for all but the most recent two decades, the accuracy of the estimates of forcing may be limited, being based entirely on proxy data for solar irradiance and on limited surface data for volcanoes. There are some indications that solar irradiance fluctuations have indirect effects in addition to direct radiative heating, for example due to the substantially stronger variation in the UV band and its effect on ozone, or hypothesised changes in cloud cover (see Chapter 6). These mechanisms remain particularly uncertain and currently are not incorporated in most efforts to simulate the climate effect of solar irradiance variations, as no quantitative estimates of their magnitude are currently available.

Anthropogenic forcing
The representation of greenhouse gases and the effect of sulphate aerosols has been improved in models. However, some of the smaller forcings, including those due to biomass burning and changes in land use, have not been taken into account in formal detection studies. The major uncertainty in anthropogenic forcing arises from the indirect effects of aerosols. The global mean forcing is highly uncertain (Chapter 6, Figure 6.8). The estimated forcing patterns vary from a predominantly Northern Hemisphere forcing similar to that due to direct aerosol effects (Tett *et al.*, 2000) to a more globally uniform distribution, similar but opposite in sign to that associated with changes in greenhouse gases (Roeckner *et al.*, 1999). If the response to indirect forcing has a component which can be represented as a linear combination of the response to greenhouse gases and to the direct forcing by aerosols, it will influence amplitudes of the responses to these two factors estimated through optimal detection.

Estimates of response patterns
Finally, there remains considerable uncertainty in the amplitude and pattern of the climate response to changes in radiative forcing. The large uncertainty in climate sensitivity, 1.5 to 4.5°C for a doubling of atmospheric carbon dioxide, has not been reduced since the SAR, nor is it likely to be reduced in the near future by the evidence provided by the surface temperature signal alone. In contrast, the emerging signal provides a relatively strong constraint on forecast transient climate change under some emission scenarios. Some techniques can allow for errors in the magnitude of the simulated global mean response in attribution studies. As noted in Section 12.2, there is greater pattern similarity between simulations of greenhouse gases alone, and of greenhouse gases and aerosols using the same model, than between simulations of the response to the same change in greenhouse gases using different models. This leads to some inconsistency in the estimation of the separate greenhouse gas and aerosol components using different models (see Section 12.4.3).

In summary, some progress has been made in reducing uncertainty, particularly with respect to distinguishing the responses to different external influences using multi-pattern techniques and in quantifying the magnitude of the modelled and observed responses. Nevertheless, many of the sources of uncertainty identified in the SAR still remain.

12.6 Concluding Remarks

In the previous sections, we have evaluated the different lines of evidence on the causes of recent climate change. Here, we summarise briefly the arguments that lead to our final assessment. The reader is referred to the earlier sections for more detail.

20th century climate was unusual.
Palaeoclimatic reconstructions for the last 1,000 years (e.g., Chapter 2, Figure 2.21) indicate that the 20th century warming is highly unusual, even taking into account the large uncertainties in these reconstructions.

The observed warming is inconsistent with model estimates of natural internal climate variability.
While these estimates vary substantially, on the annual to decadal time-scale they are similar, and in some cases larger, than obtained from observations. Estimates from models and observations are uncertain on the multi-decadal and longer time-scales required for detection. Nonetheless, conclusions on the detection of an anthropogenic signal are insensitive to the model used to estimate internal variability. Recent observed changes cannot be accounted for as pure internal variability even if the amplitude of simulated internal variations is increased by a factor of two or more. It is therefore unlikely (bordering on very unlikely) that natural internal variability alone can explain the changes in global climate over the 20th century (e.g., Figure 12.1).

The observed warming in the latter half of the 20th century appears to be inconsistent with natural external (solar and volcanic) forcing of the climate system.
Although there are measurements of these forcings over the last two decades, estimates prior to that are uncertain, as the volcanic forcing is based on limited measurements, and the solar forcing is based entirely on proxy data. However, the overall trend in natural forcing over the last two, and perhaps four, decades of the 20th century is likely to have been small or negative (Chapter 6,Table 6.13) and so is unlikely to explain the increased rate of global warming since the middle of the 20th century.

The observed change in patterns of atmospheric temperature in the vertical is inconsistent with natural forcing.
The increase in volcanic activity during the past two to four decades would, if anything, produce tropospheric cooling and stratospheric warming, the reverse to what has occurred over this period (e.g., Figure 12.8). Increases in solar irradiance could account for some of the observed tropospheric warming, but mechanisms by which this could cool the stratosphere (e.g., through changes in stratospheric ozone) remain speculative. Observed increases in stratospheric water vapour might also account for some of the observed stratospheric cooling. Estimated changes in solar radiative forcing over the 20th century are substantially smaller than those due to greenhouse gas forcing, unless mechanisms exist which enhance the effects of solar radiation changes at the ground. Palaeo-data show little evidence of such an enhancement at the surface in the past. Simulations based solely on the response to natural forcing (e.g., Figure 12.7a) are inconsistent with the observed climate record even if the model-simulated response is allowed to scale up or down to match the observations. It is therefore unlikely that natural forcing and internal variability together can explain the instrumental temperature record.

Anthropogenic factors do provide an explanation of 20th century temperature change.
All models produce a response pattern to combined greenhouse gas and sulphate aerosol forcing that is detectable in the 20th century surface temperature record (e.g., Figures 12.10, 12.12 (one model produces an estimate of internal variability which is not consistent with that observed)). Given that sulphate aerosol forcing is negative, and hence tends to reduce the response, detection of the response to the combined forcing indicates the presence of a greenhouse gas signal that is at least as large as the combined signal.

The effect of anthropogenic greenhouse gases is detected, despite uncertainties in sulphate aerosol forcing and response.
The analysis used to derive Figures 12.10a and 12.12, left box, assumes that the ratio of the greenhouse gas and sulphate aerosol responses in each model is correct. Given the uncertainty in sulphate aerosol forcing, this may not be the case. Hence one must also consider the separate responses to greenhouse gases and aerosols simultaneously. A greenhouse gas signal is consistently detected in the observations (e.g., Figure 12.10b,c, Figure 12.12 right hand boxes; North and Wu, 2001; Tett *et al.* 2000). The greenhouse gas responses are consistent with the observations in all but one case. The two component studies all indicate a substantial detectable greenhouse gas signal, despite uncertainties in aerosol forcing. The spread of estimates of the sulphate signal emphasises the uncertainty in sulphate aerosol forcing and response.

It is unlikely that detection studies have mistaken a natural signal for an anthropogenic signal.
In order to demonstrate an anthropogenic contribution to climate, it is necessary to rule out the possibility that the detection procedure has mistaken part or all of a natural signal for an anthropogenic change. On physical grounds, natural forcing is unlikely to account completely for the observed warming over the last three to five decades, given that it is likely that the overall trend in natural forcing over most of the 20th century is small or negative. Several studies have involved three or more components – the responses to greenhouse gases, sulphate aerosols and natural (solar, volcanic or volcanic and solar) forcing. These studies all detect a substantial greenhouse gas contribution over the last fifty years, though in one case the estimated greenhouse gas amplitude is inconsistent with observations. Thus it is unlikely that we have misidentified the solar signal completely as a greenhouse gas response, but uncertainty in the amplitude of the response to natural forcing continues to contribute to uncertainty in the size of the anthropogenic signal.

The detection methods used should not be sensitive to errors in the amplitude of the global mean forcing or response.
Signal estimation methods (e.g., Figures 12.10, 12.11 and 12.12)

allow for errors in the amplitude of the response, so the results should not be sensitive to errors in the magnitude of the forcing or the magnitude of the simulated model response. This would reduce the impact of uncertainty in indirect sulphate forcing on the estimated greenhouse and net sulphate signal amplitudes, to the extent that the pattern of response to indirect sulphate forcing resembles the pattern of response to direct sulphate forcing. Some models indicate this is may be the case, others do not, so this remains an important source of uncertainty. Note that if the spatio-temporal pattern of response to indirect sulphate forcing were to resemble the greenhouse response, it would lead to the amplitude of the greenhouse response being underestimated in cases where indirect sulphate forcing has not been included in the model. Detection and attribution results are also expected to be insensitive to all but the largest scale details of radiative forcing patterns. Detection is only possible at the largest spatial scales (e.g., Stott and Tett, 1998). In addition, atmospheric motions and large-scale feedbacks smooth out the response. All these arguments tend to reduce the impact of the large uncertainty in the magnitude of the forcing due to indirect sulphate aerosols. The inclusion of forcing from additional aerosols (see Chapter 6) is unlikely to alter our conclusion concerning the detection of a substantial greenhouse gas signal, though it is likely to affect estimates of the sulphate aerosol response. This is because part of the response to sulphate aerosols can be considered as surrogate for other aerosols, even though the patterns of forcing and response may differ on smaller scales. In general, the estimates of global mean forcing for other neglected factors are small (see Chapter 6, Figure 6.6).

Studies of the changes in the vertical patterns of temperature also indicate that there has been an anthropogenic influence on climate over the last 35 years.

One study finds that even when changes in stratospheric ozone and solar irradiance are taken into account, there is a detectable greenhouse gas signal in the vertical temperature record.

Observed and simulated vertical lapse rate changes are inconsistent over the last two decades, but there is an anthropogenic influence on tropospheric temperatures over a longer period.

Over the last twenty years, the observed warming trend in the lower troposphere has been smaller than at the surface. This contrasts with model simulations of the response to anthropogenic greenhouse gases and sulphate aerosols. Natural climate variability and the influence of natural external forcing, such as volcanism, can explain part of this difference. However, a discrepancy remains that cannot be accounted for with current climate models. The reduced warming in the lower troposphere does not, however, call into question the fact that the surface temperature has been warming over the satellite period (e.g., National Academy of Sciences, 2000). Over the longer period for which radiosonde data are available, an anthropogenic influence due to increasing greenhouse gases and decreasing stratospheric ozone is detected in all studies.

Natural factors may have contributed to the early century warming.

Most of the discussion in this section has been concerned with evidence relating to a human effect on late 20th century climate. The observed global mean surface temperature record shows two main periods of warming. Some studies detect a solar influence on surface temperature over the first five decades of the century, with perhaps a small additional warming due to increases in greenhouse gases. One study suggests that the early warming could be due to a combination of anthropogenic effects and a highly unusual internal variation. Thus the early century warming could be due to some combination of natural internal variability, changes in solar irradiance and some anthropogenic influence. The additional warming in the second half-century is most likely to be due to a substantial warming due to increases in greenhouse gases, partially offset by cooling due to aerosols, and perhaps by cooling due to natural factors towards the end of the period.

Appendix 12.1: Optimal Detection is Regression

The detection technique that has been used in most "optimal detection" studies performed to date has several equivalent representations (Hegerl and North, 1997; Zwiers, 1999). It has recently been recognised that it can be cast as a multiple regression problem with respect to generalised least squares (Allen and Tett, 1999; see also Hasselmann, 1993, 1997) in which a field of n "observations" $\mathbf{y}$ is represented as a linear combination of signal patterns $\mathbf{g}_1,...,\mathbf{g}_m$ plus noise $\mathbf{u}$

$$\mathbf{y} = \sum_{i=1}^{m} a_i \mathbf{g}_i + \mathbf{u} = \mathbf{G}\mathbf{a} + \mathbf{u} \qquad \text{(A12.1.1)}$$

where $\mathbf{G}=(\mathbf{g}_1|...|\mathbf{g}_m)$ is the matrix composed of the signal patterns and $\mathbf{a}=(a_1,...,a_m)^T$ is the vector composed of the unknown amplitudes. The field usually contains temperature observations, arrayed in space, either at the surface as grid box averages of surface temperature observations (typically 5×5 degrees; Santer *et al.*, 1995; Hegerl *et al.*, 1997; Tett *et al.*, 1999), or in the vertical as zonal averages of radiosonde observations (Karoly *et al.*, 1994; Santer *et al.*, 1996a; Allen and Tett, 1999). The fields are masked so that they represent only those regions with adequate data. The fields may also have a time dimension (Allen and Tett, 1999; North and Stevens; 1998; Stevens and North, 1996). Regardless of how the field is defined, its dimension n (the total number of observed values contained in any one single realisation of the field) is large. The signal patterns, which are obtained from climate models, and the residual noise field, have the same dimension. The procedure consists of efficiently estimating the unknown amplitudes $\mathbf{a}$ from observations and testing the null hypotheses that they are zero. In the event of rejection, testing the hypothesis that the amplitudes are unity for some combination of signals performs the attribution consistency test. This assumes, of course, that the climate model signal patterns have been normalised. When the signal is noise-free, estimates of the amplitudes are given by

$$\tilde{\mathbf{a}} = (\mathbf{G}^T \mathbf{C}_{\mathbf{uu}}^{-1} \mathbf{G})^{-1} \mathbf{G}^T \mathbf{C}_{\mathbf{uu}}^{-1} \mathbf{y} \qquad \text{(A12.1.2)}$$

where $\mathbf{C}_{\mathbf{uu}}$ is the $n\times n$ covariance matrix of the noise (Hasselmann, 1997, 1998; Allen and Tett, 1999; Levine and Berliner, 1999). Generalisations allow for the incorporation of signal uncertainties (see, for example, Allen *et al.*, 2000b). A schematic two-dimensional example is given in Box 12.1. In essence, the amplitudes are estimated by giving somewhat greater weight to information in the low variance parts of the field of observations. The uncertainty of this estimate, expressed as the $m\times m$ covariance matrix of $\mathbf{C}_{\mathbf{aa}}$ of $\tilde{\mathbf{a}}$, is given by

$$\mathbf{C}_{\mathbf{aa}} = (\mathbf{G}^T \mathbf{C}_{\mathbf{uu}}^{-1} \mathbf{G})^{-1} \qquad \text{(A12.1.3)}$$

This leads to a $(1-\alpha)\times 100\%$ confidence ellipsoid for the unknown amplitudes when $\mathbf{u}$ is the multivariate Gaussian that is given by

$$(\tilde{\mathbf{a}} - \mathbf{a})^T \mathbf{G}^T \mathbf{C}_{\mathbf{uu}}^{-1} \mathbf{G} (\tilde{\mathbf{a}} - \mathbf{a}) \le \chi^2_{\mathbf{1}-\alpha} \qquad \text{(A12.1.4)}$$

where $\chi^2_{1-\alpha}$ is the $(1-\alpha)$ critical value of the chi-squared distribution with m degrees of freedom. Marginal confidence ellipsoids can be constructed for subsets of signals simply by removing the appropriate rows and columns from $\mathbf{G}^T\mathbf{C}_{\mathbf{uu}}^{-1}\mathbf{G}$ and reducing the number of degrees of freedom. The marginal $(1-\alpha)\times 100\%$ confidence interval for the amplitude of signal i (i.e., the confidence interval that would be obtained in the absence of information about the other signals) is given by

$$\tilde{a}_i - z_{1-\alpha/2}(\mathbf{G}^T \mathbf{C}_{\mathbf{uu}}^{-1} \mathbf{G})_{ii} \le a_i \le \tilde{a}_i + z_{1-\alpha/2}(\mathbf{G}^T \mathbf{C}_{\mathbf{uu}}^{-1} \mathbf{G})_{ii} \qquad \text{(A12.1.5)}$$

where $Z_{1-\alpha/2}$ is the $(1-\alpha/2)$ critical value for the standard normal distribution. Signal i is said to be detected at the $\alpha/2\times 100\%$ significance level if the lower limit confidence interval (A12.1.5) is greater than zero. However, "multiplicity" is a concern when making inferences in this way. For example, two signals that are detected at the $\alpha/2\times 100\%$ significance level may not be jointly detectable at this level. The attribution consistency test is passed when the confidence ellipsoid contains the vector of units $(1,...,1)^T$.

Appendix 12.2: Three Approaches to Optimal Detection

Optimal detection studies come in several variants depending upon how the time evolution of signal amplitude and structure is treated.

Fixed pattern studies (Hegerl *et al.*, 1996, 1997, 2000a; Berliner *et al.*, 2000; Schnur, 2001) assume that the spatial structure of the signals does not change during the epoch covered by the instrumental record. This type of study searches for evidence that the amplitudes of fixed anthropogenic signals are increasing with time. The observed field $\mathbf{y}=\mathbf{y}(t)$ that appears on the left hand side of equation (A12.1.1) is typically a field of 30 to 50-year moving window trends computed from annual mean observations. The regression equation (A12.1.1) is solved repeatedly with a fixed signal matrix $\mathbf{G}$ as the moving 30 to 50-year window is stepped through the available record.

Studies with *time-varying patterns* allow the shape of the signals, as well as their amplitudes, to evolve with time. Such studies come in two flavours.

The *space-time* approach uses enlarged signal vectors that consist of a sequence of spatial patterns representing the evolution of the signal through a short epoch. For example, Tett *et al.* (1999) use signal vectors composed of five spatial patterns representing a sequence of decadal means. The enlarged signal matrix $\mathbf{G}=\mathbf{G}(t)$ evolves with time as the 5-decade window is moved one decade at a time. The observations are defined similarly as extended vectors containing a sequence of observed decadal mean temperature patterns. As with the fixed pattern approach, a separate model is fitted for each 5-decade window so that the evolution of the signal amplitudes can be studied.

The *space-frequency* approach (North *et al.*, 1995) uses annual mean signal patterns that evolve throughout the analysis period. A Fourier transform is used to map the temporal variation of each signal into the frequency domain. Only the low-frequency Fourier coefficients representing decadal-scale variability are retained and gathered into a signal vector. The observations are similarly transformed. The selection of time-scales that is effected by retaining only certain Fourier coefficients is a form of dimension reduction (see Dimension Reduction, Appendix 12.4) in the time domain. This is coupled with spatial dimension reduction that must also be performed. The result approximates the dimension reduction that is obtained by projecting observations in space and time on low order space-time EOFs (North *et al.*, 1995). A further variation on this theme is obtained by increasing the time resolution of the signals and the data by using monthly rather than annual means. Climate statistics, including means, variances and covariances, have annual cycles at this time resolution, and thus dimension reduction must be performed with cyclo-stationary space-time EOFs (Kim and Wu, 2000).

Given the same amount of data to estimate covariance matrices, the space-time and space-frequency approaches will sacrifice spatial resolution for temporal resolution.

Appendix 12.3: Pattern Correlation Methods

The pattern correlation methods discussed in this section are closely related to optimal detection with one signal pattern. Pattern correlation studies use either a centred statistic, R, which correlates observed and signal anomalies in space relative to their respective spatial means, or an uncentred statistic, C (Barnett and Schlesinger, 1987), that correlates these fields without removing the spatial means. It has been argued that the latter is better suited for detection, because it includes the response in the global mean, while the former is more appropriate for attribution because it better measures the similarity between spatial patterns. The similarity between the statistics is emphasised by the fact that they can be given similar matrix-vector representations. In the one pattern case, the optimal (regression) estimate of signal amplitude is given by

$$\tilde{a} = \mathbf{g}_1^T \mathbf{C}_{\mathbf{uu}}^{-1} \mathbf{y} \,/\, \mathbf{g}_1^T \mathbf{C}_{\mathbf{uu}}^{-1} \mathbf{g}_1 \qquad \text{(A12.3.1)}$$

The uncentred statistics may be written similarly as

$$C = \mathbf{g}_1^T \mathbf{y} \,/\, \mathbf{g}_1^T \mathbf{g}_1 \; = \mathbf{g}_1^T \mathbf{I} \mathbf{y} \,/\, \mathbf{g}_1^T \mathbf{I} \mathbf{g}_1 \qquad \text{(A12.3.2)}$$

where $\mathbf{I}$ is the $n \times n$ identity matrix. Similarly, the centred statistic can be written (albeit with an extra term in the denominator) as

$$R = \mathbf{g}_1^T (\mathbf{I}-\mathbf{U}) \mathbf{y} / [(\mathbf{g}_1^T (\mathbf{I}-\mathbf{U}) \mathbf{g}_1)^{1/2} (\mathbf{y}^T (\mathbf{I}-\mathbf{U}) \mathbf{y})^{1/2}] \qquad \text{(A12.3.3)}$$

where $\mathbf{U}$ is the $n \times n$ matrix with elements $u_{i,j}=1/n$. The matrix $\mathbf{U}$ removes the spatial means. Note that area, mass or volume weighting, as appropriate, is easily incorporated into these expressions. The main point is that each statistic is proportional to the inner product with respect to a matrix "kernel" between the signal pattern and the observations (Stephenson, 1997). In contrast with the pattern correlation statistics, the optimal signal amplitude estimate, which is proportional to a correlation coefficient using the so-called Mahalonobis kernel (Stephenson, 1997), maximises the signal-to-noise ratio.

Appendix 12.4: Dimension Reduction

Estimation of the signal amplitudes, as well as the detection and attribution consistency tests on the amplitudes, requires an estimate of the covariance matrix $\mathbf{C_{uu}}$ of the residual noise field. However, as $\mathbf{y}$ typically represents climate variation on timescales similar to the length of the observed instrumental record, it is difficult to estimate the covariance matrix reliably. Thus the covariance matrix is often estimated from a long control simulation. Even so, the number of independent realisations of $\mathbf{u}$ that are available from a typical 1,000 to 2,000-year control simulation is substantially smaller than the dimension of the field, and thus it is not possible to estimate the full covariance matrix. The solution is to replace the full fields $\mathbf{y}$, $\mathbf{g}_1,...,\mathbf{g}_m$ and $\mathbf{u}$ with vectors of dimension k, where $m<k<<n$, containing indices of their projections onto the dominant patterns of variability $\mathbf{f}_1,...,\mathbf{f}_k$ of $\mathbf{u}$. These patterns are usually taken to be the k highest variance EOFs of a control run (North and Stevens, 1998; Allen and Tett, 1999; Tett *et al.*, 1999) or a forced simulation (Hegerl *et al.*, 1996, 1997; Schnur, 2001). Stott and Tett (1998) showed with a "perfect model" study that climate change in surface air temperature can only be detected at very large spatial scales. Thus Tett *et al.* (1999) reduce the spatial resolution to a few spherical harmonics prior to EOF truncation. Kim *et al.* (1996) and Zwiers and Shen (1997) examine the sampling properties of spherical harmonic coefficients when they are estimated from sparse observing networks.

An important decision, therefore, is the choice of k. A key consideration in the choice is that the variability of the residuals should be consistent with the variability of the control simulation in the dimensions that are retained. Allen and Tett (1999) describe a simple test on the residuals that makes this consistency check. Rejection implies that the model-simulated variability is significantly different from that of the residuals. This may happen when the number of retained dimensions, k, is too large because higher order EOFs may contain unrealistically low variance due to sampling deficiencies or scales that are not well represented. In this situation, the use of a smaller value of k can still provide consistent results: there is no need to require that model-simulated variability is perfect on all spatio-temporal scales for it to be adequate on the very large scales used for detection and attribution studies. However, failing the residual check of Allen and Tett (1999) could also indicate that the model does not have the correct timing or pattern of response (in which case the residuals will contain forced variability that is not present in the control regardless of the choice of k) or that the model does not simulate the correct amount of internal variability, even at the largest scales represented by the low order EOFs. In this case, there is no satisfactory choice of k. Previous authors (e.g., Hegerl *et al.*, 1996, 1997; Stevens and North, 1996; North and Stevens, 1998) have made this choice subjectively. Nonetheless, experience in recent studies (Tett *et al.* 1999; Hegerl *et al.* 2000, 2001; Stott *et al.*, 2001) indicates that their choices were appropriate.

Appendix 12.5: Determining the Likelihood of Outcomes (*p*-values)

Traditional statistical hypothesis tests are performed by comparing the value of a detection statistic with an estimate of its natural internal variability in the unperturbed climate. This estimate must be obtained from control climate simulations because detection statistics typically measure change on timescales that are a substantial fraction of the length of the available instrumental record (see Appendix 12.4). Most "optimal" detection studies use two data sets from control climate simulations, one that is used to develop the optimal detection statistic and the other to independently estimate its natural variability. This is necessary to avoid underestimating natural variability. The p-value that is used in testing the no signal null hypothesis is often computed by assuming that both the observed and simulated projections on signal patterns are normally distributed. This is convenient, and is thought to be a reasonable assumption given the variables and the time and space scales used for detection and attribution. However, it leads to concern that very small p-values may be unreliable, because they correspond to events that have not been explored by the model in the available control integrations (Allen and Tett, 1999). They therefore recommend that p-values be limited to values that are consistent with the range visited in the available control integrations. A non-parametric approach is to estimate the p-value by comparing the value of the detection statistic with an empirical estimate of its distribution obtained from the second control simulation data set. If parametric methods are used to estimate the p-value, then very small values should be reported as being less than $1/n_p$ where n_p represents the equivalent number of independent realisations of the detection statistic that are contained in the second control integration.

References

Adcock,R.J., 1878: *The Analyst* (Des Moines, Iowa), **5**, 53.

Allen, M.R. and S.F.B.Tett, 1999: Checking for model consistency in optimal fingerprinting. *Clim. Dyn.*, **15**, 419-434.

Allen, M.R. and P.A. Stott, 2000: Interpreting the signal of anthropogenic climate change I: estimation theory. Tech. Report RAL-TR-2000-045, Rutherford Appleton Lab., Chilton, X11 0QX, UK.

Allen, M.R., N.P. Gillett, J.A. Kettleborough, R. Schnur, G.S. Jones, T. Delworth, F. Zwiers, G. Hegerl, T.P. Barnett, 2000a: Quantifying anthropogenic influence on recent near-surface temperature change", Tech. Report RAL-TR-2000-046, Rutherford Appleton Lab., Chilton, X11 0QX, UK.

Allen, M.R., P.A. Stott, R. Schnur, T. Delworth and J.F.B. Mitchell, 2000b: Uncertainty in forecasts of anthropogenic climate change. *Nature*, **407**, 617-620.

Angell, J.K.,1994: Global, hemispheric and zonal temperature anomalies derived from radiosonde records. pp. 636-672. In "Trends '93: A compendium of data on global change" (Eds. T. A. Boden *et al.*), ORNL/CDIAC-65, Oak Ridge, TN.

Bankes, H.T., R.A. Wood, J.M. Gregory, T.C. Johns and G.S Jones, 2000: Are observed changes in intermediate water masses a signature of anthropogenic climate change? *Geophys. Res. Lett.* , **27**, 2961-2964.

Barnett, T.P. and M.E. Schlesinger, 1987: Detecting changes in global climate induced by greenhouse gases. *J. Geophys. Res.,* **92**, 14772-14780.

Barnett, T.P., B.D. Santer, P.D. Jones, R.S. Bradley and K.R. Briffa, 1996: Estimates of low Frequency Natural Variability in Near-Surface Air Temperature. *The Holocene*, **6**, 255-263.

Barnett, T.P., K. Hasselmann, M. Chelliah, T. Delworth, G. Hegerl, P. Jones, E. Rasmussen, E. Roeckner, C. Ropelewski, B. Santer and S. Tett, 1999: Detection and attribution of climate change: A Status report. *Bull. Am. Met. Soc*., **12**, 2631-2659.

Barnett, T. P., G.C. Hegerl, T. Knutson and S.F.B. Tett, 2000: Uncertainty levels in predicted patterns of anthropogenic climate change. *J. Geophys.Res.*, **105**, 15525-15542.

Bengtsson, L., E.Roeckner, M.Stendel, 1999: Why is the global warming proceeding much slower than expected. *J. Geophys. Res.*, **104**, 3865-3876.

Berliner, L.M., R.A. Levine and D.J. Shea, 2000: Bayesian climate change assessment. *J.Climate,* **13**, 3805-3820.

Bertrand, C., J.-P. van Ypersele, A. Berger, 1999: Volcanic and solar impacts on climate since 1700. *Clim. Dyn.*, **15**, 355-367

Boer, G. J., G. Flato, M.C. Reader and D. Ramsden, 2000a: A transient climate change simulation with greenhouse gas and aerosol forcing: experimental design and comparison with the instrumental record for the 20th century. *Clim. Dyn.*, **16**, 405-426.

Boer, G.J., G. Flato, M.C. Reader and D. Ramsden, 2000b: A transient climate change simulation with greenhouse gas and aerosol forcing: projected for the 21st century. *Clim. Dyn.*, **16**, 427-450.

Briffa, K.R., P.D. Jones, F.H. Schweingruber and T.J. Osborn, 1998: Influence of volcanic eruptions on Northern Hemisphere summer temperature over the past 600 years. *Nature,* **393**, 450-454.

Briffa, K.R., T.J. Osborn, F.H. Schweingruber, I.C. Harris, P.D. Jones, S.G. Shiyatov and E.A. Vaganov, 2000: Low-frequency temperature variations from a northern tree-ring density network. *J.Geophys.Res*. **106**, 2929-2942.

Brown, L., G. Casella and T.G. Hwang, 1995: Optimal confidence sets, bioequivalence and the limacon of Pascal. *J. Amer. Statist. Soc.*, **90**, 880-889.

Brown, S.J., D.E. Parker, C.K. Folland and I. Macadam, 2000a: Decadal variability in the lower-tropospheric lapse rate. *Geophys. Res. Lett*., **27**, 997-1000.

Brown, S.J., D.E. Parker and D.M.H. Sexton, 2000b: Differential changes in observed surface and atmospheric temperature since 1979. Hadley Centre Technical Note No. 12, The Met. Office Bracknell, UK, pp41.

Chanin, M.-L. and V. Ramaswamy, 1999: "Trends in Stratospheric Temperatures" in WMO (World Meteorological Organization), Scientific Assessment of Ozone Depletion: 1998, Global Ozone Research and Monitoring Project - Report No. 44, Geneva. 5.1-5.59

Collins, M., T.J. Osborn, S.F.B. Tett, K.R. Briffa and F.H. Schwingruber, 2000: A comparison of the variability of a climate model with a network of tree-ring densities. Hadley Centre Technical Note 16.

Crowley, T.J., 2000: Causes of climate change over the last 1000 years, *Science*, **289**, 270-277.

Crowley, T.J. and K.-Y. Kim, 1996: Comparison of proxy records of climate change and solar forcing. *Geophys. Res. Lett*. **23**: 359-362.

Crowley, T.J. and Kim K.-Y., 1999: Modelling the temperature response to forced climate change over the last six centuries. *Geophys. Res. Lett*., **26**, 1901-1904.

Crowley, T.J. and T. Lowery, 2000: How warm was the Medieval warm period? *Ambio,* **29**, 51-54.

Cubasch, U., G.C. Hegerl and J. Waszkewitz,1996: Prediction, detection and regional assessment of anthropogenic climate change. *Geophysica*, **32**, 77-96.

Cubasch, U., G.C. Hegerl, R. Voss, J. Waszkewitz and T.J. Crowley, 1997: Simulation of the influence of solar radiation variations on the global climate with an ocean-atmosphere general circulation model. *Clim. Dyn.*, **13**, 757-767.

Delworth, T.L. and T.R. Knutson, 2000. Simulation of early 20th century global warming. *Science*, **287**, 2246-2250.

Dempster, A.P., 1998: Logicist statistics I. Models and modeling. *Statistical Science*, **13**, 248-276.

Drijfhout, S.S., R.J. Haarsma, J.D.Opsteegh, F.M. Selten, 1999: Solar-induced versus internal variability in a coupled climate model. *Geophys. Res. Lett*., **26**, 205-208.

Folland, C.K., D.M.H. Sexton, D.J.K. Karoly, C.E. Johnston, D.P. Rowell and D.E. Parker, 1998: Influences of anthropogenic and oceanic forcing on recent climate change. *Geophys. Res. Lett*., **25**, 353-356.

Forest, C.E., M.R. Allen, P.H. Stone, A.P. Sokolov, 2000: Constraining uncertainties in climate models using climate change detection techniques. *Geophys. Res. Lett*., **27**, 569-572.

Forster, P.M. and K.P. Shine, 1999: Stratospheric water vapour changes as a possible contributor to observed stratospheric cooling. *Geophys. Res. Lett*., **26**,3309-3312.

Free, M. and A. Robock, 1999: Global Warming in the Context of the little Ice Age. *J.Geophys Res*, **104**, 19057-19070.

Froehlich, K. and J. Lean, 1998: The Sun's Total Irradiance: Cycles, Trends and Related Climate Change Uncertainties since 1976. *Geophys. Res. Lett*., **25**, 4377-4380.

Fyfe, J.C., G.J. Boer and G.M. Flato 1999: The Arctic and Antarctic Oscillations and their projected changes under global warming. *Geophys. Res. Lett*., **26**, 1601-1604.

Gaffen, D.J., B.D. Santer, J.S. Boyle, J.R. Christy, N.E. Graham and R.J.Ross, 2000. Multi-decadal changes in vertical temperature structure of the tropical troposphere. *Science*, **287**, 1242-1245.

Gillett, N., M.R. Allen and S.F.B. Tett, 2000a: Modelled and observed variability in atmospheric vertical temperature structure. *Clim Dyn*, **16**, 49-61.

Gillett, N, G.C. Hegerl, M.R. Allen, P.A. Stott, 2000b: Implications of observed changes in the Northern Hemispheric winter circulation for the detection of anthropogenic climate change. *Geophys.Res.Lett.*, **27**, 993-996..

Graf, H.-F., I. Kirchner, I. Schult 1996: Modelling Mt. Pinatubo Climate Effects. NATO-ASI Series, Vol 142, The Mount Pinatubo Eruption, Fiocco G and Dua D. eds., Springer, 1996: 219-231.

Graf, H-F., I. Kirchner and J. Perlwitz,1998: Changing lower stratospheric circulation: The role of ozone and greenhouse gases. *J.*

Geophys. Res., **103**, 11251-11261.

Grieser, J.and C.-D. Schoenwiese, 1999: Parameterization of spatio-temporal patterns of volcanic aerosol induced stratospheric optical depth and its climate radiative forcing. *Atmosfera*, **12**, 111-133

Grieser, J. and C.-D. Schoenwiese, 2001: Process, forcing and signal analysis of global mean temperature variations by means of a three box energy balance model. *Clim. Change*, in press.

Haigh, J.D., 1999: A GCM study of climate change in response to the 11-year solar cycle. *Quart. J. R. Met. Soc*., **125**, 871-892.

Hansen J., Mki.Sato, R. Ruedy, A. Lacis, K. Asamoah, S. Borenstein, E. Brown, B. Cairns, G. Caliri, M. Campbell, B. Curran, S. deCastro, L. Druyan , M. Fox, C. Johnson, J. Lerner, M.P. McCormick, R. Miller, P. Minnis, A. Morrison, L. Pandolfo, I. Ramberran, F. Zaucker, M. Robinson, P. Russell, K. Shah, P. Stone, I. Tegen, L. Thomason, J. Wilder and H. Wilson 1996: A Pinatubo climate modeling investgation. In "The Mount Pinatubo Eruption: Effects on the Atmosphere and Climate", Fiocco G and Fua Visconti G, Springer Verlag, Berlin, pp 233-272.

Hansen, J., M. Sato and R. Reudy, 1997a: Radiative forcing and climate response. *J. Geophys. Res*., **102**, 6831-6864.

Hansen, J.E., M. Sato, A. Lacis and R. Reudy, 1997b: The missing climate forcing. *Roy. Soc. Phil. Trans. B*, **352**, 231-240.

Hansen, J.E., M.Sato, A. Lacis, R.Reudy, I .Tegen and E. Matthews, 1998. Climate forcings in the industrial era. *Proc. Nat. Acad. Sci. U.S.A*., **95**, 12753-12758.

Harrison, R.G. and K.P. Shine, 1999: A review of recent studies of the influence of solar changes on the Earth's climate. Hadley Centre Tech. Note 6. Hadley Centre for Climate Prediction and Research, Meteorological Office, Bracknell RG12 2SY UK pp 65

Hasselmann, K., 1976: Stochastic climate models. Part 1. Theory. *Tellus*, **28**, 473-485.

Hasselmann, K., 1979. On the signal-to-noise problem in atmsopheric response studies. Meteorology over the tropical oceans, D.B. Shaw ed., Roy Meteorol. Soc., 251-259

Hasselmann, K., 1993: Optimal fingerprints for the Detection of Time dependent Climate Change. *J. Climate*, **6**: 1957-1971.

Hasselmann, K. ,1997: Multi-pattern fingerprint method for detection and attribution of climate change. *Clim. Dyn.*, **13:** 601-612.

Hasselmann, K., 1998: Conventional and Bayesian approach to climate-change detection and attribution. *Quart. J. R. Met. Soc.*, **124**, 2541-2565.

Hasselmann, K., L. Bengtsson , U. Cubasch, G.C. Hegerl, H. Rodhe, E. Roeckner, H. von Storch, R.Voss and J. Waskewitz,1995: Detection of an anthropogenic fingerprint. In:*Proceedings of Modern Meteorology" Symposium in honour of Aksle Wiin-Nielsen, 1995.* P. Ditvelson (ed) ECMWF.

Haywood, J.M., R. Stouffer, R. Wetherald, S. Manabe and V. Ramaswamy, 1997: Transient response of a coupled model to estimated changes in grenhouse gas and sulphate concentrations. *Geophys. Res. Lett.* , **24**, 1335- 1338.

Hegerl, G.C. and G.R. North 1997: Statistically optimal methods for detecting anthropogenic climate change. *J. Climate*, **10**: 1125-1133.

Hegerl, G.C. and M.R. Allen, 2000: Physical interpretation of optimal detection. Tech Report RAL-TR-2001-010, Rutherford Appleton Lab., Chilton, X11 0QX, U.K.

Hegerl, G.C., von Storch, K. Hasselmann, B.D. Santer, U. Cubasch and P.D. Jones 1996: Detecting Greenhouse Gas induced Climate Change with an Optimal Fingerprint Method. *J. Climate*, **9**, 2281-2306.

Hegerl, G.C., K Hasselmann, U. Cubasch, J.F.B. Mitchell, E. Roeckner, R. Voss and J. Waszkewitz 1997: Multi-fingerprint detection and attribution of greenhouse gas- and aerosol forced climate change. *Clim. Dyn.* **13**, 613-634

Hegerl, G.C., P. Stott, M. Allen, J.F.B.Mitchell, S.F.B.Tett and U.Cubasch, 2000: Detection and attribution of climate change: Sensitivity of results to climate model differences. *Clim. Dyn*., **16**, 737-754

Hegerl, G.C., P.D. Jones and T.P. Barnett. 2001: Effect of observational sampling error on the detection of anthropogenic climate change. *J. Climate*, **14**, 198-207.

Hill, D.C., M.R. Allen, P.A. Stott, 2001: Allowing for solar forcing in the detection of human influence on atmospheric vertical temperature structures. *Geophys. Res. Lett*., **28**, 1555-1558.

Hoyt, D.V. and K.H. Schatten,1993: A discussion of plausible solar irradiance variations, 1700-1992. *J. Geophys. Res.*, **98**, 18895-18906.

IPCC, 1990: Climate change: the IPCC scientific assessment [Houghton, J.T., G.J. Jenkins and J.J. Ephraums (eds.)] Cambridge University Press, Cambridge, United Kingdom, 365pp.

IPCC, 1992: Climate Change 1992: The Supplementary Report to the Intergovernmental Panel on Climate Change Scientific Assessment [Houghton, J.T., B.A. Callander and S.K. Varney (eds.)]. Cambridge University Press, Cambridge, United Kingdom and New York, NY, USA, 100 pp.

IPCC,1996: Climate Change 1995. The IPCC second scientific assessment. Houghton JT, L.G. Meira Filho, B.A. Callander, N. Harris, A. Kattenberg , K. Maskell (eds.). Cambridge University Press, Cambridge, 572 pp.

Johns, T.C., J.M. Gregory, P. Stott and J.F.B. Mitchell, 2001: Assessment of the similarity between modelled and observed near surface temperature changes using ensembles. *Geophys. Res. Lett*. 28, 1007-1010.

Jones, A., D.L. Roberts and M.J. Woodage, 1999: The indirect effects of anthropogenic aerosl simulated using a climate model with an interactive sulphur cycle . Hadley Centre Tech. Note 14. Hadley Centre for Climate Prediction and Research, Meteorological Office, Bracknell RG12 2SY UK, pp39.

Jones, P.D. and G.C. Hegerl, 1998: Comparisons of two methods of removing anthropogenically related variability from the near—surface observational temperature field. *J.Geophys.Res*., **103**, D12: 1377-13786

Jones, P.D., K.R. Briffa, T.P. Barnett and S.F.B. Tett, 1998: High-resolution paleoclimatic records for the last millenium. *The Holocene* **8**: 467-483.

Jones, P.D., T.J. Osborn, K.R. Briffa, C.K. Folland, B. Horton, L.V. Alexander, D.E. Parker and N.A. Raynor, 2001:Adjusting for sampling density in grid-box land and ocean surface temperature time series, *J. Geophys. Res.*, **106**, 3371-3380

Karoly, D. J. and K. Braganza, 2001: Identifying global climate change using simple indices. *Geophys. Res. Lett*., in press.

Karoly, D.J., J.A. Cohen, G.A. Meehl, J.F.B. Mitchell, A.H. Oort, R.J. Stouffer, R.T. Weatherald, 1994: An example of fingerprint detection of greenhouse climate change. *Clim. Dyn*, **10**, 97-105.

Kattenberg, A., F. Giorgi, H. Grassl, G.A. Meehl, J.F.B. Mitchell, R. Stouffer, T. Tokioka, A.J. Weaver and T.M.L. Wigley, 1996: Climate Models - Projections of Future Climate. Houghton *et al.* (eds.), The IPCC Second Scientific Assessment. Cambridge University Press, Cambridge, 285-357.

Kaufmann, R.K. and D.I. Stern, 1997: Evidence for human influence on climate from hemispheric temperature relations. *Nature*, **388**, 39-44.

Kelly, P.M., P.D. Jones, J. Pengqun, 1996: The spatial response of the climate system to explosive volcanic eruptions. *Int. J. Climatol.* **16**, 537-550.

Kim, K.-Y. and Q. Wu, 2000: Optimal detection using cyclostationary EOFs. *J. Climate*, **13**, 938-950.

Kim, K.-Y., G.R. North, S.S. Shen, 1996: Optimal estimation of spherical harmonic components from a sample of spatially nonuniform covariance statistics. *J. Climate*, **9**, 635-645.

Kirchner, I., G.L. Stenchikov, H.-F.Graf, A.Robock and J.C.Antuna, 1999: Climate model simulation of winter warming and summer cooling following the 1991 Mount Pinatubo volcanic eruption. *J. Geophys. Res*., **104**, 19,039-19,055.

Knutson, T.R., T.L. Delworth, K. Dixon and R.J. Stouffer, 2000: Model

assessment of regional surface temperature trends (1949-97), *J. Geophys. Res.*, **104**, 30981-30996.

Labitzke, K. and H.van Loon, 1997: The signal of the 11-year sunspot cycle in the upper troposphere-lower stratosphere. *Space Sci. Rev*., **80**, 393-410.

Lamb, H. H., 1970: Volcanic dust in the atmosphere; with a chronology and assessment of its meteorological significance, Philosophical transactions of the Royal Society of Londen, A 266, 425-533

Laut, P. and J. Gunderman, 1998: Does the correlation between the solar cycle and hemispheric land temperature rule out any significant global warming from greenhouse gases? *J. Atmos. Terrest. Phys*., **60**, 1-3.

Lean, J., 1997: The Sun's Variable Raditation and its relevance for earth. *Annu. Rev. Astrophys*. **35**, 33-67

Lean, J., J.Beer and R.Bradley, 1995: Reconstruction of solar irradiance since 1600: Implications For climate change. *Geophys. Res. Lett.*, **22**, 3195-3198.

Lean, J., D. Rind, 1998: Climate Forcing by Changing Solar Radiation. *J. Climate*, **11**, 3069-3094.

Legates, D. R. and R. E. Davis, 1997 The continuing search for an anthropogenic climate change signal: limitations of correlation based approaches. *Geophys. Res. Lett.*, **24**, 2319-2322

Leroy, S., 1998: Detecting Climate Signals: Some Bayesian Aspects. *J. Climate* **11**, 640-651.

Levine, R.A. and L.M. Berliner, 1999: Statistical principles for climate change studies. *J. Climate*, **12**, 564-574.

Lockwood, M. and R. Stamper 1999: Long-term drift of the coronal source magnetic flux and the total solar irradiance, *Geophys. Res. Lett*., **26**, 2461-2464

Mann, M.E., R.S. Bradley, M.K. Hughes, 1998: Global scale tmperature patterns and climate forcing over the past six centuries. *Nature*, **392**, 779-787.

Mann, M.E., E. Gille, R.S. Bradley, M.K. Hughes, J.T. Overpeck, F.T. Keimig and W. Gross, 2000b: Global temperature patterns in past centuries: An interactive presentation. *Earth Interactions*, **4/4**, 1-29.

Mao, J. and A. Robock, 1998: Surface air temperature simulations by AMIP general circulation models: Volcanic and ENSO signals and systematic errors. *J. Climate*, **11**, 1538-1552.

Michaels, P.J. and P.C. Knappenburger, 1996: Human effect on global climate? *Nature*, **384**, 523-524.

Mitchell, J.F.B. and T.C. Johns, 1997: On the modification of greenhouse warming by sulphate aerosols. *J. Climate*, **10**, 245-267

Mitchell, J.F.B., R.A. Davis, W.J. Ingram and C.A. Senior, 1995a: On surface temperature, greenhouse Gases and aerosols, models and observations. *J. Climate*, **10**, 2364-3286.

Mitchell, J.F.B., T.J. Johns, J.M. Gregory and S.F.B. Tett, 1995b: Transient climate response to Increasing sulphate aerosols and greenhouse gases. *Nature*, **376**, 501-504.

National Academy of Sciences, 2000; Reconciling observations of global temperature change. 85pp. Nat. Acad. Press, Washington, DC.

North, G.R. and M. Stevens,1998: Detecting Climate Signals in the Surface Temperature Record. *J. Climate,* **11**,: 563-577.

North, G.R. and Q. Wu, 2001: Detecting Climate Signals Using Space Time EOFs. *J. Climate,* **14**, 1839-1863.

North, G.R., K-Y Kim, S. Shen and J.W. Hardin 1995: Detection of Forced Climate Signals, Part I: Filter Theory. *J. Climate*, **8**, 401-408.

Osborn, T.J., K.R. Briffa, S.F.B. Tett, P.D. Jones and R.M. Trigo, 1999: Evaluation of the North Atlantic Oscillation as simulated by a coupled climate model. *Clim. Dyn*. **15**, 685-702.

Overpeck, J., K. Hughen, D. Hardy, R. Bradley, R. Case, M. Douglas, B. Finney, K. Gajewski, G. Jacoby, A. Jennings, S. Lamoureux, A. Lasca, G. MacDonald, J. Moore, M. Retelle, S. Smith, A. Wolfe, G. Zielinksi,1997: Arctic Environmental Change of the Last Four Centuries. *Science,* **278**, 1251-1256.

Paeth, H. and H. Hense, 2001: Signal Analysis of the northern hemisphere atmospheric mean temperature 500/1000 hPa north of 55N between 1949 and 1994. *Clim. Dyn.*, in press.

Paeth, H., A. Hense, R. Glowenka-Hense, R.Voss and U.Cubasch, 1999: The North Atlantic Oscillation as an indicator for greenhouse gas induced climate change. *Clim. Dyn.*, **15**, 953-960.

Parker, D.E., M.Gordon, D.P.M.Cullum, D.M.H.Sexton, C.K.Folland and N.Rayner 1997: A new global gridded radiosonse temperature data base and recent temperature trends. *Geophys. Res. Lett*., **24**, 1499-1502.

Parkinson, C. L., D. J. Cavalieri, P. Gloersen, H. J. Zwally and J. C.Comiso, 1999: Arctic sea ice extents, areas and trends, 1978-1996, *J. Geophys. Res*., **104**, 20,837-20,856.

Priestley, M. B., "Spectral Analysis and Time-series", Volume 1, Academic Press, 1981.

Reader, M.C. and G.J. Boer, 1998: The modification of greenhouse gas warming by the direct effect of sulphate aerosols. *Clim. Dyn.*, **14**, 593-607.

Rind, D., J. Lean and R. Healy, 1999: Simulated time-depended climate response to solar radiative forcing since 1600. *J. Geophys. Res*. 104: 1973-1990.

Ripley, B.D. and M. Thompson, 1987: Regression techniques for the detection of analytical bias. *Analyst*, **112**, 377-383.

Risbey, J., M. Kandlikar and D. Karoly, 2000: A framework to articulate and quantify uncertainty in climate change detection and attribution. *Clim. Res*., **16**, 61-78.

Robock, A. and J. Mao 1992: Winter warming from large volcanic eruptions. *Geophys. Res. Lett*. **19**, 2405-2408.

Robock, A. and M. Free,1995: Ice cores as an index of global volcanism from 1850 to the present, *J. Geophys. Res*., **100**, 11567-11576.

Robock, A. and M. Jianping, 1995: The volcanic signal in surface temperature observations. *J. Climate*, **8**, 1086-1103.

Roeckner, E., L. Bengtsson, J. Feichter, J. Lelieveld and H. Rodhe, 1999: Transient climate change simulations with a coupled atmosphere-ocean GCM including the tropospheric sulfur cycle. *J. Climate*, **12**, 3004-3032.

Santer, B.D., T.M.L. Wigley and P.D. Jones, 1993:Correlation methods in fingerprint detection studies. *Clim Dyn*., **8**, 265-276.

Santer, B.D., K.E. Taylor, J.E. Penner, T.M.L. Wigley, U. Cubasch and P.D. Jones, 1995: Towards the detection and attribution of an anthropogenic effect on climate. *Clim. Dyn*., **12**, 77-100.

Santer, B.D., K.E. Taylor, T.M.L. Wigley, P.D. Jones, D.J. Karoly, J.F.B. Mitchell, A.H. Oort, J.E.Penner, V. Ramaswamy, M.D. Schwarzkopf, R.S. Stouffer and S.F.B. Tett, 1996a: A search for human influences on the thermal structure in the atmosphere. *Nature*, **382**, 39-46.

Santer, B.D., K.E. Taylor, T.M.L. Wigley, T.C. Johns, P.D. Jones, D.J. Karoly, J.F.B. Mitchell, A.H. Oort, J.E. Penner, V. Ramaswamy, M.D. Schwartzkopf, R.J. Stouffer and S.F.B. Tett, 1996b: Human effect on global climate? *Nature*, **384**, 522-524.

Santer, B.D., T.M.L. Wigley, T.P. Barnett, E. Anyamba, 1996c: Detection of climate change and attribution of causes. in: J. T. Houghton *et al.* (eds.) Climate change 1995. The IPCC Second Scientific Assessment, Cambridge University Press, Cambridge, pp. 407-444.

Santer, B.D., T.M.L. Wigley, D.J. Gaffen, C. Doutriaux, J.S. Boyle, M. Esch, J.J. Hnilo, P.D. Jones, G.A. Meehl, E. Roeckner, K.E. Taylor and M.F. Wehner 2000: Interpreting Differential Temperature Trends at the Surface and in the lower Troposphere, *Science*, **287**, 1227-1231.

Sato, M., J.E. Hansen, M.P. McCormick and J. Pollack, 1993: Statospheric aerosol optical depths (1850-1990). *J. Geophys. Res*. **98**, 22987-22994

Schönwiese, C.-D., M. Denhard, J. Grieser and A. Walter, 1997: Assessments of the global anthropogenic greenhouse and sulphate signal using different types of simplified climate models. *Theor. Appl. Climatol*., **57**, 119-124.

Schneider T and I. Held, 2001: Discriminants of twentieth-century changes in Earth surface temperatures. *J. Climate,* **14**, 249-254.

Schnur, R., 2001: Detection of climate change using advanced climate diagnostics: seasonal and diurnal cycle. Max-Planck-Institut fuer Meteorologie, Report No. 312, Bundesstr. 55, 20146 Hamburg, Germany.

Sexton, D.M.H., D.P. Rowell, C.K. Folland and D.J. Karoly, 2001: Detection of anthropogenic climate change using an atmospheric GCM. *Clim. Dyn*., in press.

Shindell, D. T., R.L. Miller, G. Schmidt and L. Pandolfo, 1999: Simulation of recent northern winter climate trends by greenhouse-gas forcing. *Nature*, **399**, 452-455.

Shindell, D. T., G.Schmidt, R.L. Miller and D. Rind, 2001: Northern Hemispheric climate response to greenhouse gas, ozone, solar and volcanic forcing. *J. Geophys. Res*. (Atmospheres), in press.

Simkin, T., L.Siebert, L.McClelland, D.Bridge, C.G.Newhall and J.H. Latter, 1981: Volcanoes of the World, 232 pp. Van Nostrand Reinhold, New York, 1981

Smith, R.L., T.M.L. Wigley and B.D. Santer, 2001: A bivariate time-series approach to anthropogenic trend detection in hemospheric mean temperatures. *J. Climate*, in press.

Stephenson, D.B., 1997: Correlation of spatial climate/weather maps and the advantages of using the Mahalonbis metric in predictions. *Tellus*, **49A**, 513-527.

Stevens, M.J. and G.R. North, 1996: Detection of the climate response to the solar cycle. *J. Atmos. Sci*., **53**, 2594-2608.

Stothers, R.B., 1996. Major optical depth perturbations to the stratosphere from volcanic eruptions: Pyrheliometric period 1881-1960. *J.Geophys. Res*., **101**, 3901-3920.

Stott, P. A. and S.F.B. Tett,1998: Scale-dependent detection of climate change. *J. Climate*, **11**: 3282-3294.

Stott, P.A., M.R. Allen and G.S. Jones, 2000a: Estimating signal amplitudes in optimal fingerprinting II: Application to general circulation models. Hadley Centre Tech Note 20, Hadley Centre for Climate Prediction and Response, Meteorological Office, RG12 2SY UK.

Stott, P.A., S.F.B. Tett, G.S. Jones, M.R. Allen, J.F.B.Mitchell and G.J. Jenkins, 2000b: External control of twentieth century temperature variations by natural and anthropogenic forcings. *Science,* **15**, 2133-2137.

Stott, P.A., S.F.B. Tett, G.S. Jones, M.R. Allen, W.J. Ingram and J.F.B. Mitchell, 2001: Attribution of Twentieth Century Temperature Change to Natural and Anthropogenic Causes. *Clim. Dyn.* **17**,1-22.

Stouffer, R.J., G.C. Hegerl and S.F.B. Tett, 1999: A comparison of Surface Air Temperature Variability in Three 1000-Year Coupled Ocean-Atmosphere Model Integrations. *J. Climate*, **13**, 513-537.

Svensmark, H. and E. Friis-Christensen, 1997: Variations of cosmic ray flux and global cloud coverage – a missing link in solar-climate relationships. *J. Atmos. Solar-Terrestrial Phys*., **59**, 1226-1232.

Svensmark, H., 1998: Influence of cosmic rays on Earth's climate. *Phys. Rev. Lett*., **81**, 5027-5030.

Tett, S.F.B., J.F.B. Mitchell, D.E. Parker and M.R. Allen, 1996: Human Influence on the Atmospheric Vertical Temperature Structure: Detection and Observations. *Science,* **274**, 1170-1173.

Tett, S.F.B., P.A. Stott, M.A. Allen, W.J. Ingram and J.F.B. Mitchell, 1999: Causes of twentieth century temperature change. *Nature*, **399**, 569-572.

Tett, S.F.B., G.S. Jones, P.A. Stott, D.C. Hill, J.F.B. Mitchell, M.R. Allen, W.J. Ingram, T.C. Johns, C.E. Johnson, A. Jones, D.L. Roberts, D.M.H. Sexton and M.J. Woodage, 2000: Estimation of natural and anthropogenic contributions to 20th century. Hadley Centre Tech Note 19, Hadley Centre for Climate Prediction and Response, Meteorological Office, RG12 2SY, UK pp52.

Thejll, P. and K. Lassen, 2000: Solar forcing of the Northern Hemisphere land air temperature: New data. *J. Atmos. Solar-Terrestrial Phys,* **62**,1207-1213.

Thompson, D.W.J. and J.M. Wallace, 1998: The Arctic oscillation signature in the wintertime geopotential height and temperature fields. *Geophys. Res. Lett*., **25**, 1297-1300.

Thompson, D.W.J., J.M. Wallace and G.C. Hegerl 2000: Annular Modes in the Extratropical Circulation. Part II Trends. *J. Climate*, **13**, 1018-1036 .

Tol, R.S.J. and P. Vellinga, 1998: 'Climate Change, the Enhanced Greenhouse Effect and the Influence of the Sun: A Statistical Analysis', *Theoretical and Applied Climatology,* **61**, 1-7.

Tol, R.S.J. and A.F. de Vos, 1998: A Bayesian statistical analysis of the enhanced greenhouse effect. *Clim. Change*, **38**, 87-112.

van Loon, H. and D. J. Shea, 1999: A probable signal of the 11-year solar cycle in the troposphere of the Northern Hemisphere, *Geophys. Res. Lett.*, **26**, 2893-2896.

van Loon, H. and D. J. Shea, 2000: The global 11-year solar signal in July-August. *J. Geophys. Res*., **27**, 2965-2968.

Vinnikov, K. Y., A.Robock, R. J.Stouffer, J.E.Walsh, C. L. Parkinson, D.J.Cavalieri, J.F.B Mitchell, D.Garrett and V.F. Zakharov, 1999: Global warming and Northern Hemisphere sea ice extent. *Science*, **286**, 1934-1937.

Volodin, E.M. and V.Y. Galin, 1999: Interpretation of winter warming on Northern Hemisphere continents 1977-94. *J. Climate*, 12, 2947-2955.

Walter, A., M. Denhard, C.-D. Schoenwiese, 1998: Simulation of global and hemispheric temperature variation and signal detection studies using neural networks. Meteor. Zeitschrift, N.F. **7**, 171-180.

Weber, G.R., 1996: Human effect on global climate? *Nature*, **384**, 524-525.

White, W.B., J. Lean, D.R. Cayan and M.D. Dettinger, 1997: A response of global upper ocean temperature to changing solar irradiance. *J. Geophys. Res*., **102**, 3255-3266.

Wigley, T.M.L., P.D. Jones and S.C.B. Raper, 1997: The observed global warming record: What does it tell us? *Proc. Natl. Acad. Sci. USA*, **94**, 8314-8320.

Wigley, T.M.L., R.L. Smith and B.D. Santer, 1998a: Anthropogenic influence on the autocorrelation structure of hemispheric-mean temperatures. *Science*, **282**, 1676-1679.

Wigley, T.M.L., P.J. Jaumann, B.D. Santer and K.E Taylor, 1998b: Relative detectablility of greenhouse gas and aerosol climate change signals *Clim Dyn*, **14**, 781-790.

Wigley, T.M.L., B.D.Santer and K.E.Taylor, 2000: Correlation approaches to detection. *Geophys. Res. Lett*. **27**, 2973-2976.

WMO, 1999: Scientific assessment of ozone depletion : 1998, Global Ozone Research and Monitoring Project, World Meteorological Organisation, Report No. 44, Geneva.

Wong, A.P.S., N.L. Bindoff and J.A. Church, 1999: Large-scale freshening of intermediate water masses in the Pacific and Indian Oceans. *Nature*, **400**, 440-443.

Zheng, X. and R.E. Basher, 1999: Structural time-series models and trend detection in global and regional temperature series. *J. Climate*, **12**, 2347-2358.

Zwiers, F.W., 1999: The detection of climate change. In "Anthropogenic Climate Change", H. von Storch and G. Floeser, eds., Springer-Verlag, 161-206.

Zwiers, F.W. and S.S. Shen, 1997: Errors in estimating spherical harmonic coefficients from partially sampled GCM output. *Clim. Dyn*., **13**, 703-716.